Design of a cable-driven upper limb exosuit: a simulation study

AUTHOR: ALESSANDRO PIRELLI

ADVISOR: Prof.ssa EMILIA AMBROSINI, Ing. ELENA BARDI, Prof.ssa MARTA GANDOLLA

ACADEMIC YEAR: 2020-2021

1. Introduction

Preservation of motor ability is strongly associated with independence and quality of life. Together with joint mobility and neuromuscular control efficiency, muscular force (intended as the ability of muscles to contract and generate forces) is one of the main key factors contributing to motor mobility. However, many different conditions and diseases can undermine it, causing muscle weakness and in turn negatively affecting motor ability. In this scenario, soft exoskeletons, also called *exosuits*, are among the most innovative instruments that can be used to provide assistance, compensating for muscular deficits. Their reliance on soft and deformable materials makes them extremely compliant to the complex movements allowed by our musculoskeletal system, without restricting movements or burdening the user excessively. Portability and usability greatly benefit from soft materials, making them valid instruments to use in rehabilitation programs and daily living assistance.

2. State of the art and objective

In [1] an in depth analysis of the current state of the art in the field of exosuit is provided. Research in this field is still at an early phase, but the results are rather promising and the interest is growing.
Exosuits are classified according to their actuation system: i) Tensile robotic suits: these devices deliver power to the human body by tensioning functional units (i.e. cables), actuating joints by pulling limbs' segments, ii) Expansive robotic suits: these robotic suits feature inflatable structures that move limbs' segments by changing size and shape; iii) Passive-adaptive robotic suits: unlike the previous ones, this kind of devices do not rely on actuators to function, but rather exploit materials' intrinsic characteristic to provide the assistance required; however, being also active devices, the engagement of such passive systems is controlled by other active systems.

In this scenario, tensile exosuits are the most interesting devices, as they provide relevant assistance with high transparency and low encumbrance. Examples of this kind of devices are presented in [2]-[5], where also their efficacy has been assessed with numerous studies.

After researching tensile exosuits in literature, the main objective of this thesis was to design the cable routing for a tensile exosuit specific for the upper limb. Unlike any of the studies previously found, a simulation-based approach has been developed to analyze the effects of different cables' configurations on a musculoskeletal model, obtaining valuable data used to determine which configuration led to minimal mechanical requirements and to assess the effects on biomechanical quantities of each configuration in order to maximize efficacy. Finally, data obtained from simulations has been used to size the actuation system of a prototype.

3. Materials & methods

The project has been developed using OpenSim, an open-source software that allows to perform musculoskeletal analysis in a simulation environment. The model used in this thesis was the model Arm_26, which has been developed by the OpenSim team. It represents the right upper body,

featuring 2 degrees of freedom of the arm (elbow flexion-extension and shoulder elevation) and 6 muscles representing biceps brachii (BIClong, BICshort), brachialis (BRA) and triceps brachii (TRIlong, TRIlat, TRImed). All muscles have been implemented as Hill-type musculo-tendon actuators. In this thesis, I focused my analysis on a single DOF (elbow flexion-extension).

Using MATLAB, the Arm_26 model was customized in order to include sets of cables (implemented as path actuators) with anchor points on the arm and forearm, placed along the frontal half of circumferences centered on the model's bodies (i.e. bones) and spaced 45° between each other. Single and double cables configurations were built. Then, using the OpenSim's CMCTool, the tensions required to be applied to the cables in order to perform elbow flexion have been computed. The elbow joint had to cover and angle between 20° and 120° in periods of time of 1s, 3s, 5s and 7s. In these first simulations, the model's muscles have been kept deactivated, so only the cables could generate the forces required to perform the elbow flexion. This procedure was repeated for each cable configuration (9 in total) and then the *Opt* value was computed as:

$$Opt_i = \frac{T_i^{max}}{\max{(T_i^{max})}} * 0.4 + \frac{T_i^{mean}}{\max{(T_i^{mean})}} * 0.3 + \frac{\Delta T_i^{max}}{\max{(\Delta T_i^{max})}} * 0.3$$

Where:

- T_i^{max} stands for the maximum value of the sum of the cables' tensions of the ith configuration.
- T_i^{mean} stands for the average value of the sum of the cables' tensions of the ith configuration.
- ΔT_i^{max} stands for the maximum difference between the cables' tension of the ith configuration (in case of the single cable configuration, this term was set to 0, and the weights of the other two terms was set to 0.5).

Each term of the cost function was normalized to the maximum value achieved among all the configurations. All terms of the cost function are functional in defining components requirements, as the maximum tension determines the maximum required motor torque, the average tension provides information about power consumption, and the equality between the cables' tension defines whether or not a single motor can be used to actuate both cables.

The best configuration was selected as the one with the lowest *Opt* value, and once found it was further studied to assess its efficiency and impact on the model behaviour.

Specifically, effects of the device on muscle activation, passive forces, metabolic costs and joint reaction forces/torques at the elbow were observed. Muscle activation is defined as the percentage of the maximum force generable by muscles required to perform a movement. In OpenSim, the minimum absolute amount of muscle activation is equal to 2%. Muscle passive forces are generated by muscles as responses to their state (intended as the muscle's length and lengthening speed). Metabolic cost is defined as the power consumed by a muscle over a period of time. Joint reaction forces and torques are internal forces/torques that generate at joints in response to external forces.

To obtain the desired data, CMCTool and FDTool simulations were run, performing elbow flexion movement in 1s and 7s covering an angle between 20° and 120°. To simulate different degrees of assistance, cables' tension was prescribed as 50%, 75% and 100% as the one required to perform elbow flexion without any of the muscles' intervention.

Regarding the device's design (Figure 1), taking inspiration from the works studied in literature, the idea was to use a motor to make a spool rotate, in order to wrap the cables around it, effectively pulling the forearm towards the arm. The cables would be anchored to garments on the arm and the forearm and thus performing the elbow flexion movement.
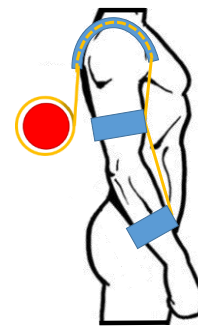

Figure 1: Exosuit concept.

At the time being, a motor and a reductor were already provided. The motor was the EC flat produced by Maxon Motor, which is a brushless 70W motor able to produce up to 128 mNm torques. The reductor was the GP 42, produced by Maxon Motor, which had a reduction parameter of

156:1. The reductor multiplies the motor's torque by its reduction factor, at the cost of the output speed which is equal to the motor's one divided by the same reduction factor. The only missing component for the actuation system was the spool, which dimensions had to be calculated. Using data acquired from simulations (specifically the one in which the elbow flexion was performed in 1s) and specifics of the available components, it was possible to calculate the spool's radius length range according to both performance requirements and hardware limitations using the following equation:

$$\frac{60 * v_{Max}^{Cables}}{2 * \pi * rpm_{Max}^{Red}} < R_{Spool} < \frac{C_{Max}^{Red}}{T^{Cables}}$$

Where:

- v_{Max}^{Cables} stands for the cables' maximum lengthening speed required to perform the movement defined.
- rpm_{Max}^{Red} stands for the reductor's maximum rotation velocity provided by datasheet.
- R_{Spool} stands for the spool's radius.
- C_{Max}^{Red} is the maximum torque that the reductor can exercise provided by datasheet.
- T^{Cables} is the cables' maximum tension, computed as the maximum of the sum of both cables' tension.

4.   Results

Following the optimization criteria defined previously, the *Opt* values of each configuration for each movement were computed.

The model U0H2 (Figure 2) was selected as the one with the best cables' configuration, since its *Opt* value was the lowest for all of the simulations, and therefore, it was used to perform the following biomechanical analyses.
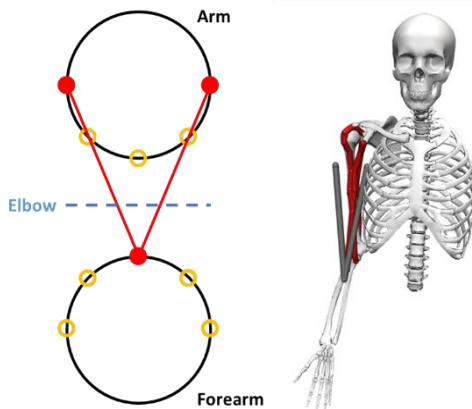
Figure 2: Model U0H2 scheme and rendering.

These analyses were performed running simulations in which cables' tension were prescribed as 50%, 75% and 100% (to simulate different degrees of assistance) of the tension required by the cables to perform elbow flexion (Figure 3) in 1s and 7s.
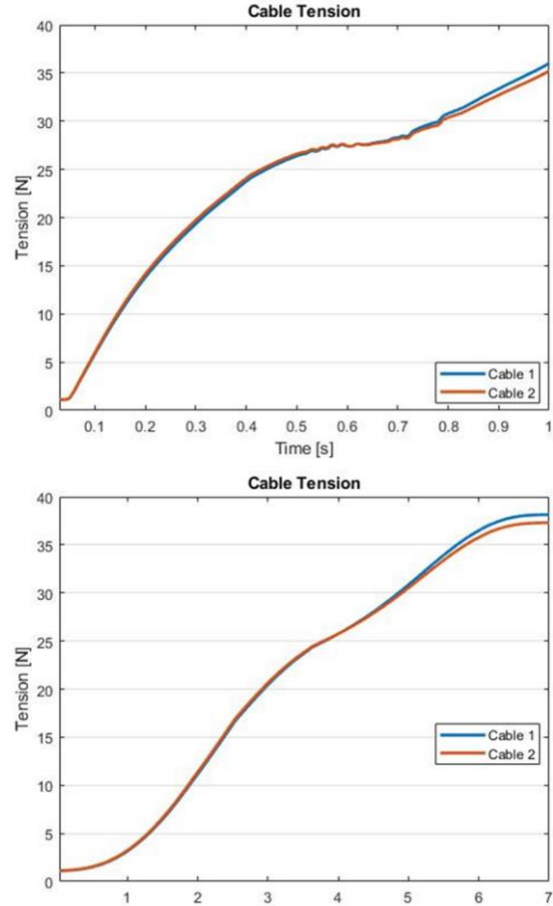
Figure 3: Cables' tension required to perform elbow flexion in 1s (top) and 7s (bottom) without muscles' intervention.

Figure 4 shows the effects of the cables' action on the agonist (BIClong, BICshort, BRA) muscles' activation. This quantity was the most interesting to study, as the goal of an assistive device is to reduce the load on muscles to perform movements. As expected, cables' intervention is effective in reducing the agonist muscles' activation (almost completely when 100% assistance is provided) as the assistance's degree increases. On the other hand, activation of antagonist muscles was basically unaffected or slightly increased, but still was close to the absolute minimum.

Regarding all other analysis, summaries of the comparison between different assistance's levels and the natural arm are reported in Table 1-3.
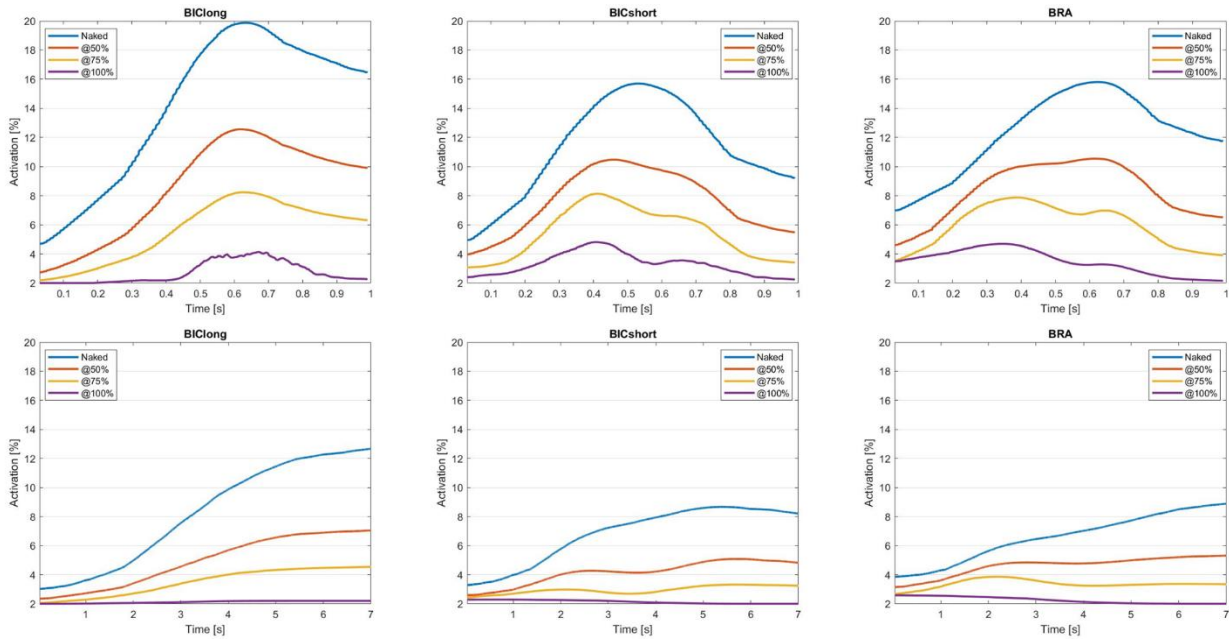
3

Figure 4: Activation of agonist muscles during elbow flexion extension movement lasting 1s (top row) and 7s (bottom row).

	@50%		@75%		@100%	
Muscle	1s	7s	1s	7s	1s	7s
BIClong	2%	2%	2%	2%	5%	1%
BICshort	2%	3%	4%	4%	7%	7%
BRA	2%	3%	7%	6%	8%	9%
TRIlong	-1%	0%	0%	0%	1%	1%
TRImed	0%	0%	0%	0%	0%	0%
TRIlat	-4%	-2%	1%	-2%	-23%	-22%

Table 1: Muscles' passive force reduction (in percentage) from the physiological case for each muscle in each condition tested.

	@50%		@75%		@100%		@eq	
Muscle	1s	7s	1s	7s	1s	7s	1s	7s
BIClong	-41%	-36%	-61%	-52%	-79%	-68%	-88%	-73%
BICshort	-32%	-34%	-51%	-50%	-69%	-61%	-83%	-65%
BRA	-32%	-26%	-50%	-42%	-69%	-57%	-77%	-47%
TRIlong	0%	0%	1%	0%	1%	0%	47%	8%
TRImed	-1%	0%	-1%	1%	5%	12%	46%	2%
TRIlat	0%	1%	-1%	1%	5%	13%	50%	2%

Table 2: Muscles' metabolic cost reduction (in percentage) from the physiological case for each muscle in each condition tested.

	@50%		@75%		@100%	
React.	1s	7s	1s	7s	1s	7s
F_x	-5%	-4%	-7%	-5%	-6%	-1%
F_y	-11%	-10%	-17%	-15%	-22%	-18%
F_z	-1%	4%	0%	9%	12%	25%
M_x	-1%	-4%	-1%	-4%	0%	-3%
M_y	46%	111%	76%	170%	108%	229%
M_z	2%	5%	4%	7%	6%	9%

Table 3: Joint reaction reduction (in percentage) from the physiological case for each muscle in each condition tested. On the right is a reference system centered on the ulna's head.

These tables show percentile changes from the physiological case at the various degrees of assistance of muscles' passive forces (Table 1), metabolic costs (Table 2) and reaction forces at the elbow (Table 3).

Looking at the results in Table 1, it can be stated that generally providing assistance of any magnitude did not affect any of the muscles' passive behaviour, with the only exception being TRIlat, for which passive forces dropped of 22-23% at 100% assistance. This means that the device's

4

action does not produce excessive muscles' strain, which could potentially lead to muscles' reaping and tearing. As such, the device can be deemed safe to use under this point of view.

In Table 2, data obtained from the model's resting condition (found for elbow flexion at 20°) is added as *@eq* values. Since metabolic cost is strictly related to muscle activation, it was expected to observe changes similar to those regarding muscles' activation. This hypothesis proved to be correct, as for agonist muscles (BIClong, BICshort, BRA), metabolic costs do indeed get lower and closer to the *@eq* values. Basically, this means that providing 100% of assistance, agonist muscles consume almost as much power as when they are in the elbow's resting condition. On the other hand, for antagonist muscles (TRIlong, TRImed, TRIlat), the values stay almost the same or slightly increase for higher degrees of assistance, in accordance with the results in muscles' activation.

Results in Table 3 show that forces along X axis and moments on X and Z axes do not get affected in a relevant way by the cable's action. The same cannot be said regarding forces along Z axis and the moment on Y axis, as they increase as the assistance degree raises, potentially affecting prono-supination of the forearm (but due to the model's limits it could not be verified). Anyways, this phenomenon could be explained by errors in the placement of the cables' anchor points, which may not be exactly symmetrical respect the limb's longitudinal axis. Also, the raise for higher degrees of assistance could be due to disparities in the cables' tension profiles. On the other hand, forces along Y axis decrease for higher degrees of assistance, thus the device's action reduces compressive stress on the elbow joint.

Finally, to size the spool for the actuation system the missing data was researched: the maximum lengthening velocity of the cables was found equal to 0.2m/s, while the maximum force required, considering the peak of both cables, was about 70N. However, to account for possible lack of power due to friction, possible higher weight of the arm and to potentially allow faster movements, 80N were considered.

With these pieces of information and the datasheets of the components at hand, it was calculated that the spool's radius had to be between 6cm (to guarantee the cables' maximum lengthening velocity required) and 18cm (this upper limit has been set by the maximum output torque of the motor-reductor system). Using the data acquired, the schematic in Figure 5 was developed. The center pieces are the motor and the reductor; the spool, which radius was set of 7cm to use the motor under the maximum of its operational range, is placed on the side and is actuated by the motor using a couple of bevel gears as transmission system. All components are up to scale.
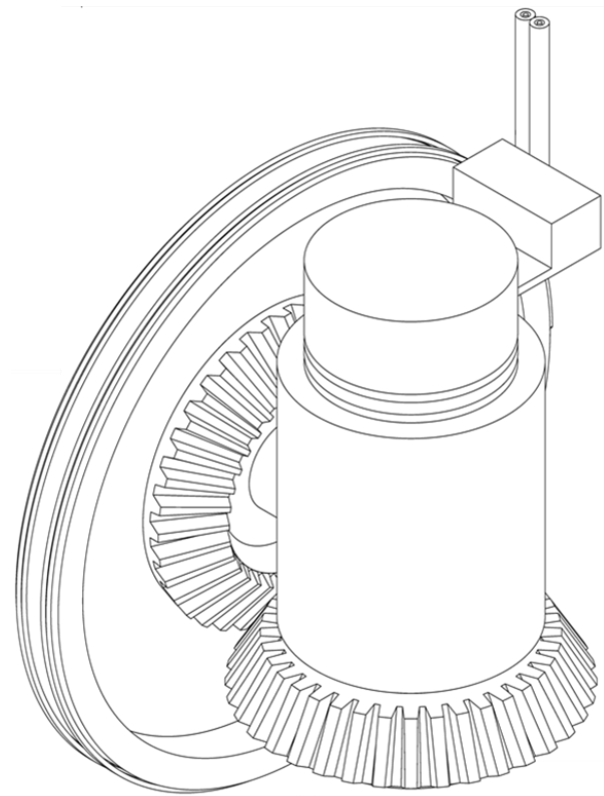

Figure 5: Actuation system prototype.

5.   Conclusions

The analysis regarding the best cables' configuration led to an important conclusion: in order to optimize the tension profile during elbow flexion, double cable systems are better than those relying on a single cable, as they require less maximum and average tension to pull the limb's segments.

Looking at the results in Figure 4, it is safe to say that the employment of the device succeeded in reducing the recruitment of the model's agonists muscles (BIClong, BICshort, BRA) needed to perform the desired elbow flexion movement, which lowers as the assistance provided by the cables increases. The same cannot be said about the antagonist muscles (TRIlong, TRImed, TRIlat). Indeed, it was initially expected to record no

sensible change in these muscles' activation, as the cables action was thought not to affect their behaviour. However, although there is a raise in their activation for higher percentages of assistance, the values obtained are still close to the absolute minimum. Also, this behaviour may be functional in correcting the movement's trajectory. Data of muscles' metabolic consumption (Table 2) are analogue to those regarding muscles' activation, as these two quantities are strictly correlated. Regarding passive forces and joint reactions at the elbow joint (Table 1 and Table 3), the aim was to make sure that cables' action wouldn't result in possible harmful situations, such as excessive strain on muscle, leading to high passive forces, or high reaction forces at the elbow joint. The data computed by simulations suggests that no excessive increases were measured for any of those values; therefore, using the exosuit with the proposed cables configuration should not result in harmful and dangerous situations. However, the raise of M_y as a result of the cables's action may affect forearm prono-supination.

6.   Future developments

The main limits of this project were determined by the model's simplicity in terms of number of muscles and degrees of freedom. A more realistic model, including more degrees of freedom, more muscle groups and a more realistic behaviour of existing muscles, would have led to more robust results. It's worth stating that trials were performed using other models (specifically the MoBL_ARM and the DAS3) which include more muscles and more degrees of freedom than the Arm_26. However, the results of the CMCTool were not reliable for these more complex models and therefore, the analysis was based on the Arm_26 model. For these reasons, in order to further develop the project (for instance to design and study cables' routing to assist other arm movements such as elbow extension or forearm pronation and supination), it is fundamental to find or build a more realistic musculoskeletal model. Meanwhile, the final goal of this project was to fully develop a portable exosuit to assist the upper limb. As such, the device has to be as small as possible, but currently the results are underwhelming. Given the current motor and reductor, the actuation system (alone) would be way too cumbersome, as the minimum diameter

for the spool would have to be 12cm. A possible solution to reduce the actuation system's size is to use a different motor and reductor, allowing the possibility to reach the appropriate maximum angular speed needed to perform physiological movements. With respect to the torque requirements, it is possible to reduce the gear ratio, since the present gear ratio is highly conservative. By reducing the gear ratio, not only the gear weight and dimensions could be reduced, but also the spool's radius length range would be shifted towards lower values and, therefore, the whole system's dimension would be reduced, lowering its weight, volume and thus increasing its portability.

7.   Bibliography

[1]   M. Xiloyannis *et al.*, "Soft Robotic Suits: State of the Art, Core Technologies, and Open Challenges," *IEEE Trans. Robot.*, pp. 1–20, Jun. 2021, doi: 10.1109/TRO.2021.3084466.

[2]   N. Li *et al.*, "Bio-inspired upper limb soft exoskeleton to reduce stroke-induced complications," *Bioinspiration and Biomimetics*, vol. 13, no. 6, Aug. 2018, doi: 10.1088/1748-3190/aad8d4.

[3]   S. Lessard, P. Pansodtee, A. Robbins, J. M. Trombadore, S. Kurniawan, and M. Teodorescu, "A Soft Exosuit for Flexible Upper-Extremity Rehabilitation," *IEEE Trans. Neural Syst. Rehabil. Eng.*, vol. 26, no. 8, pp. 1604–1617, Aug. 2018, doi: 10.1109/TNSRE.2018.2854219.

[4]   J. L. Samper-Escudero, A. Gimenez-Fernandez, M. A. Sanchez-Uran, and M. Ferre, "A Cable-Driven Exosuit for Upper Limb Flexion Based on Fibres Compliance," *IEEE Access*, vol. 8, pp. 153297–153310, 2020, doi: 10.1109/ACCESS.2020.3018418.

[5]   D. C. Scuola *et al.*, "Design and Embedded Control of a Soft Elbow Exosuit HUMAN-MACHINE INTERFACES BASED ON ELECTRO-BIOLOGICAL SIGNALS FOR ROBOTIC APPLICATIONS AND NEUROREHABILITATION View project CENTAURO-Robust Mobility and Dexterous Manipulation in Disaster Response by Full," doi: 10.1109/ROBOSOFT.2018.8405386.

DESING OF A CABLE-DRIVEN UPPER LIMB EXOSUIT: A SIMULATION STUDY

Author: **Alessandro Pirelli**

Abstract

Motor ability is essential in determining the quality of life of any individual. However, aging, myopathologies, neuropathologies and trauma can lead to partial or total loss of the ability to move.

For this reason, it is essential to research and develop new solutions to restore motor ability when impaired. Among the newest solutions, exosuits are emerging as promising in providing assistance with activities of daily living (ADLs). These devices are composed of soft fabric, or polymers, and work in parallel with the users' muscles without relying on rigid links. The use of such materials and the lack of rigid links, make them lighter, easier to wear and to use with respect to conventional stiff exoskeletons.

The goal of this thesis is to identify the best cable routing configuration for an upper limb cable-driven exosuit. In particular, the targeted movement was elbow flexion. In order to carry out this activity, OpenSim, a software that allows to run simulations of movements with musculoskeletal models, was used. Through this software different configurations for the cables were explored and evaluated. The optimization analysis led to the optimal design that minimizes the tension to be applied to the cables, while keeping to a minimum medium tension during movement and disparity between tensions of the cables. The resulting configuration is composed by two cables connected to the sides of the arm and forearm in a symmetrical way with respect to the longitudinal axis of the whole arm.

Such configuration was then evaluated in simulation for different percentages of assistance in order to study its effects in terms of muscle activation, passive forces generated by the muscles, metabolic consumption of the muscles and joint reaction forces at the elbow with respect to the natural movement without assistance. The results proved that the device's assistance lowered muscle activation without affecting too much passive forces and joint reactions at the elbow, assessing its safety. Furthermore, starting from the data collected in simulation and the current available components, a prototype of the actuation system was dimensioned and improvements were suggested.

Key-words: exosuit, assistance, rehabilitation, upper limb, cable based actuation.

Abstract in lingua italiana

La capacità motoria è essenziale nel determinare la qualità della vita di ogni individuo. Tuttavia, invecchiamento, miopatologie, neuropatologie e traumi possono portare alla perdita parziale o totale della capacità di movimento.

Per questo motivo è fondamentale ricercare e sviluppare nuove soluzioni per ripristinare la capacità motoria in caso di compromissione. Tra le soluzioni più recenti, gli exosuit stanno emergendo come promettenti nel fornire assistenza nelle attività della vita quotidiana. Questi dispositivi sono composti da tessuti morbidi, o polimeri, e lavorano in parallelo con i muscoli degli utenti senza fare affidamento su collegamenti rigidi. L'utilizzo di tali materiali e l'assenza di maglie rigide, li rendono più leggeri, più facili da indossare e da utilizzare rispetto ai tradizionali esoscheletri rigidi.

L'obiettivo di questa tesi è identificare la migliore configurazione di instradamento dei cavi per un'esotuta guidata da cavi dell'arto superiore. In particolare, i movimenti mirati erano la flessione del gomito. Per svolgere questa attività è stato utilizzato OpenSim, un software che permette di eseguire simulazioni di movimenti con modelli muscoloscheletrici. Attraverso questo software sono state esplorate e valutate diverse configurazioni per i cavi. L'analisi di ottimizzazione ha portato a un design ottimale che minimizza tensione da applicare ai cavi, tensione media durante il movimento e disparità tra le tensioni dei cavi. La configurazione risultante è composta da due cavi collegati ai lati del braccio e dell'avambraccio in modo simmetrico rispetto all'asse longitudinale dell'intero braccio.

Tale configurazione è stata poi valutata in simulazione per diverse percentuali di assistenza al fine di studiarne gli effetti in termini di attivazione muscolare, forze passive generate dai muscoli, consumo metabolico dei muscoli e forze di reazione articolari al gomito. Inoltre, partendo dai dati raccolti in simulazione e dai componenti attualmente disponibili, è stato anche dimensionato un prototipo del sistema di attuazione e sono stati suggeriti miglioramenti.

Parole chiave: exosuit, assistenza, riabilitazione, arto superiore, attuazione basata su cavi.

Contents

1. Chapter one: Introduction

When evaluating quality of life, there's no doubt that motor mobility is one of the key parameters to account for.

Being able to freely move our bodies in space, although bound to physics' laws, allows us to perform a plethora of tasks, starting from the most basic ones, such as eating or walking, to the extremely complex acrobatics showcased by olympic athletes.

Motor mobility is linked to 3 main features: joint mobility, neuromotor control and muscle force.

The first one, is defined as the range of motion of a joint, and is affected by how the bones, muscles, tendons and ligaments are arranged.

Neuromotor control is the coordination between muscular action and the nervous system, which requires both the ability to process inputs from our surroundings and to deliver signals to control timing of muscle recruitment as well as muscle contraction.

Finally, by muscle force is intended the ability of muscles to exert forces. Muscles actuate joints by contracting and thus pulling different body segments to which they are attached.

Motor mobility as a whole can be affected by a variety of things: training for one can be useful in enhancing performances and skills, but on the other hand diseases and traumatic events can have a negative impact.

While there are numerous diseases and conditions that target joint mobility and neuromotor control, for the purpose of this thesis a focus on muscle weakness and some of its causes is in order.

As the name states, muscle weakness is a condition that causes muscles to not perform at physiological levels, limiting the amount of force that they can exert and thus affecting both joints' range of motion and maximum bearable loads.

Depending on its extent, this condition can seriously compromise motor ability, resulting in a loss of independence and thus dramatically lower quality of life.

Muscle weakness is generally linked to the natural process of aging: like the rest of our body, muscle fibers deteriorate over time.

Of course, factors like training, dieting and genetics can change the rate at which this process takes place.

However, muscle weakness can also be a symptom related to diseases: stroke survivors, for example, commonly suffer from it as a drawback, and there are plenty of examples of myopathies that cause dysfunctions of muscle fibers resulting in muscle weakness.

Especially, but not exclusively, in these pathological cases, rehabilitation and assistance play major roles in reestablishing the lost quality of life.

Fortunately, scientific progress and technological development made, and keep on making, available new instruments aimed to aid in these specific fields.

For this thesis in particular, soft wearable devices (i.e. exosuits) have been considered the most relevant. Being light-weight, easy to use and wear, exosuits could be potentially be used autonomously by patients affected by motor deficits outside

clinical environments, providing assistance in everyday life scenarios, and most importantly overcoming usability issues typical of their rigid counterparts.

In this project, the objective was to develop and design the cable routing for a cable based exosuit specific for arm and study the device's effects on the human body.

2. Chapter two: State of the art

Currently, many devices to assist limbs are already available. These of course vary in shape, form, typology of assistance and technology used.

According to [1], wearable robots aimed at empowering limbs can be classified following a taxonomical method, much like it is done in biology, based on a series of dichotomies. This taxonomy is showed in Figure 2.1 and will be described in the following sections.
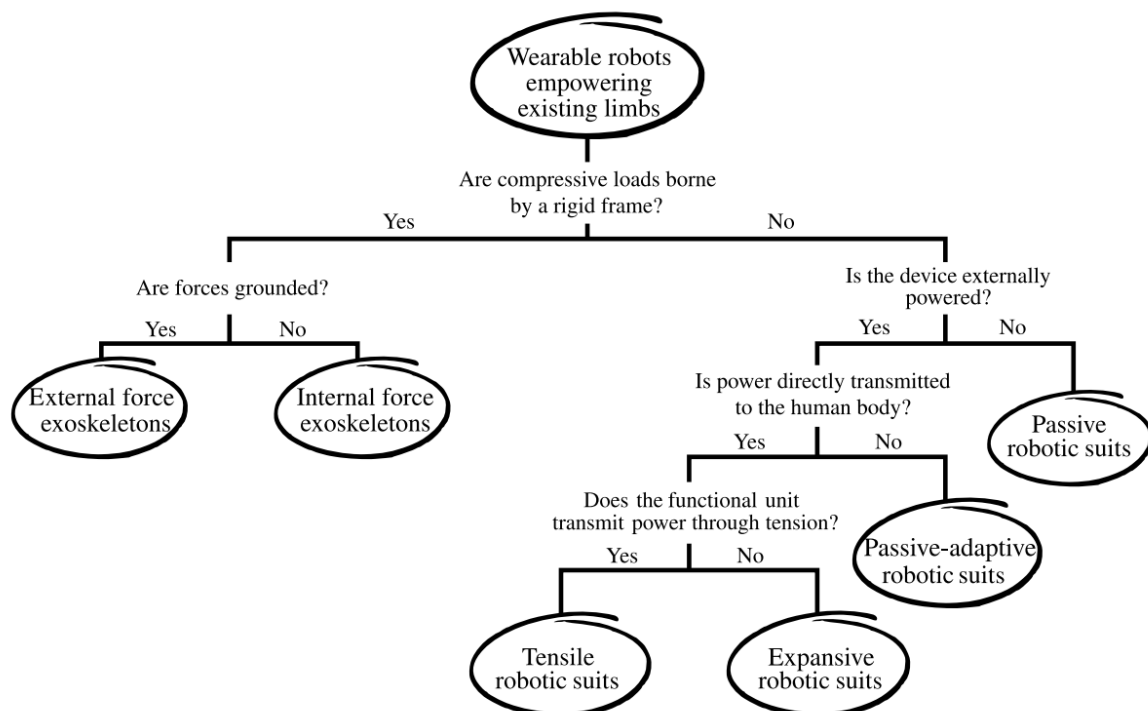
Figure 2.1: Taxonomy of wearable assisting robots. Taken from [1]

2.1   Rigid vs soft exoskeletons

The first main distinction that can be made on wearable robotic devices is between those that are referred to as rigid exoskeletons and those that are referred to as soft exoskeletons.

By rigid exoskeleton, or rather just exoskeleton, given the intrinsic rigidity of this kind of devices, is defined a wearable robot which features a solid external structure to which the user's body is bounded, so that the actuation of the external frame causes the user's limbs to be moved along.

Exoskeletons can be either grounded, and they are called external force exoskeletons, or not, and they are referred to as internal force exoskeletons. This distinction is important as it is directly linked to the device's performance. In fact, external force exoskeletons can extend human strength beyond its natural limits by transmitting power to an external base, while the latter, since they transfer power between the device and the user, which of course can withstand only forces of limited magnitude, are typically used to provide assistance in case of weak motor abilities. Regarding their field of use, in [2] exoskeleton systems can be broadly categorized into assistive devices meant to replace impaired human functioning, rehabilitation devices aimed at recovering functionality lost due to injury or medical conditions, augmentation exoskeletons designed to enhance the users' abilities above their normal levels, and other devices such as those used for teleoperation or entertainment.

On the other hand, soft exoskeletons, or *exosuits*, as they will be referred to from now on, take the wearable definition to a further extent, appearing like what seem pieces of clothes with the addition of actuation units like cables, shape changing materials or inflatable structures to mobilize the user's limbs.

Both categories, exoskeletons and exosuits, come with their respective pros and cons. Starting with exoskeletons, they have the ability to potentially provide large forces to the user, while maintaining precise control over the trajectory of the movements performed. For these reasons, such devices are appropriate in case of patients affected by severe conditions that require high levels of assistance [2].

Still, their cumbersome structure makes them bulky and heavy, their rigidity requires precise alignment between their links and the user's joints, their power consumption is not negligible and due to their complexity, in order to be operated safely, the assistance of specialized and trained personnel is required.

All these disadvantages negatively affect their usability, pricing and overall availability. For all these reasons, the use of exoskeletons in rehabilitation and assistance is limited to clinical environments only. However, especially simpler passive devices are steadily spreading in the industrial context, such as the Paexo by Ottobock [3].

However, is worth noticing that the latest advancements in the technologies involved in their production and functioning led to improvements on all fronts.

Given the current scenario, as stated in [4], nowadays research groups are investigating the field of exosuits, as they could be a valid alternative to their rigid counterpart. By using soft materials such as fiber and polymers to build their frame, exosuits can still provide assistance but with higher transparency, increased comfort and ease of wear due to their compliance. Also, characteristics such as weight, encumbrance, power consumption and cost can benefit from the employment of soft materials and the lack of rigid links.

As a result, the portability and usability of exosuits is much better than that of exoskeletons, thus in cases such as rehabilitation outside clinical environment and everyday life assistance they can potentially prove to be more effective.

2.2   Exosuits

Moving on with the taxonomy, exosuits (as well as exoskeletons) can be either passive, when the device passively stores and releases energy (e.g. springs) according to the movements of the user, or active, when it requires a power source in order to function.

Focusing on active exosuits, these can be divided in 3 main categories based on their characteristics:

- Tensile robotic suits: these devices deliver power to the human body by tensioning functional units (i.e. cables), actuating joints by pulling limbs' segments. Devices of this kind are presented in [5]–[8].

- Expansive robotic suits: while the working principle of tensile exosuit is based on the pulling action of cables to mobilize the user's joints, expansive robotic suits feature inflatable structures that move limbs' segments by changing size and shape. Examples of this kind of devices are the Exomuscle [9], the exosuit developed by Koh et al. [10] and other exosuits presented in [11]–[14].

- Passive-adaptive robotic suits: Unlike the previous ones, this kind of devices do not rely on actuators to function, but rather exploit materials' intrinsic characteristic to provide the assistance required; however, being also active devices, the engagement of such passive systems is controlled by other active systems. An example of such devices is described in [15], where electromagnetic clutches regulate the involvement of elastic bands to provide passive support to the shoulder joint.

In the following paragraphs, only devices belonging to the first category will be presented, as the purpose of this thesis was to develop and design the cable routing of a cable based exosuit for the upper limb.

Also, the controlling methods have not been investigated in detail since, at the current stage, the main objective was to determine the approach to follow in order to optimize the cables' configuration only, but will be kept in mind when further developing the device.

2.2.1 Tensile robotic suits

Among the previous explained categories of active exosuits, in particular, four devices representative of this category have been analyzed and studied, each one featuring systems of cables arranged in different designs in order to assist the upper limbs in performing different movements.

In Table 2.1 a brief recap of the devices' main characteristics is provided. Specifically, the number of degrees of freedom actuated, the portability, and the number of cables used have been considered.

Device/Study	DOF	Portable	# of cables
Li et al	7	No	13
ExoFlex	2	No	2
Xiloyannis et al.	2	Yes	3
Crux	8	Yes	7

Table 2.1: Exosuits' main characteristics

The first device studied, presented in [5], allows to control all the 7 of the degrees of freedom of the arm (3 of the shoulder joint, 1 of the elbow joint, 1 of the forearm joint, 2 of the wrist joint), and features 13 Bowden cables anchored to a wearable sleeve.

The cables' routes (shown in Figure 2.2-6) have been determined after an anatomical study of the upper limb: each and every cable has been placed in order to follow the tension lines of the actual anatomical muscles of the arm whose action it was aimed to replicate.
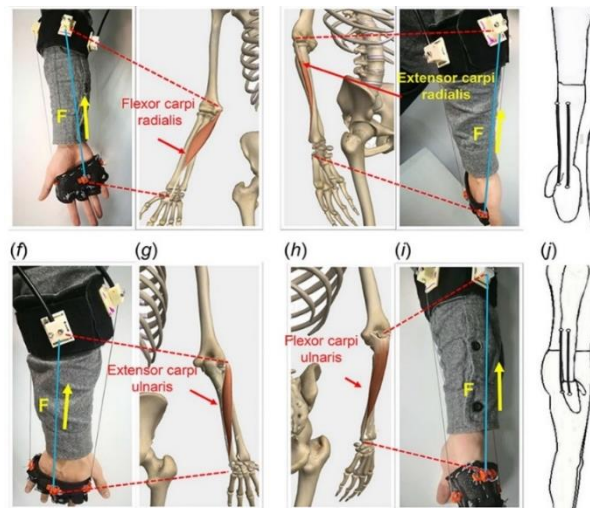
Figure 2.2: Cable routing for wrist deviation [5]
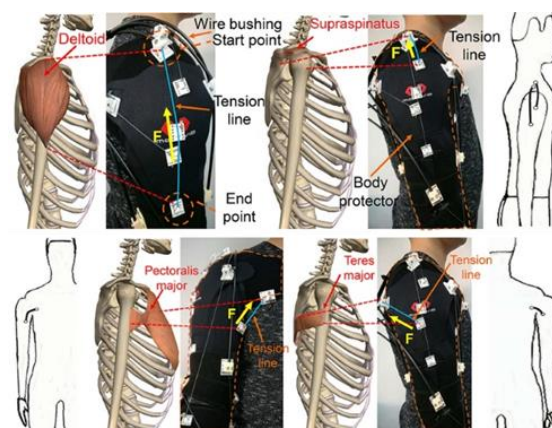
Figure 2.3: Cable routing for shoulder elevation, adduction and abduction [5]
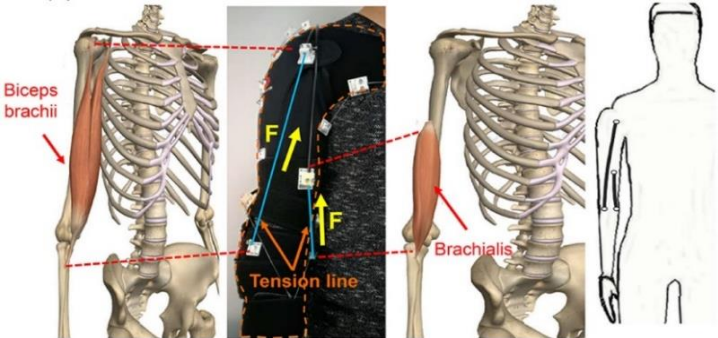
Figure 2.6: Cable routing for elbow flexion [5].
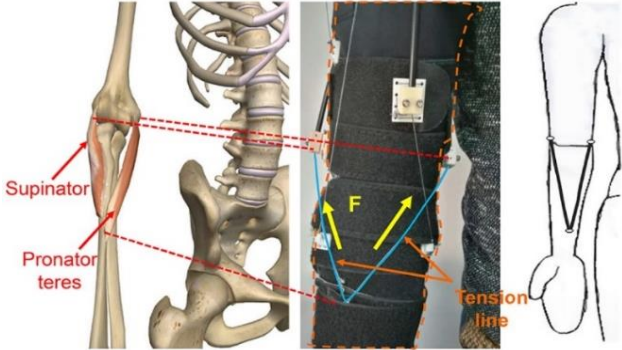
Figure 2.5: Cable routing for forearm pronation
and supination [5].
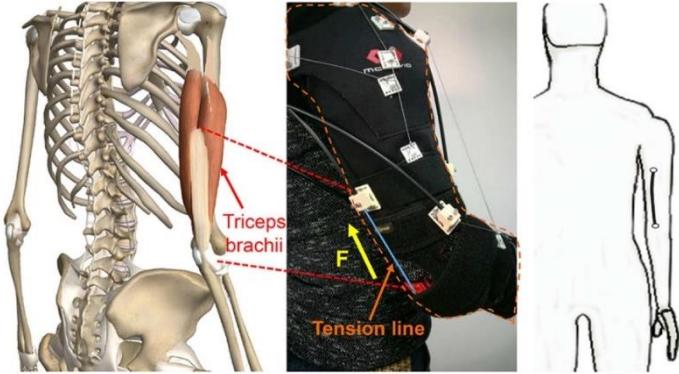
Figure 2.4: Cable routing for elbow
extension [5].

About the actuation of the device, the tension to the cables is applied by 10 brushless DC motors controlled by an ARM-based processor and alimented by 3 switching mode power supplies.

To control the exosuit, first healthy subjects have been monitored while performing tasks (specifically water-drinking) using motion capture systems. In addition, each joint's angle has been obtained. Then, the cables' lengths and the motors rotation amounts have been calculated according to the data collected.

At the current state, the prototype (Figure 2.7) had all of the actuation and control systems placed on a movable tray external to the wearable part of the device, but eventually it will all fit in a backpack to be portable.
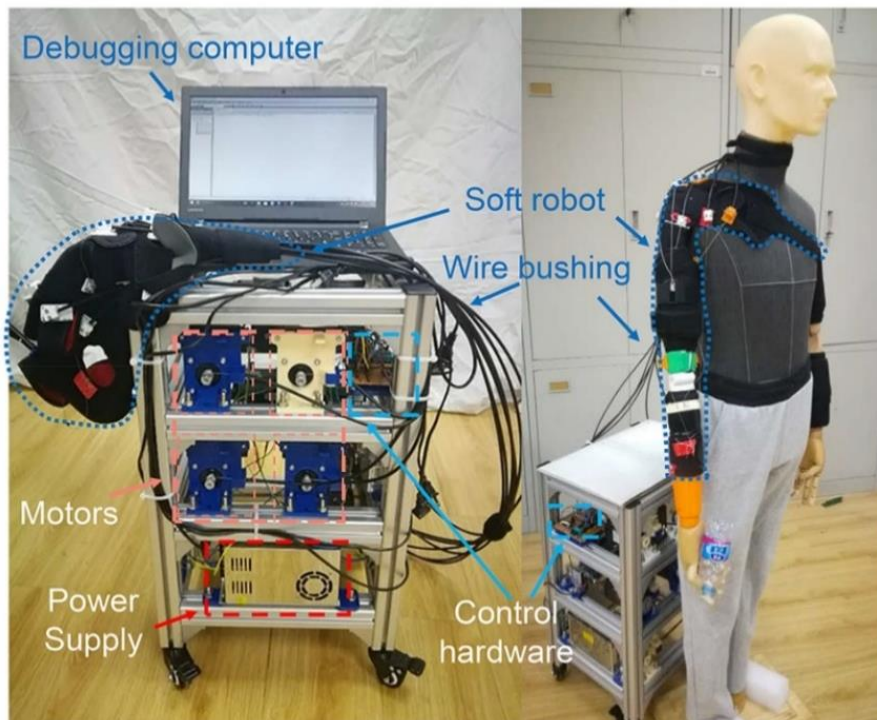
Figure 2.7: Soft robot's prorotype with control and actuation systems [5].

2.2.1.2 ExoFlex

Another device which has been studied is the one presented in [6].

The ExoFlex (Figure 2.8) has been developed in order to assist the elbow flexion movement in its whole range of motion and the shoulder elevation up to 100 degrees.
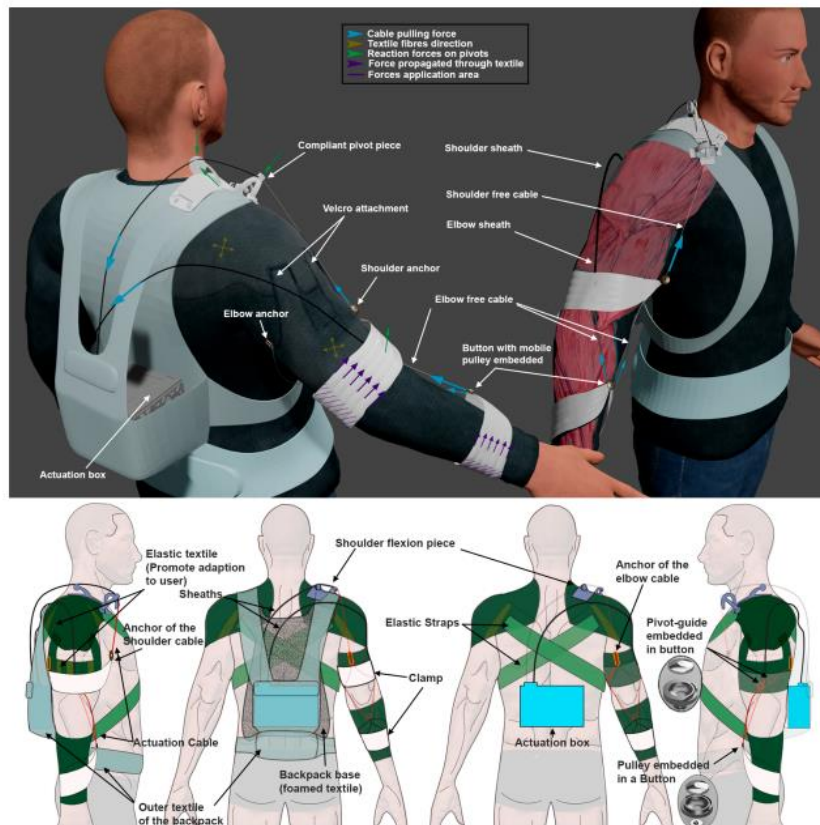
Figure 2.8: ExoFlex rendering [6].

This exosuit has only 2 cables, one for each degree of freedom, and features the ability to actuate them separately since both are linked to their own independent motor. Specifically, the device features two 24V at 0.5A geared Maxon motors with torque exertion up to 5Nm chosen for their light weight and easiness to modify the output range. A 5cm pulley is the used to deliver assistance forces up to 130N for both motors.

Regarding the cables, the exosuit uses 0.68mm Bowden steel cables which, due to their characteristics, provide reduced curvature radius and significant resistance values.

Currently the device is alimented by an external DC power supply.

All of the motors and electronics, and eventually also the power supplies, are placed in a rearranged baby-carrier used as a backpack, which will affectively make the device portable.

About the routing of the cables, the design process has not been explained in detail in the papers available, but it's stated that the main factors in designing the routing were the shear forces acting on the cables and the volume's changes of the muscles while performing movements to grant both comfort and safety.

 As such, the routing has been designed in order to minimize shear stress on the fabric and to avoid collisions between the cables and the contracted muscles.

To function, the exosuit uses feedback from encoders and mechanical sensors.

2.2.1.3   Xiloyannis et al. exosuit

In [7] the design of a soft exosuit for assisting elbow flexion and extension is presented.

Figure 2.9: Exosuit developed
by Xiloyannis et al [7].

The exosuit (shown in Figure 2.9) comprises an actuation stage, driving a pair of tendons, and a wearable component.

The tendon-driving unit comprises the following components: a brushless motor (Maxon EC-i, Ø 40 mm, 70W) coupled to a planetary gearhead (reduction of 28:1), whose angular position is sensed by a quadrature encoder (Maxon Encoder MR, 1000 CPR) and a spool around which two cables are coiled in opposite directions, so that rotation of the motor in one direction causes retraction of one tendon and releases the other, in an antagonistic fashion.

The two tendons, made of superelastic NiTi wire, are routed from the actuator unit on the harness to the elbow joint through a Bowden sheath, one passing in the front of the arm, the on the back, so that when tensioned the cables provide assistance in elbow flexion and extension respectively.

The whole actuation mechanism is enclosed in a 3D-printed case and carried in a plastic backpack with the electronics and power supply.

The exosuit for the elbow is made of two straps: a proximal one anchored to the arm and chest, designed by modifying an existing orthosis (MASTER03, Reh4mat) and a distal one tightened around the forearm, which fastens as it is pulled for more stability.

Finally, to route the tendons along the load paths 3D printed anchor points were sewn on each side of the joint.

Also, to sense the tension on the tendons, the distal anchor points house a subminiature load-cell (Futek, LLB210, 220 N).

2.2.1.4 Crux

Last but not least, the Crux exosuit (presented in [8], shown in Figure 2.10) has been studied and analyzed.

Figure 2.10: Crux exosuit [8].

This device, which weighs only 1.3kg, assists the user in performing both movements of the shoulder (adduction, abduction, extension and flexion) and of the arm (elbow extension and flexion, forearm pronation and supination) reaching significant amounts in terms of range of motion.

With the main target being post-stroke patients, and thus having mobility issues on one side of their body, the suit has been developed to record with IMU sensors the movements of the leading arm and use the data to assist the other impaired arm in performing those same movements using cable driven actuators.

The system features 7 Bowden cables rated to 220N. The actuation is up to 6 independent DC brushed micromotors each with a stall torque of 88.3 Nm and a gear ration of 1000:1, all under the management of a 32kB microcontroller.

All the electronics are powered by a three cell 3500 mAh lithium polymer battery which provides between 11.1 – 12.6 V and up to 50 A.

In this case, the routing of the cables (Figure 2.11) has been studied in order to reduce the lines of extension upon the skin of the cables, using methods involving motion capture and 3D modeling, and as a result, the exosuit provides significant assistance without inhibiting the flexibility of the user.
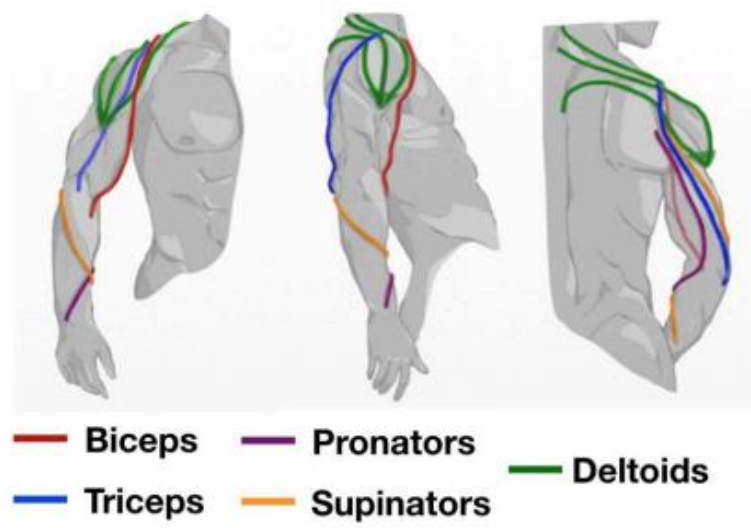
Figure 2.11: Crux's cable routing scheme [8].

2.3 Thesis' objective

After researching and studying tensile exosuits in literature, the main objectives of this work were to optimize the design of a cable-driven exosuit in a simulation environment and to define a simulation workflow to evaluate the resulting configuration.

In particular, for what concerns the optimization, the aim of this process was to design the cable routing of the device, in order to obtain cables' arrangement that would lead to minimal mechanical requirements actuation-wise, keeping both the device's encumbrance and costs to a minimum.

Regarding the evaluation of the configuration obtained, data from simulations has been analyzed to assess the efficacy of the device. Specifically, the effects of the cables' assistance on muscles' activation, passive force, metabolic costs and joint reaction forces have been observed.

The main advantages of working in a simulation environment are:

- Otherwise difficult to obtain data can be easily collected, and, as long as appropriate models and tools are used, the results can be deemed representative of what would actually be recorded in real file. This data can then be used both in the optimization process and to evaluate the device, as will be explained in the following chapters.

- Being defined by basic parts and inputs, the whole process can be easily generalized to be used in similar studies. In this specific case, an exosuit for supporting the elbow flexion was investigated, but by using a different model and changing some parameters the same optimization process could be potentially exploited for other arm movements or even for other limbs.

Finally, data obtained from simulations and specifics of some available components have been used to size the actuation system of a potential prototype.

3. Chapter three: Materials & methods

This chapter is aimed to explain how OpenSim [16]–[18], the software used to develop the project, works, and how its tools have been used for the development of the project.

First, a brief description of OpenSim is provided, with insights on all its tools, among which the Computed Muscle Control Tool and the Forward Dynamics Tool played a major role in this project.

Then, the whole project development process is described in detail.

3.1 Opensim

Figure 3.1: OpenSim logo

OpenSim (SimTK) is an open source and freely available software package. It allows to build, exchange, and analyze models of the musculoskeletal system and perform dynamic simulations of any movement.

OpenSim version 1.0 was introduced at the American Society of Biomechanics Conference in 2007, and with version 2.0, an application programming interface (API) was added, allowing researchers to access and customize OpenSim core functionality.

The latest version is OpenSim 4.2, was released on March 14, 2021, which is the version that has been used in this project.

OpenSim features a graphical user interface (GUI) which allows to observe and customize the model while performing the desired tasks in real time.

Furthermore, all the tools featured in the OpenSim software are available on MATLAB thanks to the Simbody library, which is an open-source multibody dynamics engine developed to create mathematical models of biological dynamics.

3.1.1 .osim models

In OpenSim, the neuromuscular and musculoskeletal dynamics of a human or animal are represented by models, which are files characterized by the .osim extension.

A model is made up of components corresponding to parts of the physical system that combine to generate or describe movement.

The key parts of a model are: bodies, joints and actuators, plus other components which more specifically define certain characteristics of the model.

In OpenSim, a model's skeletal system is represented by rigid bodies, characterized by specified geometries, mass and inertial properties.

Joints define how two bodies, termed parent and child bodies, can move with respect to one another. Constraints can also be applied to limit the range of motion joints.

Actuators can apply pure forces or torques that are directly proportional to the input control (i.e., excitation) via their optimal force (i.e., a gain). Forces and torques are applied between bodies.

Muscles are a specific kind of actuators, and can be implemented choosing among many different models available in OpenSim.

They are generally modeled as specialized force elements that act at muscle points (e.g., insertion and origin points) connected to rigid bodies. The force of a muscle is typically dependent on the path through muscle points comprised of muscle fiber and tendon lengths, the rate of change of the fiber lengths, and the level of muscle activation.

OpenSim also has a variety of other forces, which represent externally applied forces (e.g., ground reaction forces), passive spring-dampers (e.g., ligaments), and controlled linear and torsional actuators.

3.1.2 OpenSim Tools

As stated before, OpenSim features many tools which can be used to carry out different studies on a biomechanical model:

- **Scale Tool**: the Scale Tool alters the anthropometry of a model so that it matches a particular subject as closely as possible. Scaling is typically performed by comparing experimental marker data to virtual markers placed on a model. In addition to scaling a model, the Scale Tool can be used to adjust the locations of virtual markers so that they better match the experimental data.

- **Inverse Kinematics (IK) Tool**: the IK Tool steps through each time frame of previously collected experimental data and positions the model in a pose that "best matches" experimental marker and coordinate data for that time step. This

"best match" is the pose that minimizes a sum of weighted squared errors of markers and/or coordinates. Obtaining accurate results from the IK Tool is essential for using later tools like Static Optimization, Residual Reduction Algorithm, and Computed Muscle Control.

- **Inverse Dynamics (ID) Tool**: the ID Tool determines the generalized forces (e.g., net forces and torques) at each joint responsible for a given movement. Given the kinematics (e.g., states or motion) describing the movement of a model and the external loads applied to the model, the ID Tool performs an inverse dynamic analysis. Classical mechanics mathematically expresses the mass-dependent relationship between force and acceleration, $F = m \times a$, by means of the equations of motion. The Inverse Dynamics Tool solves these equations, in the inverse dynamics sense, to yield the net forces and torques at each joint which produce the movement.

- **Static Optimization Tool**: Static optimization is an extension of the inverse dynamics tool that further resolves the net joint moments into individual muscle forces for each time-instant. The muscle forces are computed by minimizing the sum of squared muscle activations.

- **Residual Reduction Algorithm (RRA) Tool**: the purpose of residual reduction is to minimize the effects of modeling and marker data processing errors that aggregate and lead to large nonphysical compensatory forces called residuals. Specifically, residual reduction alters the torso mass center of a subject-specific model and permits the kinematics of the model from Inverse Kinematics to vary in order to be more dynamically consistent with the ground reaction force data.

- **Computed Muscle Control (CMC) Tool**: the purpose of CMC is to compute a set of muscle excitations (or, more generally, actuator controls) that will drive a

dynamic musculoskeletal model to track a set of desired kinematics in the presence of applied external forces (if applicable).

- **Forward Dynamics Tool**: given the controls (e.g., muscle excitations) computed by the Computed Muscle Control (CMC) or another approach, the Forward Dynamics Tool can drive a forward dynamic simulation. A forward dynamics simulation is the solution (integration) of the differential equations that define the dynamics of a musculoskeletal model. Also, by using different analyses, more detailed biomechanical data (for instance muscles' metabolic costs) can be collected.

- **Analyze Tool**: as the name suggests, this tool runs a set of analyses on the model studied. For instance, this tool may be used to get configurations of bodies, states of actuators, joints' coordinates and reaction forces during a simulation run.

Among all these tools, the ones most involved in the developing of the project were the Computed Muscle Control Tool and the Forward Dynamics Tool, which will be further described in the next paragraphs.

3.1.3 Computed Muscle Control Tool

As briefly stated before, the CMC Tool, given a model and a desired kinematic set as inputs, returns the necessary values of activation of the actuators featured in a model to reproduce the kinematic behaviour given as input.

Once selected in the Tool's tab, the Computed Muscle Control (CMC) Tool's window opens.
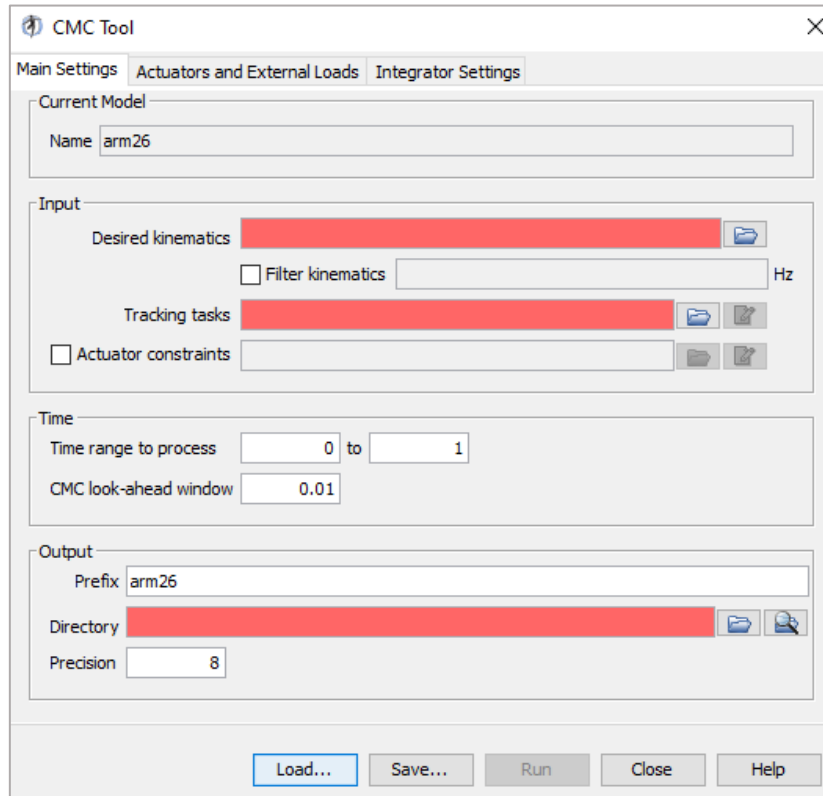
Figure 3.2: CMCTool control window on main settings pane.

- In the *Main Settings* pane (Figure 3.2), the user has access to different inputs:

  o *Desired kinematics* file, which can be optionally low-pass filtered at a specified frequency.

  o *Tracking tasks* file, which specifies which of the model's coordinates have to follow the kinematics uploaded in the *Desired kinematics* file. Additionally, it's possible to set a weight to each coordinate that represents how precise the tracking of the trajectory should be with respect to the input desired kinematics.

o   By checking the *Actuator constraints* box, the user can upload a constraints file which sets boundaries to the model's actuators' controls, either setting minimum and maximum values, or prescribing the activation during the processing period.

o   In the *Time* section, the user can select the time window of the *Desired kinematics* file in which the CMCTool has to operate and customize the look-ahead window.

o   In the *Output* section, the user can select the output files' prefix (analyzed model's name by default) and the output directory.
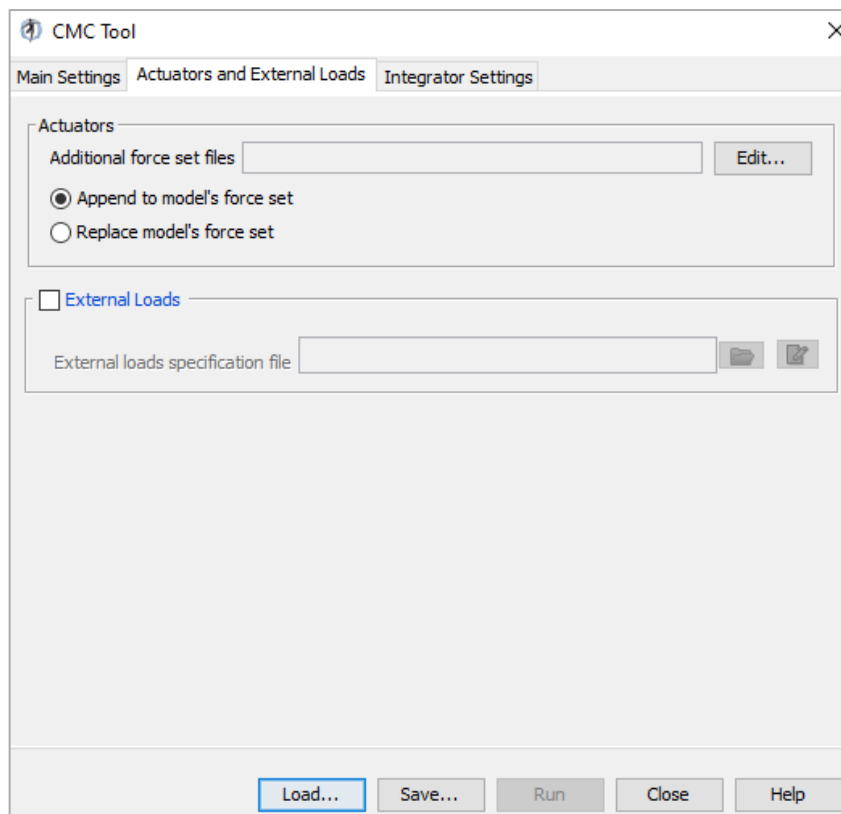
Figure 3.3: CMCTool actuators and external loads pane.

- In the *Actuators and External Loads* pane (Figure 3.3), the user can upload other force files, either *Actuators* or *External loads*, to the model. For the *Actuators*, these

forces can be either appended to the model's force set or used to replace them completely.
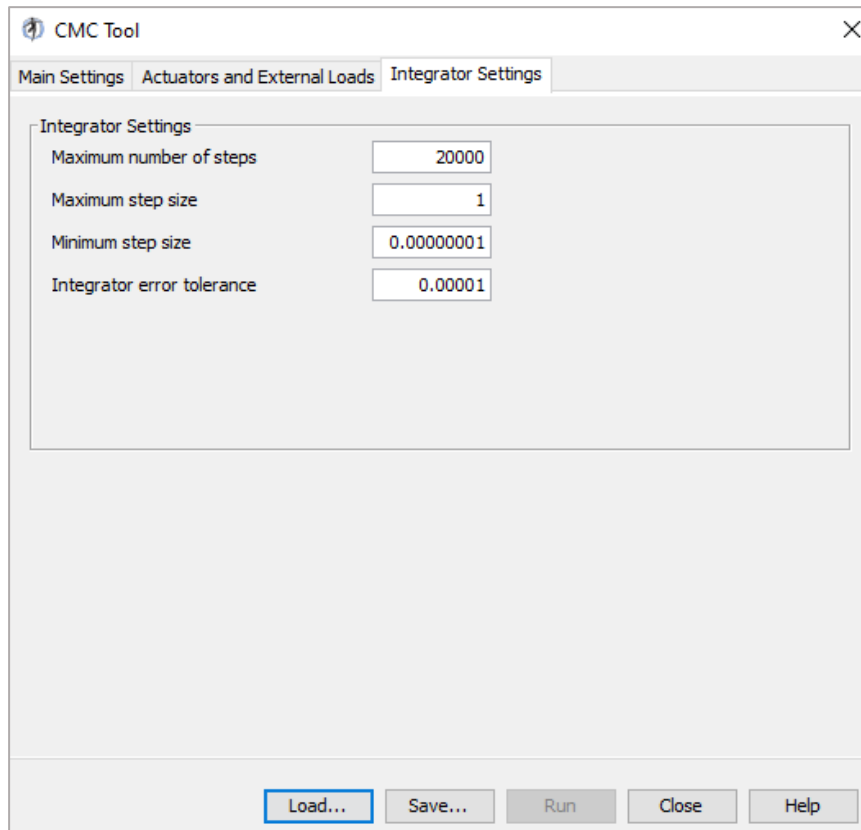
Figure 3.4: CMCTool integrator settings pane.

- In the *Integrator Settings* pane, the CMCTool's specifics (shown in Figure 3.4) can be fully customized according to the user's needs

- On the bottom part of the window, the *Control Panel*, there are 5 buttons:

   o *Load…* allows to select a setup file already available to the user

   o *Save…* saves the current setup as a .xml file which can be further customized

   o *Run* starts the tools

   o *Close* closes the window

    o *Help* opens acts as a link to the Simtk's site explaining how the tool works

Regarding the tool's methods of operation, the whole process is explained in depth by the developers themselves in [19], and is reported in the following:

To compute the actuators activations that will drive the model's coordinates towards the desired trajectory, the CMCTool uses a combination of proportional derivative (PD) control and static optimization.

Before starting the CMC algorithm, initial states (joint angles, joint angular velocities, muscle activation levels and fiber lengths) for the model are computed.

The first step in the CMC algorithm is to compute the accelerations to drive the model coordinates using:

$$\ddot{q}^*(t+T) = \ddot{q}_{exp}(t+T) + k_v\left[\dot{q}_{exp}(t) - \dot{q}(t)\right] + k_p[q_{exp}(t) - q(t)] \qquad (3.1)$$

Where:

- *$\ddot{q}^*$ are the accelerations to drive the model*
- *q are the model coordinated*
- *q_{exp} are the desired coordinate*
- *k_v is the feedback gain in velocity errors*
- *k_p is the feedback gains on position errors*

These accelerations are computed for small intervals of time (T).

To drive errors to zero without over-shooting or over-damping, the velocity feedback gain can be set as:

$$k_v = 2\sqrt{k_p} \qquad (3.2)$$

Usually, error gains k_v=20 and k_p=100 are used.

The next step in CMC is to compute the actuator controls to obtain the previously computed accelerations. x that will achieve the desired accelerations $\ddot{q}^*(t + T)$.

Static optimization is used to distribute the load across synergistic actuators. It is called "static" optimization because the performance criterion (i.e., the cost index) is confined to quantities that can be computed at any instant in time during a simulation.

Two formulations of the static optimization problem are currently available in CMC, the slow target and the fast target.

In this project the latter has been used, which *is the sum of squared controls augmented by a set of equality constraints $C_j = 0$ that requires the desired accelerations to be achieved within the tolerance set for the optimizer:*

$$J = \sum_{i=1}^{n_x} x_i^2 \tag{3.3}$$

$$C_j = \ddot{q}_j^* - \ddot{q}_j \quad \forall j \tag{3.4}$$

The fast target is both faster and generally produces better tracking.

However, if the constraints cannot be met, the fast target will fail and CMC will exit with an error message. Often the reason for the failure is that the musculoskeletal model is not strong enough.

To prevent the fast target from failing, it is possible to add a number of reserve actuators to a model in order to make up for strength deficiencies in muscles. The reserve actuators have very low strength (or optimal force) and so require very high excitations to apply substantial load to the model, and as such their employment is highly penalized.

The final step in the CMC algorithm is to use the computed controls to conduct a standard forward dynamic simulation, advancing forward in time by T.

These steps—computing the desired accelerations, static optimization, and forward dynamic simulation—are repeated until time is advanced to the end of the desired movement interval.

3.1.4   Forward Dynamics Tool

In order to function the Forward Dynamics Tool requires controls for the model's actuators, which are used to drive forward dynamic simulations.

The output of the tool is the kinematic behavior of the model due to the input files provided.

It is important to notice that any actuator, including muscles, requires controls in order to provide active force during a Forward Dynamics simulation, otherwise it will only exert passive forces, granted they are featured in the actuators' characteristics, dependent on the actuator's states (length and lengthening speed).

The force provided by actuators is equal to the product of the control value supplied to it and its own optimal force parameter.

Like the CMCTool, the Forward Dynamics Tool is accessible from the Tool tab in the OpenSim GUI, and once selected its own control window appears.
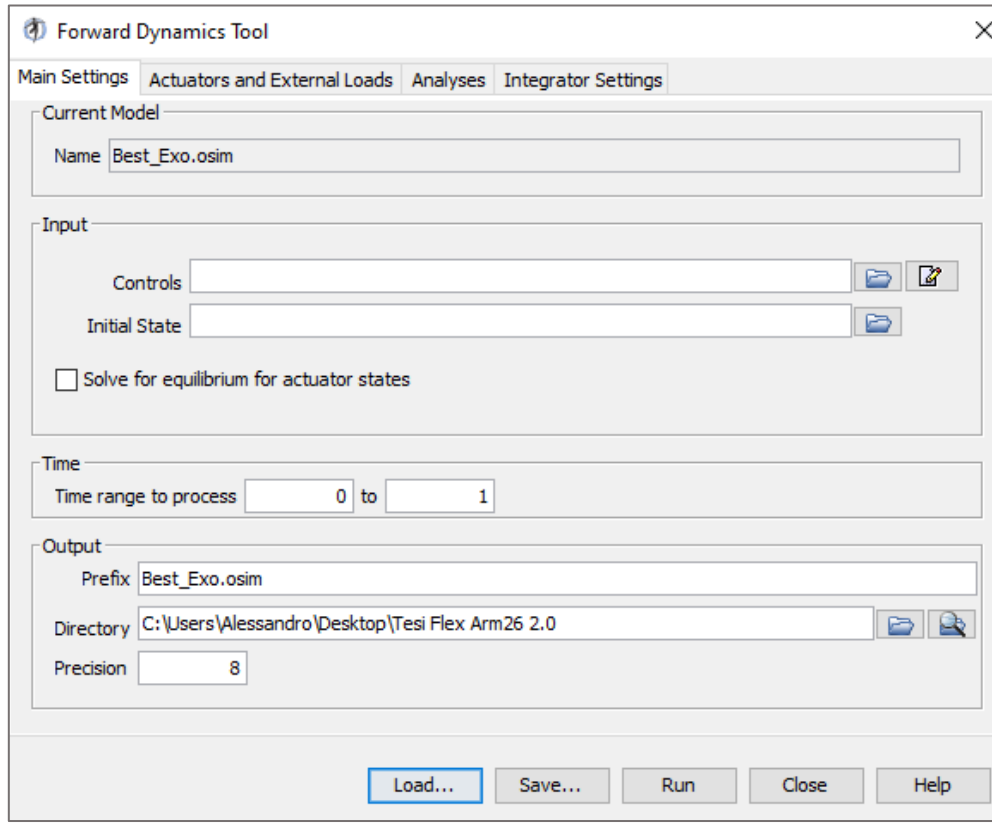
Figure 3.5: FWDTool Main Settings pane.

- The Main Settings pane (Figure 3.5) specifies parameters related to the controls and states that will be input into the model, the time range for the simulation, and the output of the results.

- The Actuators and External Loads pane and the Integrator Settings pane work exactly as for the Computed Muscle Control Tool explained in the previous paragraph.

- The Analyses pane (Figure 3.6) allows to investigate multiple model's variables during the simulation, all accessible by clicking the *Add* button. Once selected the desired ones, after the simulation, specific output files containing the desired data will be generated along with the standard ones.
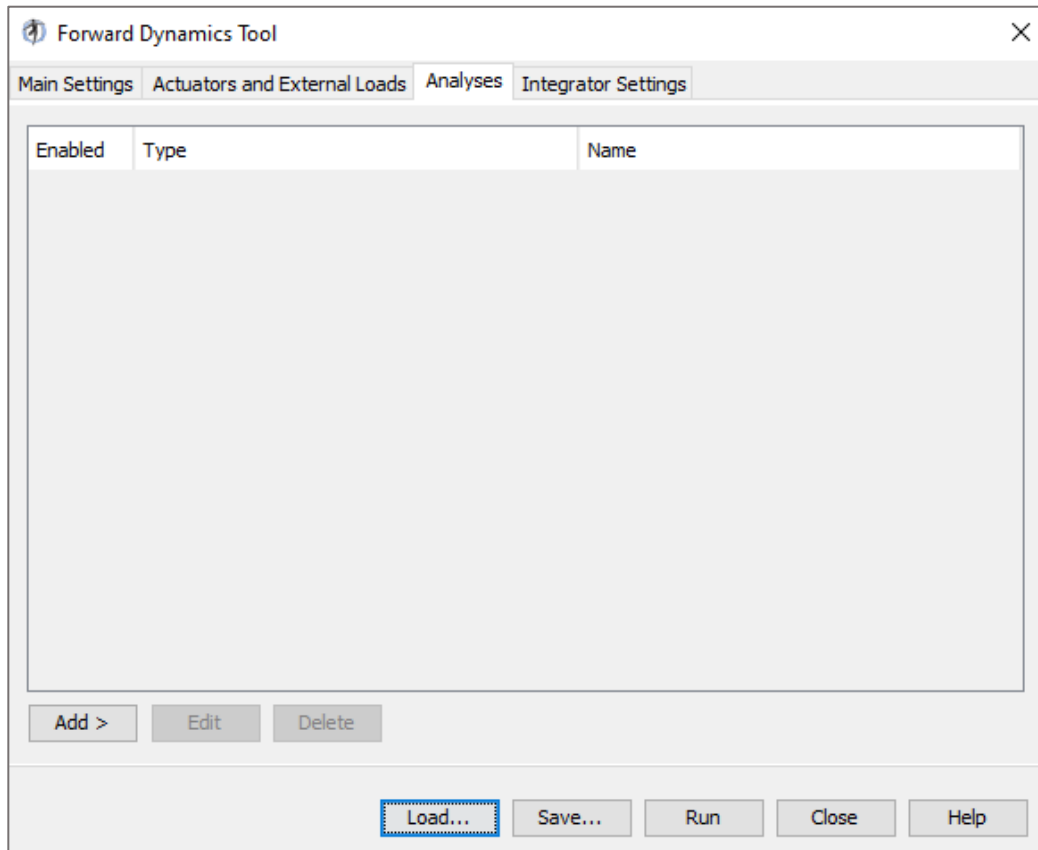
Figure 3.6: FWDTool analyses pane.

As stated previously, the Forward Dynamics requires as input the forces that drive the model to perform the motion of interest. The tool solves the Newton's second law, for a multibody system, to find the accelerations of the body's coordinates with the following:

$$\ddot{q} = [M(q)]^{-1}\{\tau + C(q, \dot{q}) + G(q) + F\} \qquad (3.5)$$

Where:

- $q, \dot{q}, \ddot{q}$ are the vectors of the generalized positions, velocity and acceleration respectively;

- $[M(q)]^{-1}$ is the inverse of the mass matrix;

- τ is the vector of the joint torques;

- $C(q, \dot{q})$ is the vector of the Coriolis and the centrifugal forces;

- $G(q)$ is the vector of the gravitational forces;

- F is the vector of other forces applied to the model;

Regarding muscles' forces acting on the system, they can be computed starting from their own muscular activations with the following equation:

$$\tau m = [R(q)]\, f(a, l, \dot{l}) \tag{3.6}$$

Where:

- τm is the vector of moments acting on the joints due to muscle forces;

- $R(q)$ is the vector of the moments arms;

- f are the muscles forces, which are functions of:

  - a muscle activations;

  - l, muscle lengths;

  - $\dot{l}$, speed of contraction of muscle fibers. This parameter depends on the muscle contraction dynamics (Λ) which has as variables the length and the activation level of the muscle (l and a) and the position and speed of the articulation ($q\ and\ \dot{q}$) on which the muscle act.

$$\dot{l} = \Lambda(a, l, q, \dot{q}) \tag{3.7}$$

In quite a similar way, contributes of any given actuator can be calculated, however their force can be a function of other parameters (for instance it could only depend on their activation values).

Finally, musculoskeletal dynamics are ruled by the following equation:

$$\dot{a} = A(a, x) \tag{3.8}$$

Where the activation rate of the actuators ($\dot{a}$) depends on their activation dynamics (A), where x stands for the model controls (i.e activation values).

3.2   Project Development

The aim of this thesis is to optimize the position of the anchor points of a set of cables to actuate an upper limb exosuit.

In order to do so, during the first stages of the project, different musculoskeletal models representing the human body were studied and analyzed, to understand how they would behave in specific conditions and to determine whether or not they could be deemed reliable in simulating the actual physiological human musculoskeletal behaviour. Then, once assessed the models' limits and capabilities, the most suitable for our analysis was selected.

The exosuit's cable routing optimization was performed by means of the minimization of selected cost functions. Different cable-routing designs were therefore built and analyzed in the simulated environment as it will be described in the following sections. The best design was selected according to the optimization cost functions.

Finally, further simulation studies were conducted on the best design to assess how it would affect the model's behaviour in terms of metabolic cost and reaction forces at the joints.

All the steps of the project development will be thoroughly analyzed in the next paragraphs.

3.2.1 Musculoskeletal Model Selection

The first steps in the project development were: i) finding a suitable musculoskeletal model for the analysis, and ii) defining the trajectories of the movements to perform.

As for the model, the ideal one should have all the degrees of freedom of the real human arm, in particular it should be able to perform elbow flexion and extension along with forearm pronation and supination, and a feasible set of muscles which would behave as closely as possible as the actual muscles, mimicking both their active and passive contribution during any given movement.

While searching for a model that featuring these characteristics, different ones were studied and analyzed.

3.2.1.1 MoBL-ARMS

The first model tested was the MoBL-ARMS [20]–[29] (shown in Figure 3.7).
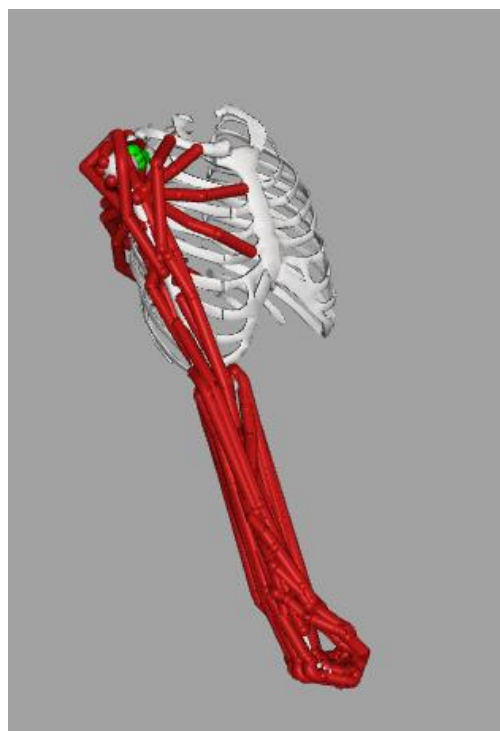
Figure 3.7: MoBL-ARM rendering

This model has all 7 degrees of freedom of the arm implemented (shoulder adduction and abduction, shoulder elevation, shoulder rotation, elbow flexion and extension, forearm pronation and supination, wrist flexion and extension, wrist lateral deviation) as long as a complex musculoskeletal system, featuring 50 muscles modeled as *Millard2012EquiilibriumMuscle* actuators (described in [26]) and also a set of ligaments.

While its complexity makes this model basically a complete representation of the upper limb, it also makes its computationally load extremely heavy, negatively affecting simulations' running times.

To solve this problem, at first the model was simplified by removing most of its muscles and keeping only those which contribution was most relevant to perform movements of the elbow (flexion and extension) and the forearm (pronation and supination), specifically have been kept:

- Biceps brachii,
- Brachialis
- Brachioradialis
- Triceps brachii
- Anconeus
- Triceps brachii
- Anconeus
- Supinator

However, the results obtained in further studies were not deemed reliable, as the model didn't behave in a realistic way during the simulations (i.e. muscles' passive forces would trigger sudden movements or cause the model to assume unrealistic configurations), and since also testing the model without any modification led to the same results, the Mobl-ARM has been discarded.

Another model tested was the DAS3 [30] (Figure 3.8).
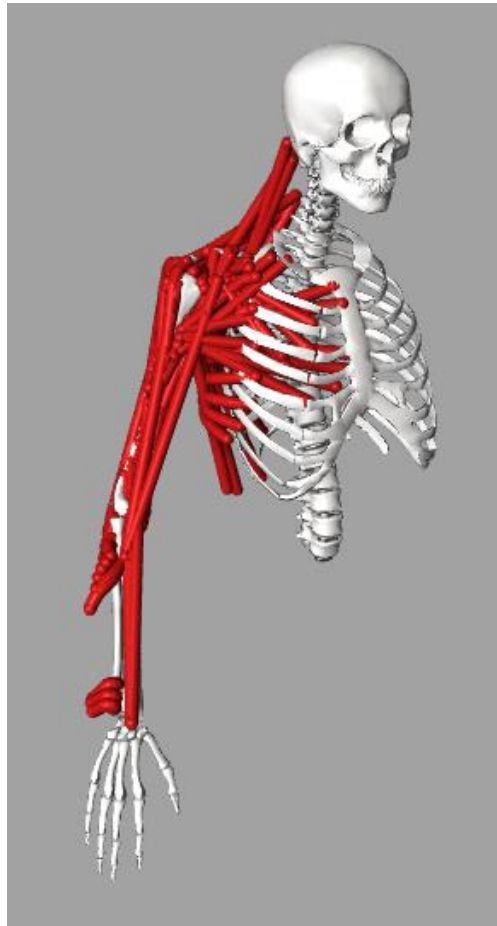
Figure 3.8: DAS3 rendering

This model features 11 degrees of freedom: most of them are related to the shoulder, while for the arm there are both elbow flexion and extension and forearm pronation and supination, although the latter doesn't seem to actually work since changing the coordinate's values in the OpenSim GUI doesn't affect the model at all.

Regarding the musculoskeletal system, the model has 29 groups of *Schutte1993Muscle_Deprecated* actuators to represent muscles of both the arm and the right side of the upper thorax. At first glance however, it is apparent that there may be some errors with the building process of the model since most of the muscles' insertion

points on the model's bones are affected by an offset and do not attach on the bodies' surface.

A similar procedure to the one explained in the previous paragraph has been followed when testing this model, and unfortunately also this model has been discarded as it presented the same reliability problems as the MoBL-ARM.

3.2.1.3   Arm26

As both the models previously tested failed and no others have been found, in the end has been decided to use the model Arm26 (Figure 3.9) to develop the project.
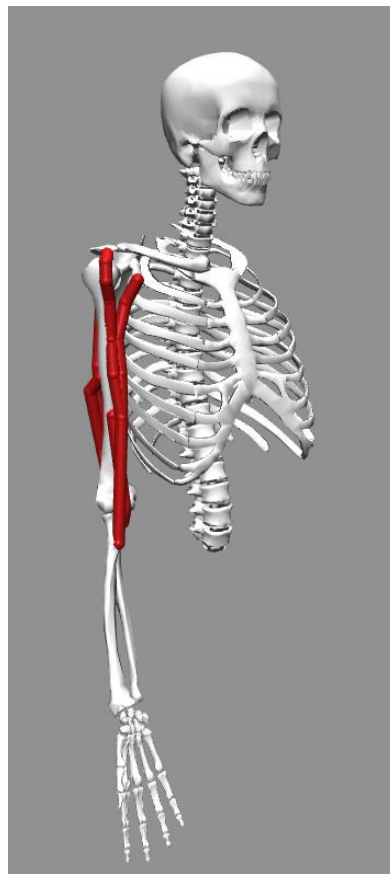
Figure 3.9: Arm26 rendering

This model, which is provided directly by OpenSim and made available with the program itself, features the complete upper right side of the human skeletal system along with 6 of the main upper limb muscles being: TRIlong, TRIlat, TRImed representing the triceps brachii; BIClong, BICshort representing the biceps brachii; BRA standing for the brachialis.

All the muscles are implemented as a specific class of actuator implemented by OpenSim called Thelen2003Muscle, which implements muscles as Hill-type musculo-tendon actuators (Figure 3.10) defined by their actuation and fiber length.
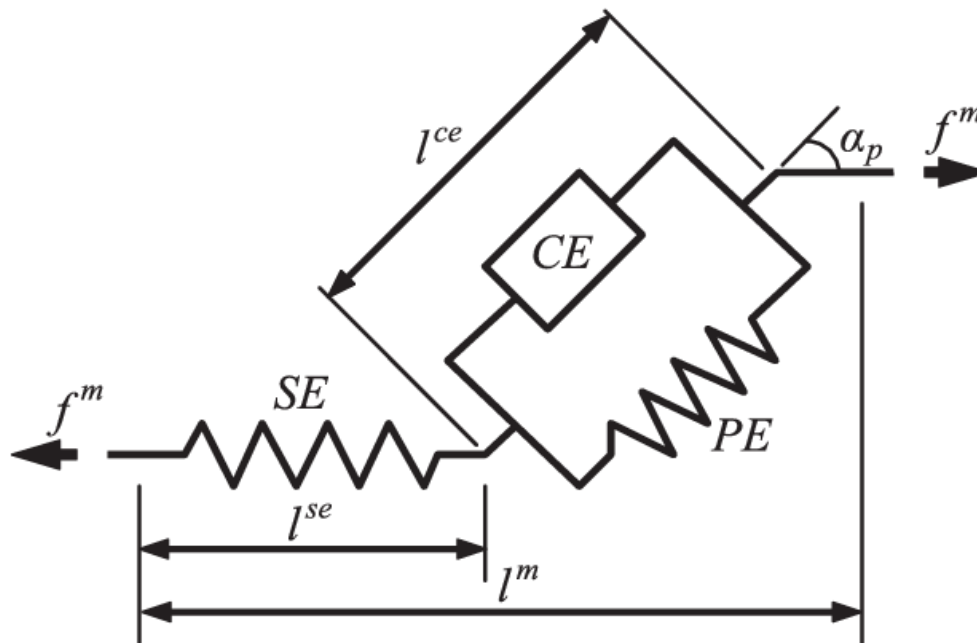
Figure 3.10: Hill-type musculo-tendon model. SE = series element, PE = parallel element, CE = contractile element

Regarding the skeletal system model, every bone is configured in order to feature properties such as mass and inertial values similar to the actual human ones, although some simplifications were introduced: the bones making up the whole torso-neck-head area were implemented as one single body, and so have been the ones of the forearm and hand area.

The model features 2 joints, one at the shoulder and the other at the elbow.

Both are pin joints allowing the rotation on the frontal axis only (see Figure 3.11), but are characterized by different ranges of motions: the shoulder joint (r_shoulder_elv) can rotate between -90° and 180°, with 0° being the position show in Figure 3.9, while the elbow joint (r_elbow_flex) can rotate between 0° and 130° (in Figure 3.9 it's at 20°).
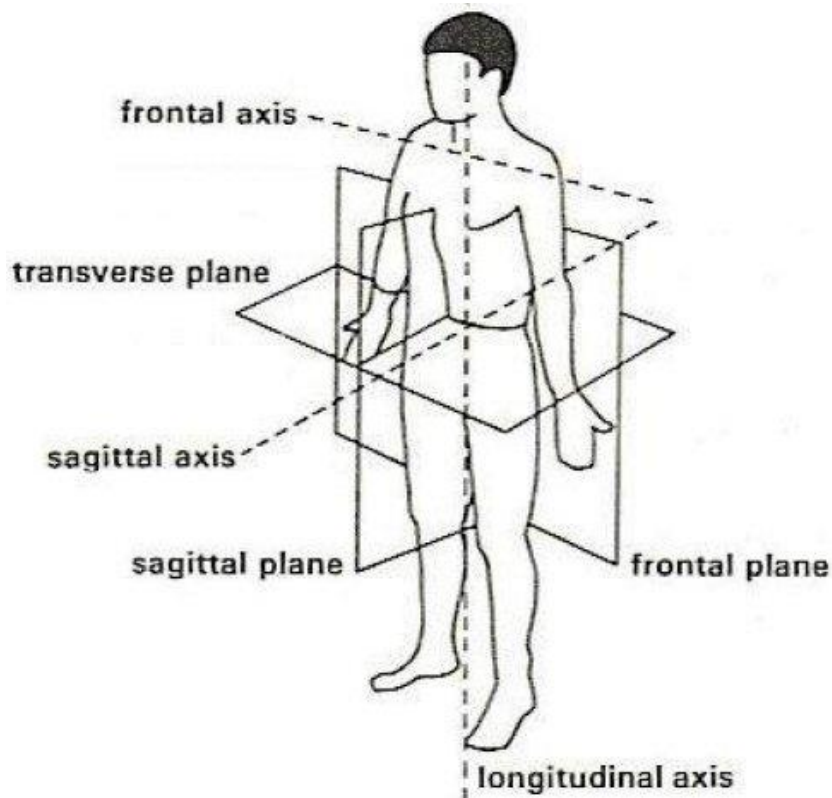
Figure 3.11: axes and planes of the human body

The Arm26 however presents some limitations: its simplicity, although useful to drastically lower computational loads and thus cutting simulations' running times, makes it an approximation, at best, of the real human body, and can't be considered completely reliable.

3.2.2 Movement definition

Given the chosen model's limits, it's been established that only cable-routing designs for the actuation of the elbow flexion and extension would be investigated. The first step in this process was to study the model itself, with no cables attached, while performing said movements.

At first, elbow flexion has been studied.

As stated before, the range of motion of the elbow flexion for the Arm26 is between 0° and 130°. Due to the passive properties of the muscles, the equilibrium point of the elbow was not at 0° and, therefore, the first step was to find the equilibrium point of the joint, to be used as the starting position of any movement to be tested.

Using the Forward Dynamics Tool, a simulation lasting 10 seconds has been run, starting from the model's default configuration (i.e. elbow joint and locking the shoulder joint at 0°) and without providing any kind of controls to any of the model's muscles. This way, any of the model's movements would have been due to muscles' passive forces only, which would rearrange the joint's coordinates to equilibrate gravity.

Then, with the equilibrium point known, following a protocol similar to the one used in the study presented in [31], the elbow flexion trajectory (Figure 3.12) has been determined to cover the range between 20° and 120° in a period of time of 7 seconds. Angular velocity and acceleration were computed as well.
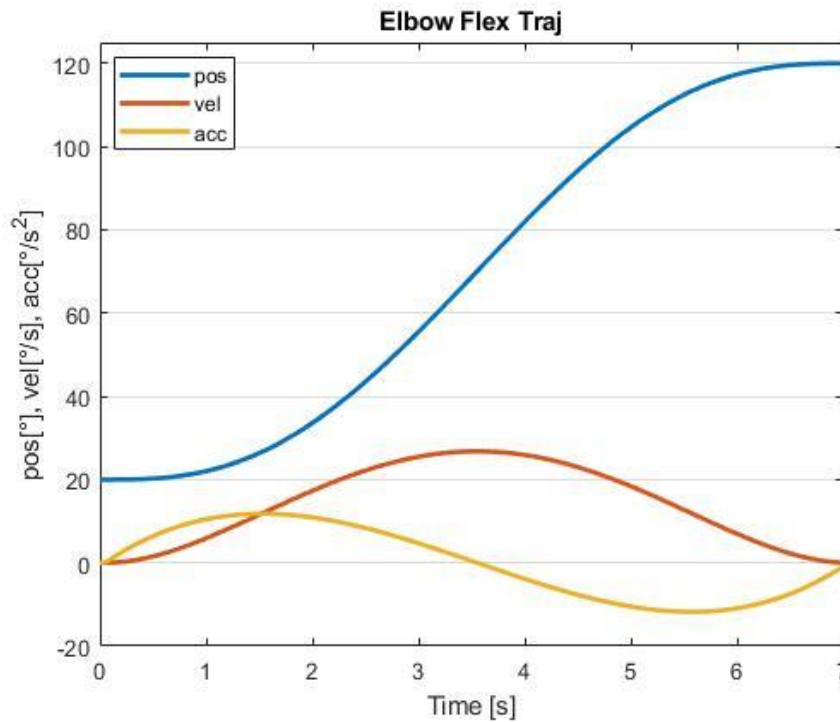
Figure 3.12: Elbow flexion trajectory (pos) complete with angular velocity (vel) and acceleration (acc)

The trajectory has been defined using the *quintcpolytraj()* function available in MATLAB and saved in a .sto file manageable by OpenSim, in order to be used later as input for other tools.

A similar procedure has been used to study the elbow extension movement.

The model was set with a starting position having the arm raised (r_shoulder_elv at 160°) and the elbow fully flexed (r_elbow_flex at 130°).

However, given the results obtained for this particular configuration, the model has not been deemed reliable in this kind of scenario, and as such studies regarding the elbow extension movement have not been possible.

3.2.3 Cables Configuration

In the pursue of finding the best configuration for the exosuit's cables, many different designs have been built and then analyzed.

The Arm26 model was customized in MATLAB, using the libraries made available by OpenSim, with the addition of PathActuators, that were used to represent the cables.

PathActuators can apply tension along their geometry path, which is the path they can move onto, behaving just like tensionable ropes.

To simulate different cables configurations, the actuators' anchor points, which are the points at which they are attached to the bodies, have been moved in different position following a specific pattern which will be described hereafter.

First, as shown in Figure 3.13, two circumferences have been defined around the model's arm and the forearm:

- The arm's circumference has been set to a distance equal to 1/4 of the arm's length from the shoulder joint.

- The forearm's circumference has been set to a distance equal to 1/8 of the forearm's length from the elbow joint.
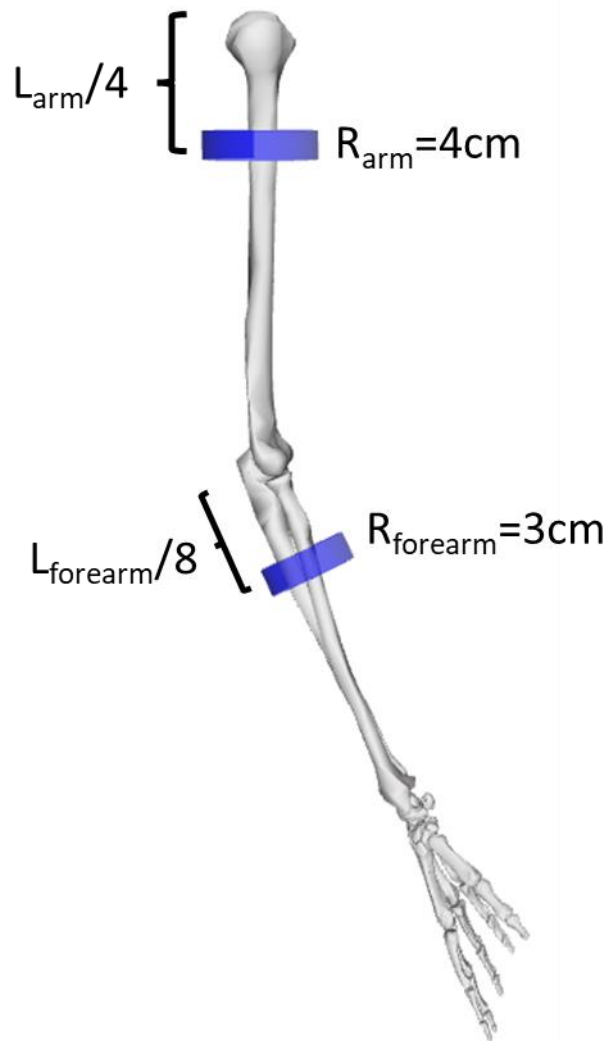
Figure 3.13: Circumferences (in blue)
placement for the cables' anchor points.

Then, on the front half of those circumferences anchor points spaced 45° between themselves have been defined, for a total of 5 points for limb.

These points act as insertion points for the cables, and have been used to define different cables' routes. Specifically, single and double cables configurations have been defined (shown in Figure 3.14). In order to prevent excessive influence on forearm pronation and supination, all the configurations have been built by trying to either center the cable along the arm's longitudinal axis (in case of the single cable

configuration only), or by having the cables' paths specular to each other with respect
to the sagittal plane centered on the arm's longitudinal axis.
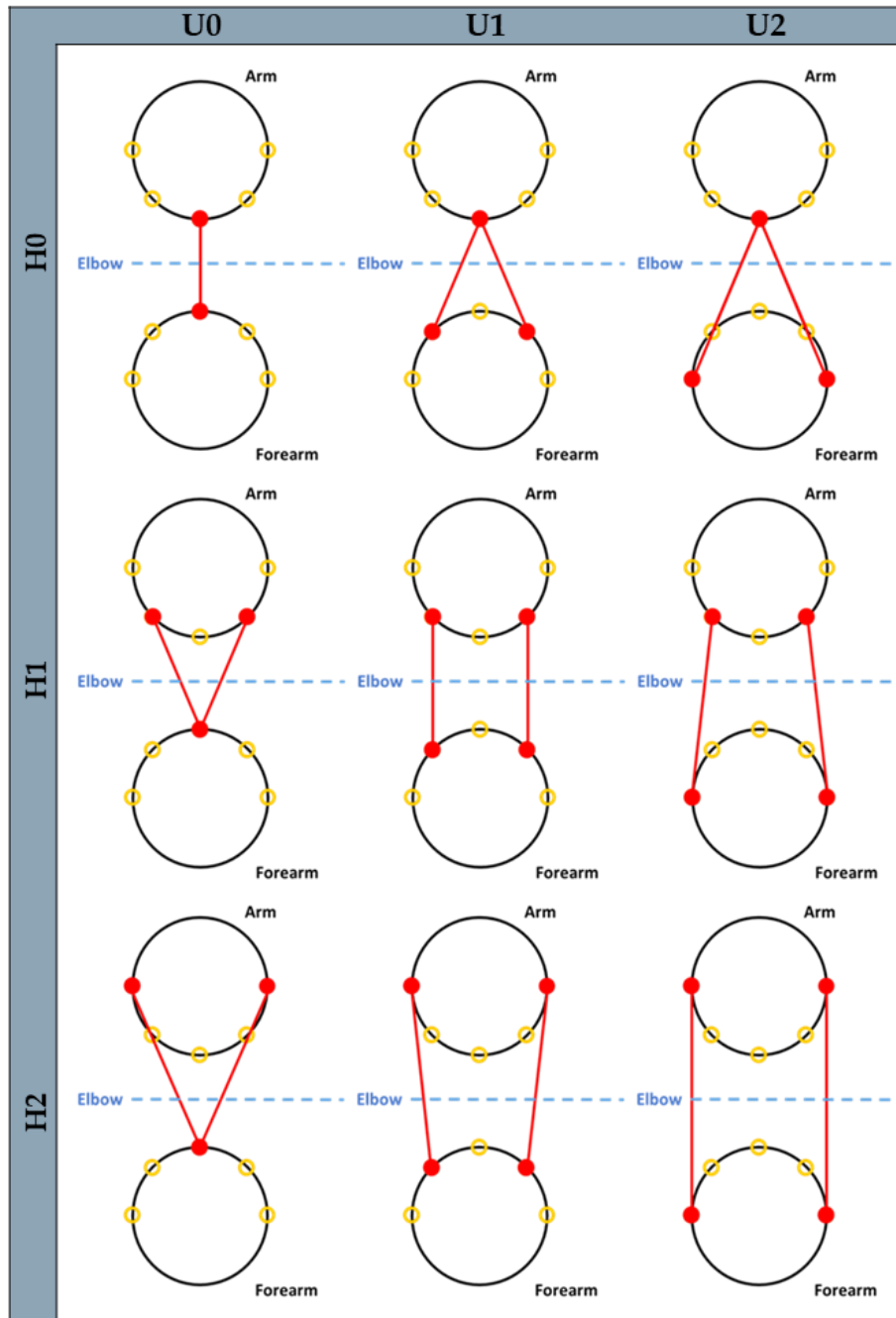
Figure 3.14: All configurations built and analyzed. In black are the
circumferences around arm and forearm; in yellow are the cables' anchor
points; in red are the cables.

Finally, using the CMCTool, the controls' set for each configuration's cables were computed. These simulations have been run keeping the model's muscles deactivated (Figure 3.15) so that the only the cables could be used to perform the movement established by the trajectory file.

```
<!--XML file (.xml) containing the forces applied to the model as ExternalLoads.-->
<external_loads_file />
<!--List of individual Actuators by individual or user-defined group name  to be excluded from CMC's control.-->
<actuators_to_exclude> TRIlong TRIlat TRImed BIClong BICshort BRA</actuators_to_exclude>
<!--Motion (.mot) or storage (.sto) file containing the desired point trajectories.-->
<desired_points_file />
```

Figure 3.15: CMCTool's setup file extract. The muscles have been excluded and cannot be activated during the simulation.

Regarding the movements studied, elbow flexion in a range between 20° and 120° over 1,3,5 and 7 seconds has been selected. The trajectory for each movement has been defined following the same procedure explained in 3.2.2.

3.2.4 Optimal Cable Routing Selection

The next step in the project development was to determine which one among all the configurations would be the optimal one.

Since the optimization of the device is based on portability, the ideal design would feature a single motor, which should be as small as possible and with the lowest power consumption possible.

These requirements led to choose 3 main parameters based on which each configuration was evaluated:

- Maximum tension reached by the cables: the lower this value, the less powerful and thus the less cumbersome the motor can be, providing advantages on the portability of the device.

- Average tension of the cables during the whole movement: this value would provide important information regarding motor's power consumption used to actuate the device. Generally, smaller motors consume less power.

- Similarity between the cables' tensions (in case of two-cables configuration): since the idea was to develop a single motor system, it is important that the tensions produced by the two cables during the movement are similar. Moreover, considering the configuration almost symmetrical applying different tensions on the two cables would generate torques on the forearm axis that would affect the prono-supination. By making the two tensions similar, it is presumed to avoid this effect.

Based on these 3 requirements, an optimization parameter has been defined as:

$$Opt_i = \frac{T_i^{max}}{\max(T_i^{max})} * 0.4 + \frac{T_i^{avg}}{\max(T_i^{avg})} * 0.3 \\ + \frac{\Delta T_i^{max}}{\max(\Delta T_i^{max})} * 0.3 \tag{3.9}$$

Where:

- T^{max} stands for the maximum value of the sum of the cables' tensions

- T^{avg} stands for the average value of the sum of the cables' tensions

- ΔT^{max} stands for the maximum difference in value between the cables' tension

Each term of the cost function was normalized to the maximum value achieved among configurations. In case of the single cable configuration, the third value representing the difference in tension between the cables has been set to 0, and the weights of the remaining two has been set to 0.5 for both.

For a configuration to be deemed better than another, its *Opt* value would have to be lower, with the absolute best configuration bearing the one closest to 0.

3.2.5 Assistive Device Evaluation

Once selected the design deemed best among all the possible configurations (following the criteria explained in the previous section), and obtained its cables' controls, its efficiency in assisting the movement was analyzed.

Four main aspects were considered to assess the device's efficacy with different levels of support, with respect to the case in which the movement is performed without assistance, using the tools provided by OpenSim:

- Reduction in muscles' activation: the lower the muscles would get involved to perform the elbow flexion, the more the device would be effective in assisting the user to perform the movement.

- Muscles' passive forces analysis: it is important to be sure that the device's action would cause the muscles to be compliant to its action, without responding in potentially harmful ways.

- Metabolic cost reduction: along with muscles' activation, the less the muscles consume in terms of metabolic costs, the better the device's capability to relieve the load from the user.

- Joint reaction analysis: since by pulling the cables new external forces are introduced and applied to the body, it is fundamental to compute the internal forces at the elbow joint and make sure that they would not cause excessive discomfort or potential harm to the user.

All these studies have been performed actuating the device with 100%, 75% and 50% of the controls computed by the CMCTool to perform elbow flexion from 20° to 120° in 1 and 7 seconds.

This was done in order to evaluate the effects of different assistance levels.

The first 3 aspects (reduction in muscles' activation, muscles' passive forces analysis and metabolic cost reduction) were evaluated running the Computed Muscle Control Tool on the best exosuit's model.

In the CMCTool, it is possible to impose a priori actuators' activation by customizing the ControlConstaints file, which is used by the CMC Setup file to determine the activation limits of the model's actuators.

For these evaluations, the cables' actuation has been prescribed as a percentage of the one computed by the first CMCTool run during the exosuit's building phase (paragraph 3.2.2).

However, in order to customize the ControlConstraints file, the .sto file outputted by the CMCTool containing the actuation data had to be converted in a .xml file.

This file conversion was done using the Forward Dynamics Tool: the actuation .sto file has been uploaded as the *Controls* input, then by clicking on the customization icon a pop-up window appeared (Figure 3.16).

From this window, the cables' boxes have been checked and then by pressing *OK* another window appeared from where the controls are generated as .xml files and can be saved as such.

It's important to notice that the Forward Dynamics Tool has not been actually run.

The data contained in the .sto and the .xml files is identical, the only difference being the format in which it is stored.
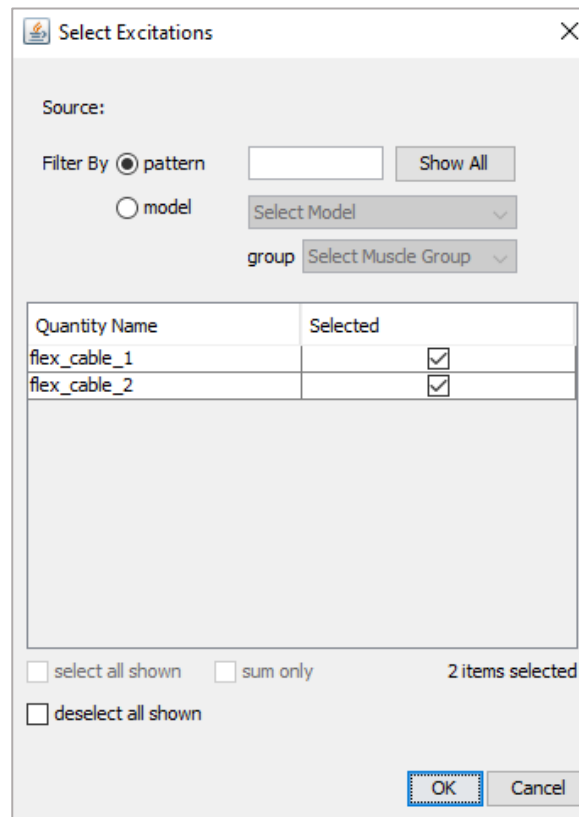
Figure 3.16: Excitation customization pop-up window. The cables' excitations have been selected to be converted from .sto files to .xml files.

In both cases, for each time instant, the activation of an actuator, which are the cables in this specific case, is defined.

This conversion was necessary since the ControlConstraints file itself is in a .xml format, so once the actuation files have been converted, the ControlConstraints file used by the CMC_Setup file could be updated to not only feature the model's muscles' activation boundaries, but also to impose the desired activation in each time instant of the cables. This is obtained by adding new fields to file regarding the excitation of the cables (flex_cable_1 and flex_cable_2 in Figure 3.17), and by simply copying and

pasting the data under the <x_nodes> field of the previously generated .xml file in the <min_nodes> and <max_nodes> fields of the current one.

```xml
1    <?xml version="1.0" encoding="UTF-8"?>
2    <OpenSimDocument Version="20302">
3        <ControlSet name="Control Set">
4        <defaults>
5            <ControlLinear name="default">
18       </defaults>
19       <objects>
20           <ControlLinear name="TRIlong.excitation">
33           <ControlLinear name="TRIlat.excitation">
46           <ControlLinear name="TRImed.excitation">
59           <ControlLinear name="BIClong.excitation">
72           <ControlLinear name="BICshort.excitation">
85           <ControlLinear name="BRA.excitation">
86               <is_model_control> true </is_model_control>
87               <extrapolate> true </extrapolate>
88               <default_min>        0.02000000 </default_min>
89               <default_max>        1.00000000 </default_max>
90               <filter_on> false </filter_on>
91               <use_steps> true </use_steps>
92               <x_nodes/>
93               <min_nodes/>
94               <max_nodes/>
95               <kp>      100.00000000 </kp>
96               <kv>       20.00000000 </kv>
97           </ControlLinear>
98
99           <ControlLinear name="flex_cable_1.excitation">
100          <ControlLinear name="flex_cable_2.excitation">
101              <is_model_control>true</is_model_control>
102              <extrapolate>true</extrapolate>
103              <default_min>0.02</default_min>
104              <default_max>1</default_max>
105              <filter_on>false</filter_on>
106              <use_steps>false</use_steps>
107              <x_nodes>
157              <min_nodes>
177              <max_nodes>
157              <kp>100</kp>
158              <kv>20</kv>
159          </ControlLinear>
170
171      </objects>
172          <groups/>
173      </ControlSet>
174  </OpenSimDocument>
175
```

Figure 3.17: .xml file containing the actuators'
activation values created from the original .sto file.

Also, some other changes to the Setup file and the model's file have been made specifically to perform the metabolic costs analysis.

In the Setup file, an object to the <AnalysysSet> field of the type ProbeReporter called MetabolicsReporter has been added, this way the metabolics data would be made available at the end of a simulation in the output data.

In the model's file on the other hand, under the <ProbeSet> field, an object type <Umberger2010MuscleMetabolicsProbe> has been added in order to keep track and save the muscles metabolic consumption during any simulation.

Lastly, while in the first CMC simulation the model's muscles were excluded from the actuation computation, effectively keeping them deactivated during the whole simulation, in these simulations no such thing has been done as the objective was to analyze how the cables' action would affect the muscles' behaviour.

Once all this necessary setting process has been done, the simulations have been performed and their outputs saved.

Regarding the joint reaction analysis, it was performed using the Forward Dynamics Tool.

This tool allows to add multiple analysis to be performed during a simulation.

Once selected from the Tool bar in the OpenSim GUI, in the Analysis tab, the JointReaction analysis can be added by clicking Add and selecting it.

After that, the simulations have been run by providing as the Controls input the output controls files generated by the CMCs run for the previous studies.

The way the JointReaction analysis works, it returns internal forces and moments applied on the *child* body of the joint studied.

In this specific case, as the elbow was the joint of interest, all the forces and moments returned were the ones applied on the ulna, since in the elbow joint the humerus is defined as the *parent* body and the ulna as the *child* one.

3.2.6 Device Sizing

The last step in the project development was to dimension some parts of the first device.

The concept is to use a motor which would make a spool rotate in order to wrap the cables around it, effectively pulling the forearm towards the arm and thus actuating the elbow joint to perform arm flexion (Figure 3.18).
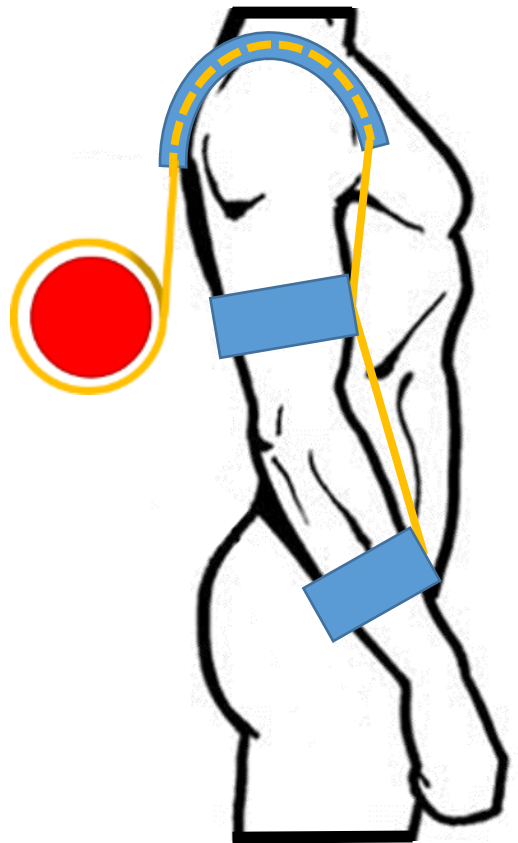
Figure 3.18: Device's scheme. In blue are the exosuit's garments, in yellow the cables, in red the spool (actuated by the motor) around which the cables would wrap around.

At this stage, the casing of the device, as well as the controlling electronics and the actual wearable garments or the cables' path along the user's body have not been investigated.

At the time being, a motor and a reductor have been already provided.

The motor is the EC flat produced by Maxon Motor, shown in Figure 3.19, which is a brushless 70 W motor with a diameter of 42.8 mm able to produce up to 128 mNm torques, weighting 140 g.

Figure 3.19: EC flat Maxon motor.

The reductor is the GP 42 (Figure 3.20), produced by Maxon Motor. This reductor has a diameter of 42 mm, has a reduction parameter of 156:1 and weights 460g.

The reductor, multiplies the motor's torque by its reduction factor, at the cost of the output speed which is equal to the motor's one divided by the same reduction factor.

Figure 3.20: GP 42 Maxon reductor.

With both components also their data sheets have been provided, which held all the necessary information regarding the component's characteristics to design the spool.

In order to determine the spool's dimensions, information on the cables' tension needed to pull the forearm to perform the elbow flexion and their lengthening speed was required.

To acquire the necessary data, further simulations have been made, similar to the ones already done in previous studies, with the only difference being the duration of the movement.

Indeed, in real life, the elbow flexion in hand-to-mouth movements takes about 1 second. Since this device is intended to be used in everyday life scenarios, the data used to determine the sizes of the necessary components has been obtained by running simulations in which the elbow flexion (still between 20° and 120°) was performed in 1 second. This movement indeed requires the strictest conditions to be performed, as the limb's velocity is higher than in the other simulations.

Then, using the CMCTool with the muscles kept deactivated, the controls for the cables arranged in the best configuration found have been computed, along with the cables' length during the movement. At this point, the maximum value of tension has been calculated as the maximum of the sum of the tensions of both cables, while the maximum lengthening speed has been found as the maximum value of the derivative of the function representing the average length of the two cables over time, calculated using the *polyfit*, *polyval* and *polyder* functions in MATLAB.

Finally, with all the necessary data computed, it has been possible to calculate the spool's radius length range according to both performance requirements and hardware limitations using the following:

$$\frac{60 * v_{Max}^{Cables}}{2 * \pi * rpm_{Max}^{Red}} < R_{Spool} < \frac{C_{Max}^{Red}}{T^{Cables}} \tag{3.10}$$

Where:

- v_{Max}^{Cables} stands for the cables' maximum lengthening speed
- rpm_{Max}^{Red} stands for the reductor's maximum rotation velocity, computed as the motor's maximum rotation velocity (31.15 rpm, obtained from datasheet) times the reductor's reduction factor (156, obtained from datasheet)
- R_{Spool} stands for the spool's radius
- C_{Max}^{Red} is the maximum torque that the reductor can exercise (15 N), obtained from its datasheet
- T^{Cables} is the cables' maximum tension, computed as the maximum of the sum of both cables' tension

4. Chapter four: Results

In this section, the results of all the studies conducted and outlined in the previous chapter are presented.

The results were obtained from simulations run using the OpenSim Arm26 model, in which the elbow joint was set to follow a specified trajectory in order to perform an elbow flexion movement.

The tools involved in these studies where the CMCTool and the FDTool.

In order, the results presented will include the following sections:

- Best cables' configuration
- Effects of cables' action on muscular activation
- Effects of cables' action on muscular passive forces
- Effects of cables' action on muscular metabolic costs
- Effects of cables' action on elbow's reaction forces

4.1   Best cables configuration

Executing the CMC tool and using the formula (3.9) explained in paragraph 3.2.4, to each configuration was assigned an *Opt* value calculated with data obtained from all the simulations performed. In these simulations, elbow flexion was performed covering and angle between 20° and 120° in 1, 3, 5 and 7 seconds.

The Opt values itself was computed as the sum of 3 components: i) *max_T*: stands for the maximum value of the sum of the cables' tensions, ii) *mean_T*: stands for the average value of the sum of the cables' tensions, iii) *delta_T*: stands for the maximum difference between the cables' tension. Each term of the cost function was normalized to the maximum value achieved among configurations and multiplied for a specific weight: 0.4 for *max_T*, 0.3 for *mean_T* and *delta_T* (with the only exception being the single cable configuration (U0H0), where the weights were adjusted to 0.5 for both *max_t* and *mean_T*, while 0 for *delta_t*).

Results for each movement simulated are shown in Figure 4.1-4 (respectively representing results obtained from 1, 3, 5 and 7 seconds lasting movements).

The aim was to determine the best among all 9 configurations built, which was identified as the one having the lowest *Opt* value.
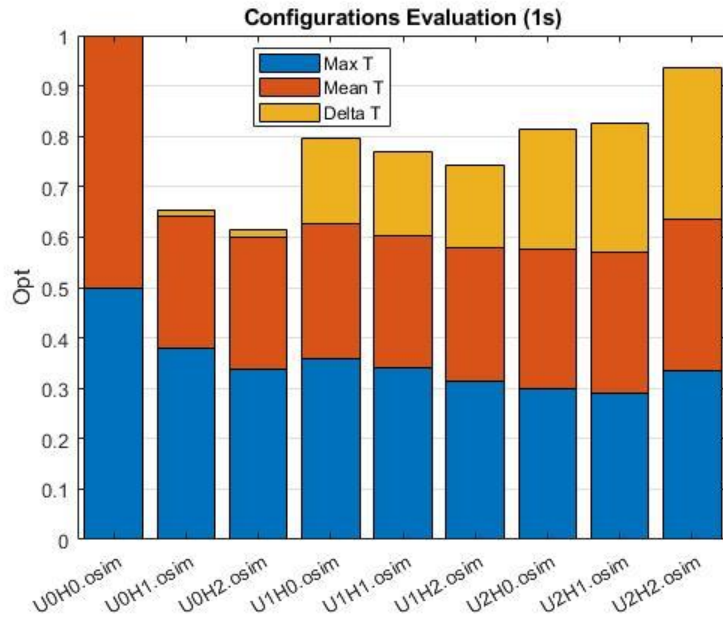
Figure 4.1: *Opt* values of each configuration (labeled by their U#H# tag, labeling explained in Figure 3.14) for 1s elbow flexion shown as the sum of *Max T* (blue), *Mean T* (orange) and *Delta T* (yellow).
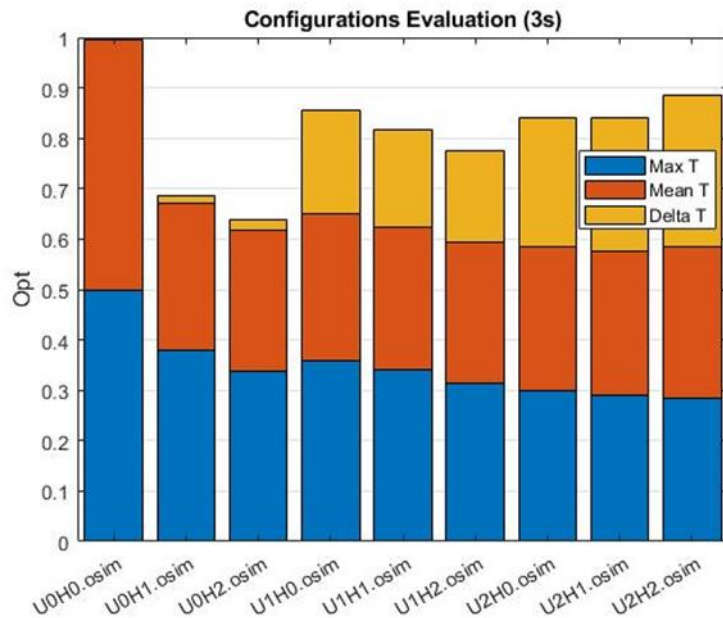
Figure 4.2: *Opt* values of each configuration (labeled by their U#H# tag, labeling explained in Figure 3.14) for 3s elbow flexion shown as the sum of *Max T* (blue), *Mean T* (orange) and *Delta T* (yellow)
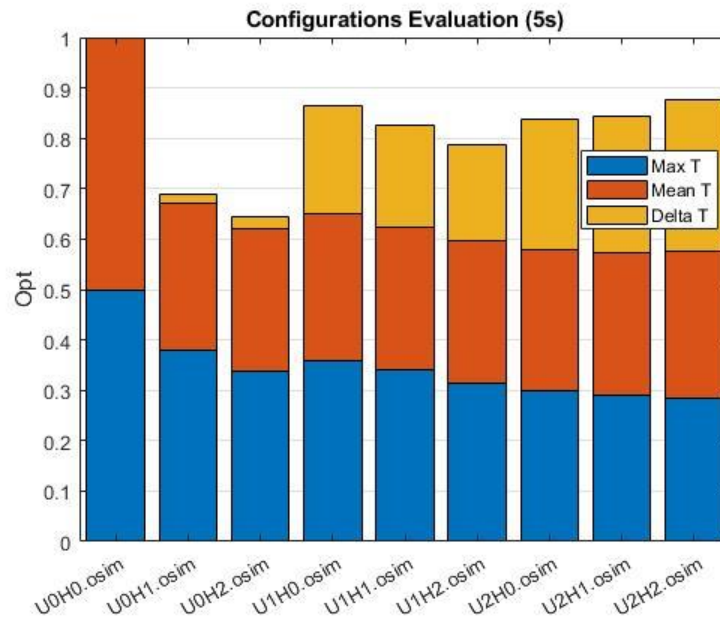
Figure 4.4: *Opt* values of each configuration (labeled by their U#H# tag, labeling explained in Figure 3.14) for 5s elbow flexion shown as the sum of *Max T*(blue), *Mean T* (orange) and *Delta T* (yellow)
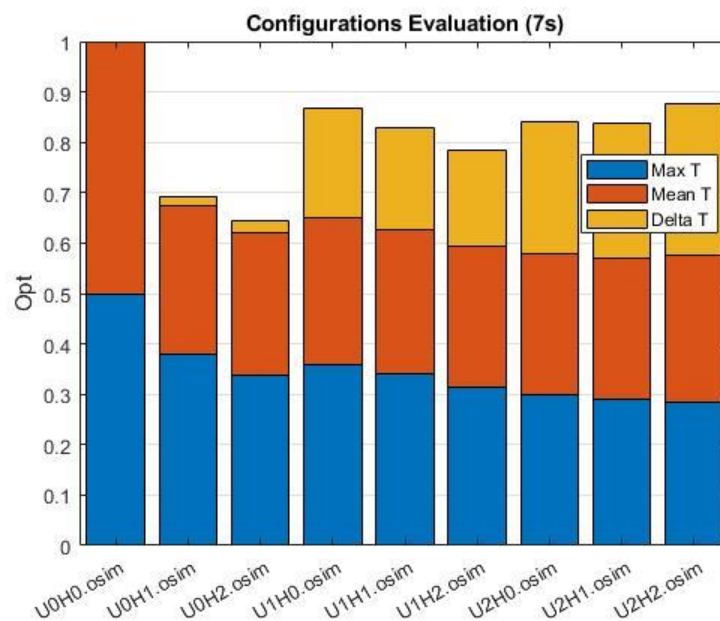
Figure 4.3: *Opt* values of each configuration (labeled by their U#H# tag, labeling explained in Figure 3.14) for 7s elbow flexion shown as the sum of *Max T*(blue), *Mean T* (orange) and *Delta T* (yellow)

Analyzing the results obtained, the model U0H2 (shown in Figure 4.5) was chosen as the best configuration and used in all further evaluations, as it bears the minimum *Opt* for all 4 simulations.

This model features 2 cables arranged in order to have a single anchor point centered on front of the forearm, and 2 other anchor points (one for each cable) placed on the sides of the arm.
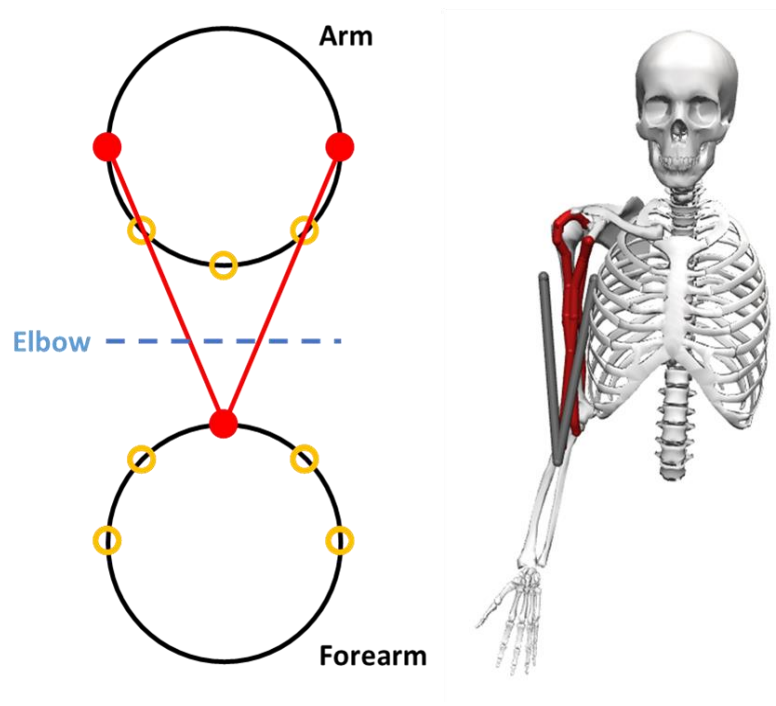
Figure 4.5: Model U021 scheme (on the left) and OpenSim rendering (on the right). In the rendering, the cables are in grey, while the model's own muscles are in red.

4.2 Biomechanical evaluations

Once selected the best cables configuration, its effects on the model behaviour were assessed by a series of tests.

While the choice of each test will be discussed in the following paragraphs, it's important to highlight that the device was evaluated (in a simulation environment) under different support conditions: the tensions applied to the cables were set to different percentages of the one required by the cables to autonomously (i.e. without any of the muscles' intervention) perform elbow flexion (Figure 4.6).

Specifically, 50%, 75% and 100% of the required cables' tensions have been provided, in order to simulate different levels of assistance.

Simulations have been run performing elbow flexion in 1s and 7s, as they were the two extremes of duration considered.
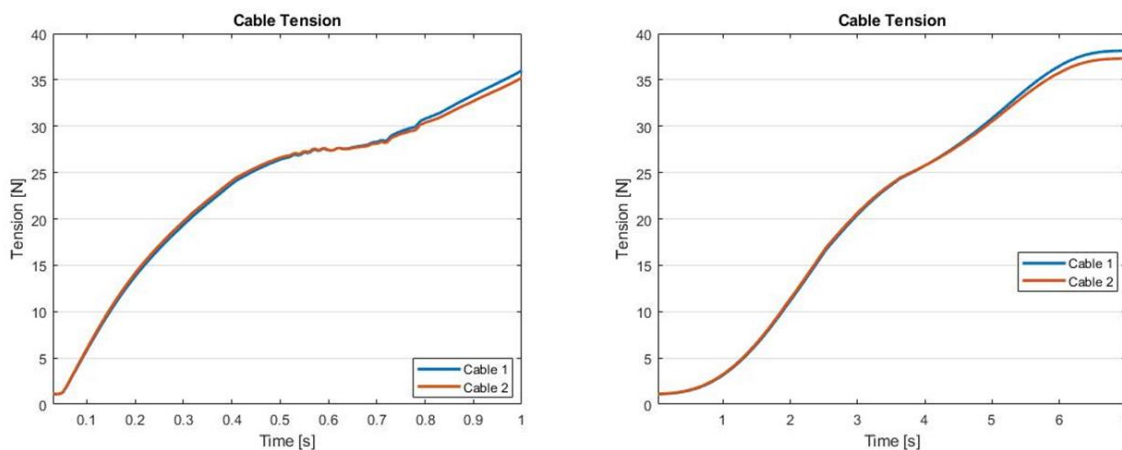
Figure 4.6: Cables' tension required to perform elbow flexion in 1s (left) and 7s (right) without muscles' intervention.

4.2.1 Muscle activation

The plots shown in this section (Figure 4.7-12) represent the model's muscles' activation while performing the elbow flexion movement.

The activation values are expressed as a percentage of the muscles' maximum possible force. Note that because of how muscles are defined in OpenSim, the minimum activation value for any muscle is set at 0.02.

In the graphs, the progression of the activation values over time while performing the elbow flexion movement in 1 and 7s are plotted.

Coupled with each graph, there is a bar plot representing the curves' integrals calculated for their respective time period, useful to better understand the quantity's changes for each different condition tested.

Values labeled as *Naked* refer to results obtained by running simulations in which the model performed elbow flexion without the cables' assistance, while values labeled as *@50%-75%-@100%* represent results obtained providing the corresponding assistance percentage through the cables.
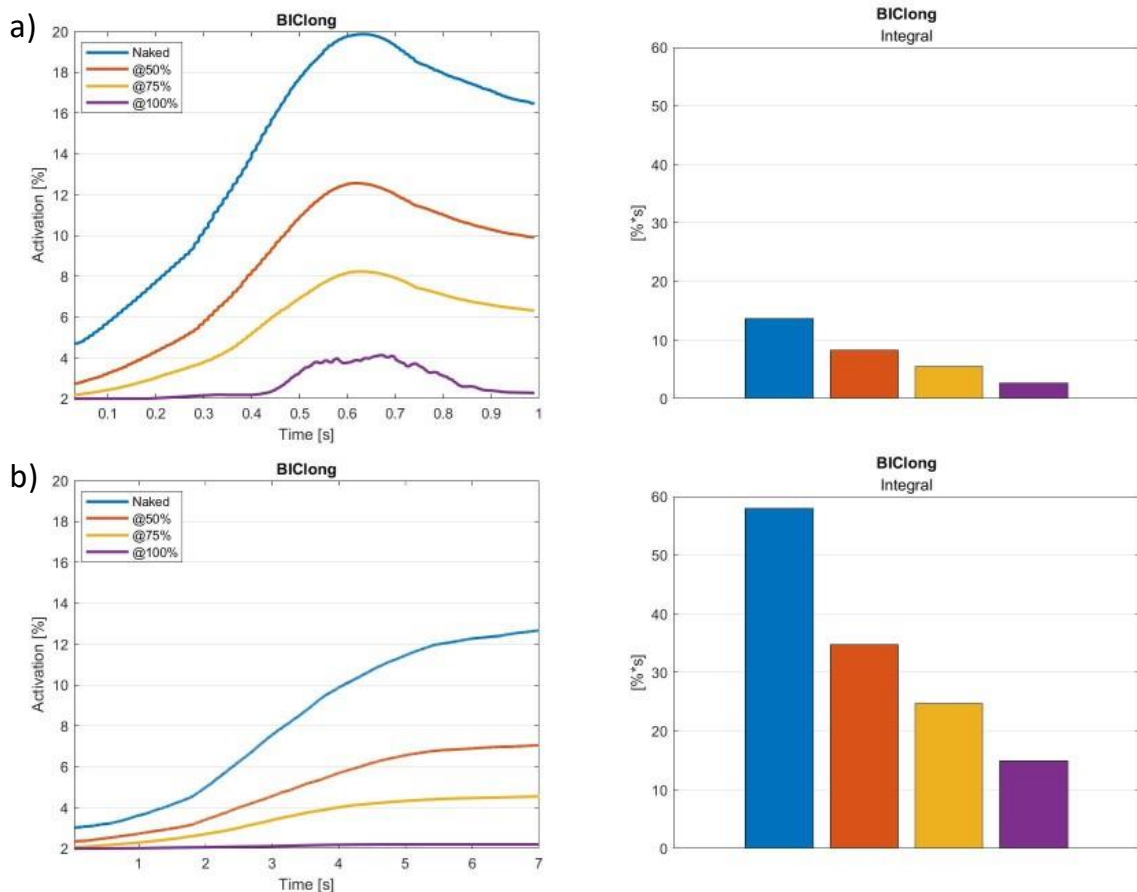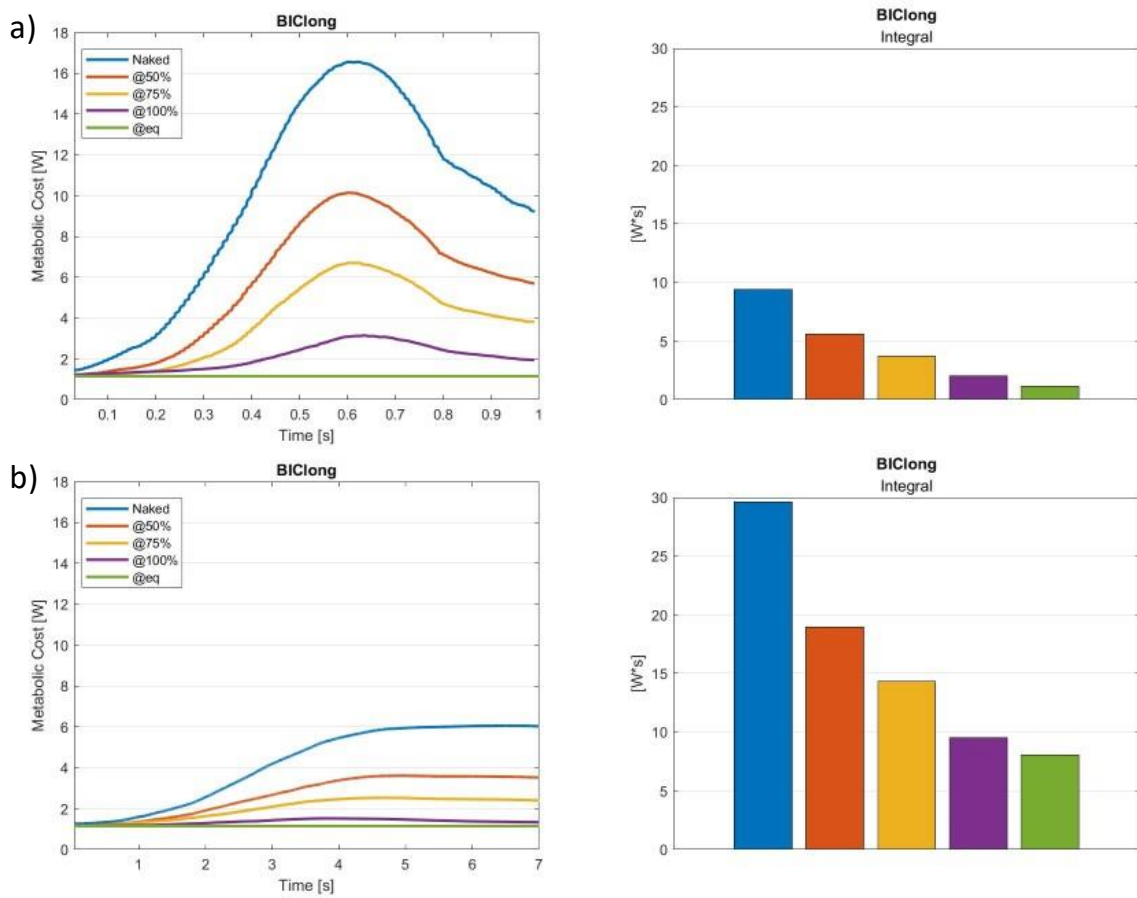

Figure 4.7: Left panels - Percentage of Biceps Long (BIClong) muscle activation during elbow flexion extension movement lasting a) 1s and b) 7 s; right panels – Integral of each curve in the right panel, color labels are the same.
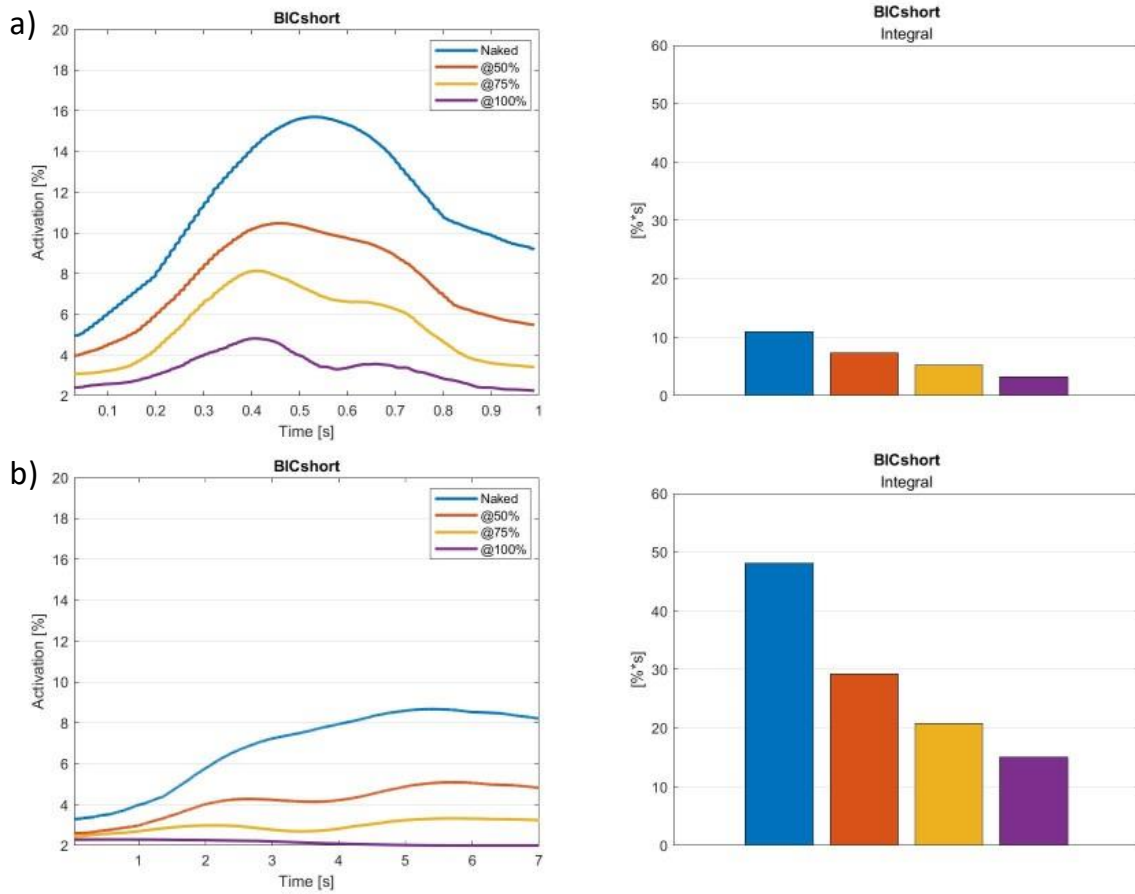
Figure 4.8: Left panels - Percentage of Biceps Short (BICshort) muscle activation during elbow flexion extension movement lasting a) 1s and b) 7 s; right panels – Integral of each curve in the right panel, color labels are the same.
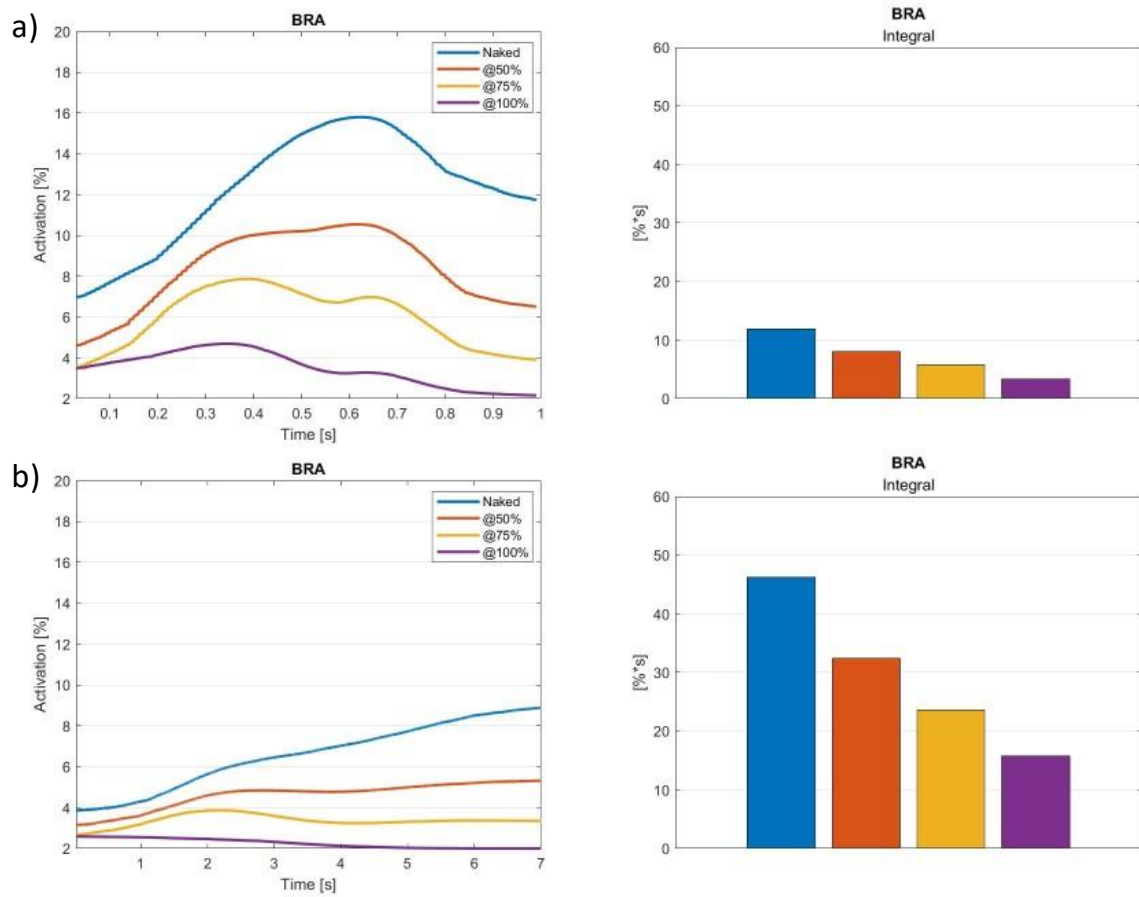
Figure 4.9: Left panels - Percentage of Brachialis (BRA) muscle activation during elbow flexion extension movement lasting a) 1s and b) 7 s; right panels – Integral of each curve in the right panel, color labels are the same.
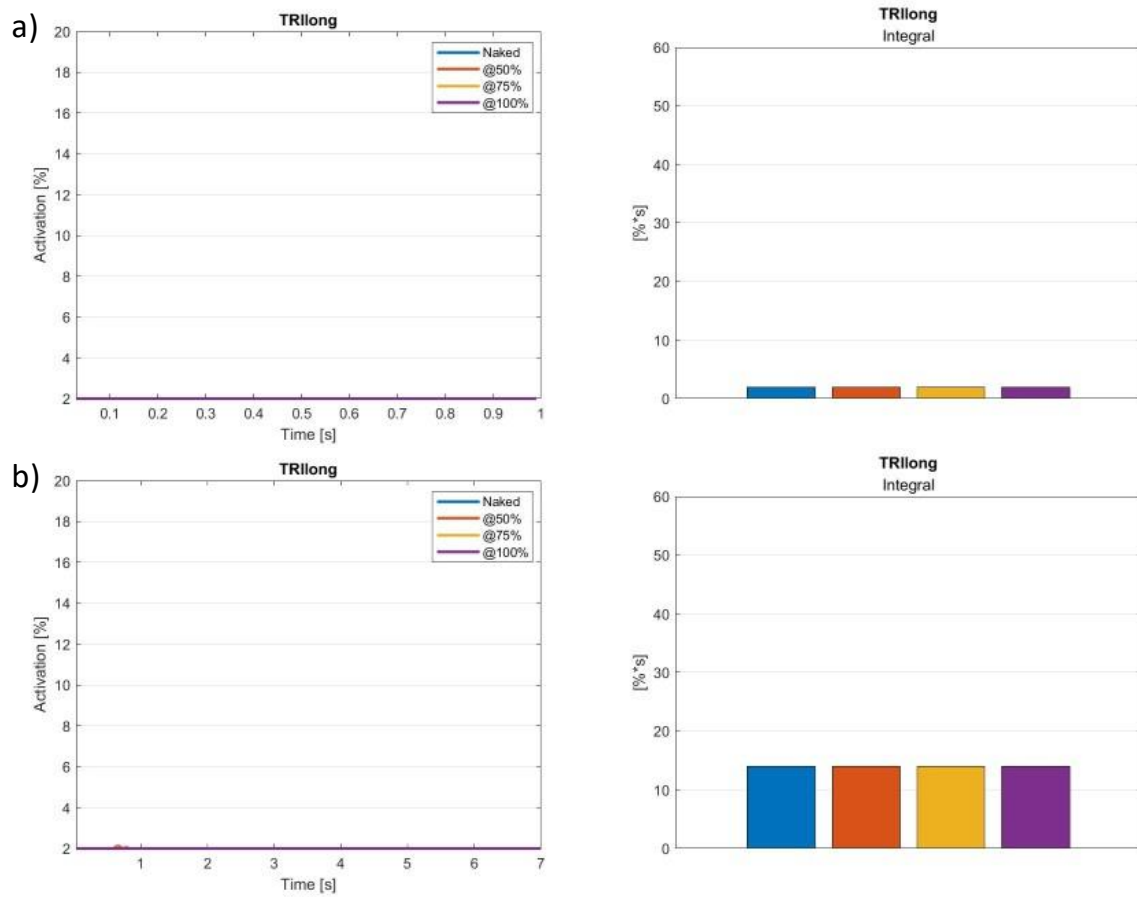
Figure 4.10: Left panels - Percentage of Triceps Long (TRIlong) muscle activation during elbow flexion extension movement lasting a) 1s and b) 7 s; right panels – Integral of each curve in the right panel, color labels are the same.
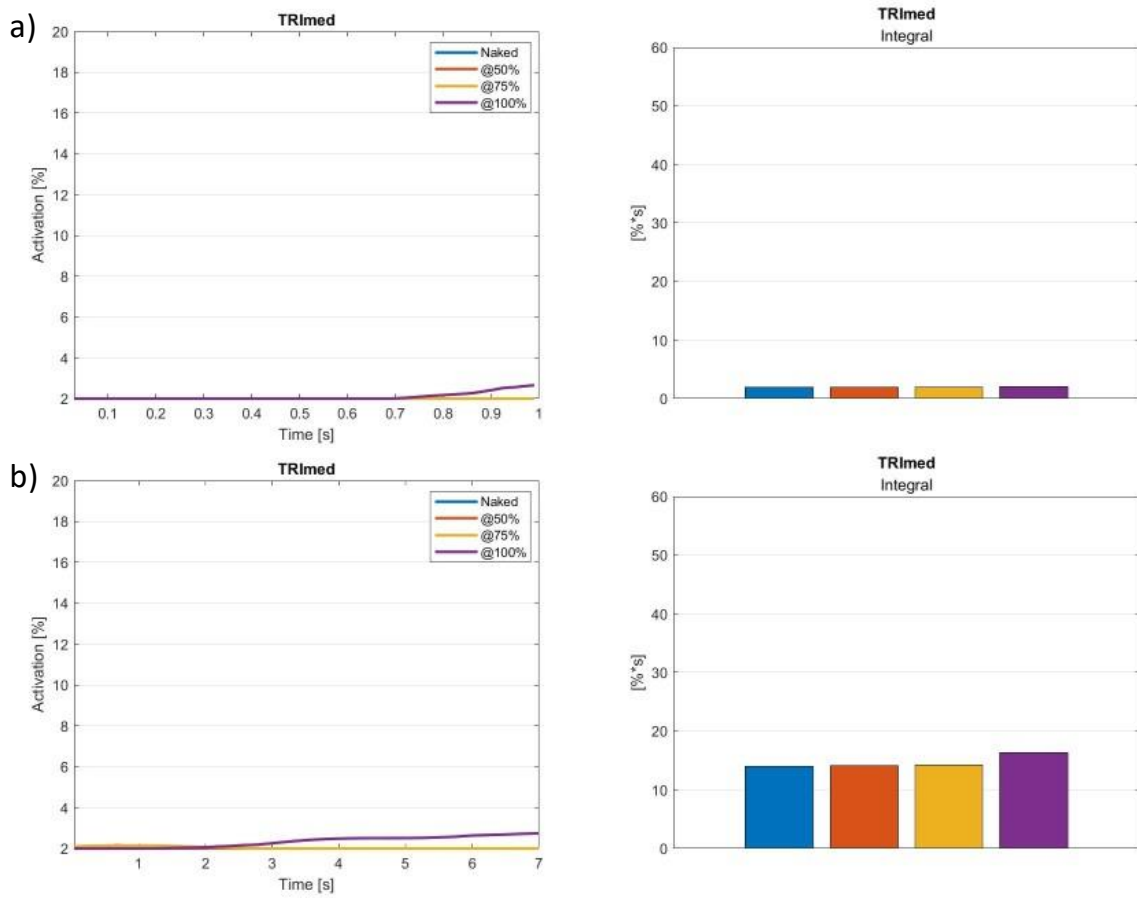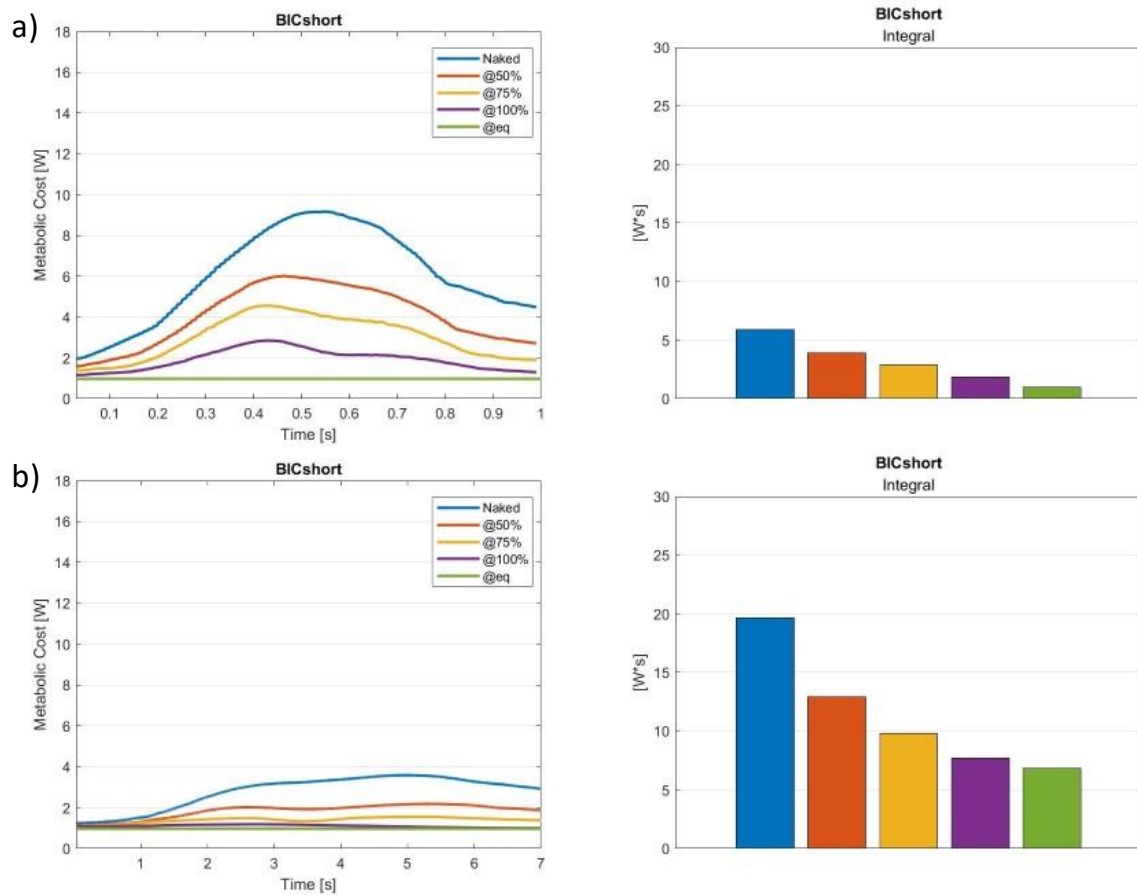
Figure 4.11: Left panels - Percentage of Triceps Medium (TRImed) muscle activation during elbow flexion extension movement lasting a) 1s and b) 7 s; right panels – Integral of each curve in the right panel, color labels are the same.
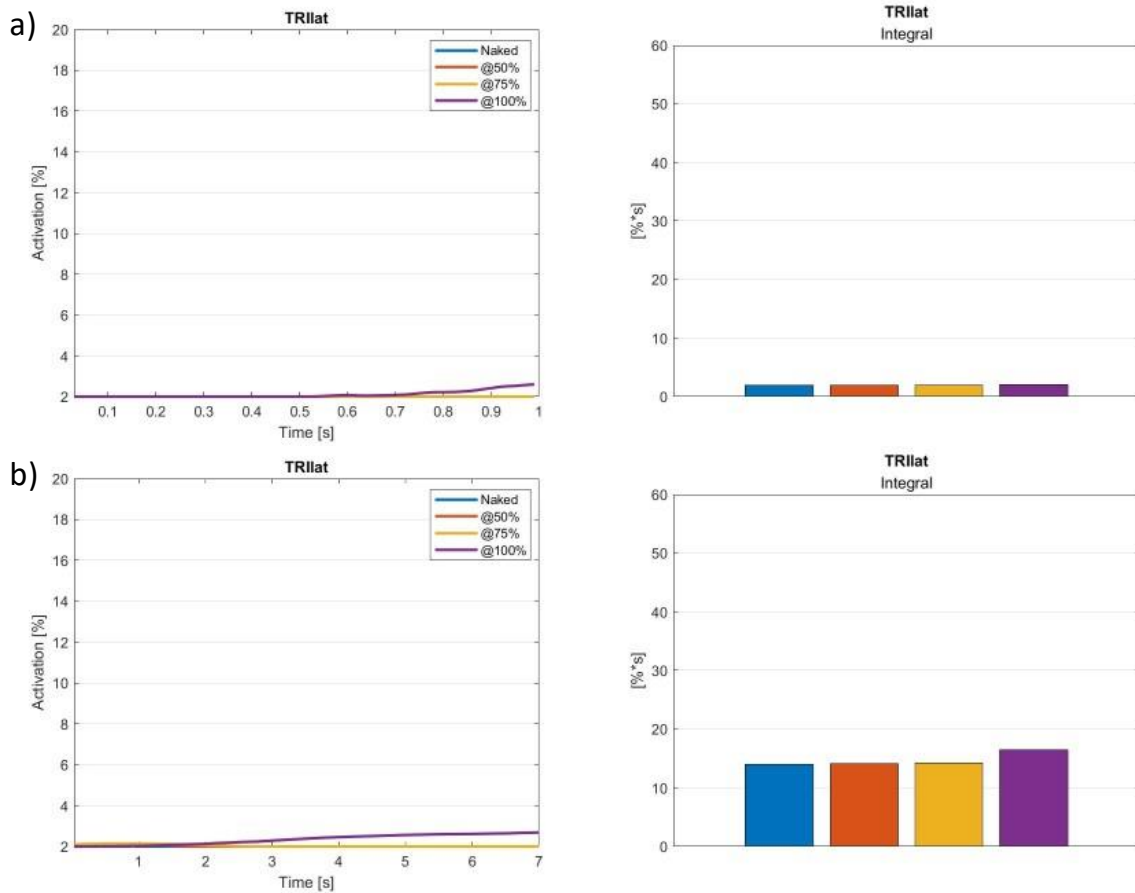
Figure 4.12: Left panels - Percentage of Triceps Lateral (TRIlat) muscle activation during elbow flexion extension movement lasting a) 1s and b) 7 s; right panels – Integral of each curve in the right panel, color labels are the same.

As seen in Figure 4.7, Figure 4.8 and Figure 4.9, the cables' intervention is effective in reducing the activation of the agonists muscles, which are BIClong, BICshort and BRA, in elbow flexion both in the 1s and 7s condition.

Regarding the other muscles (TRIlong, TRImed and TRIlat), which are defined as antagonist muscles when executing an elbow flexion movement, they show a slight increase in activation for higher percentage of assistance. However, it is also worth noticing that the activation values remain close to the absolute minimum, reaching a maximum of about 3%, when the possible absolute minimum is equal to 2%.

In Table 4.1 the reduction of the muscles' activation is shown. These values represent how much (in percentage values) the activation of the muscles has decreased (or increased in case of positive values) from the *Naked* condition as a result of the cables' assistance. Positive values represent an increase in the muscle's activation, while negative ones represent a decrease.

Muscle	@50%		@75%		@100%	
	1s	7s	1s	7s	1s	7s
BIClong	-40%	-40%	-61%	-58%	-81%	-74%
BICshort	-33%	-39%	-52%	-57%	-71%	-69%
BRA	-32%	-30%	-52%	-49%	-72%	-66%
TRIlong	0%	0%	0%	0%	0%	0%
TRImed	0%	0%	0%	2%	4%	17%
TRIlat	0%	1%	0%	2%	5%	17%

Table 4.1: Muscles' activation reduction (in percentage) from the physiological case for each muscle in each condition tested. *@50%-@75%-@100%* represent the cables' assistance percentage provided, *1s-7s* stand for the different elbow flexion durations.

4.2.2 Passive forces

Passive forces are generated by muscles as responses to their state. Specifically, they are related to muscle's length and lengthening speed.

In the graphs shown (Figure 4.13-18), the progression of passive forces, expressed in Newtons, over time while performing the elbow flexion movement are plotted.

Coupled with each graph, there is a bar plot representing the curves' integrals useful to better understand the quantity's changes for each different condition tested.

Values labeled as *Naked* refer to results obtained by running simulations in which the model performed elbow flexion without the cables' assistance, while values labeled as *@50%-75%-@100%* represent results obtained providing the corresponding assistance percentage through the cables.
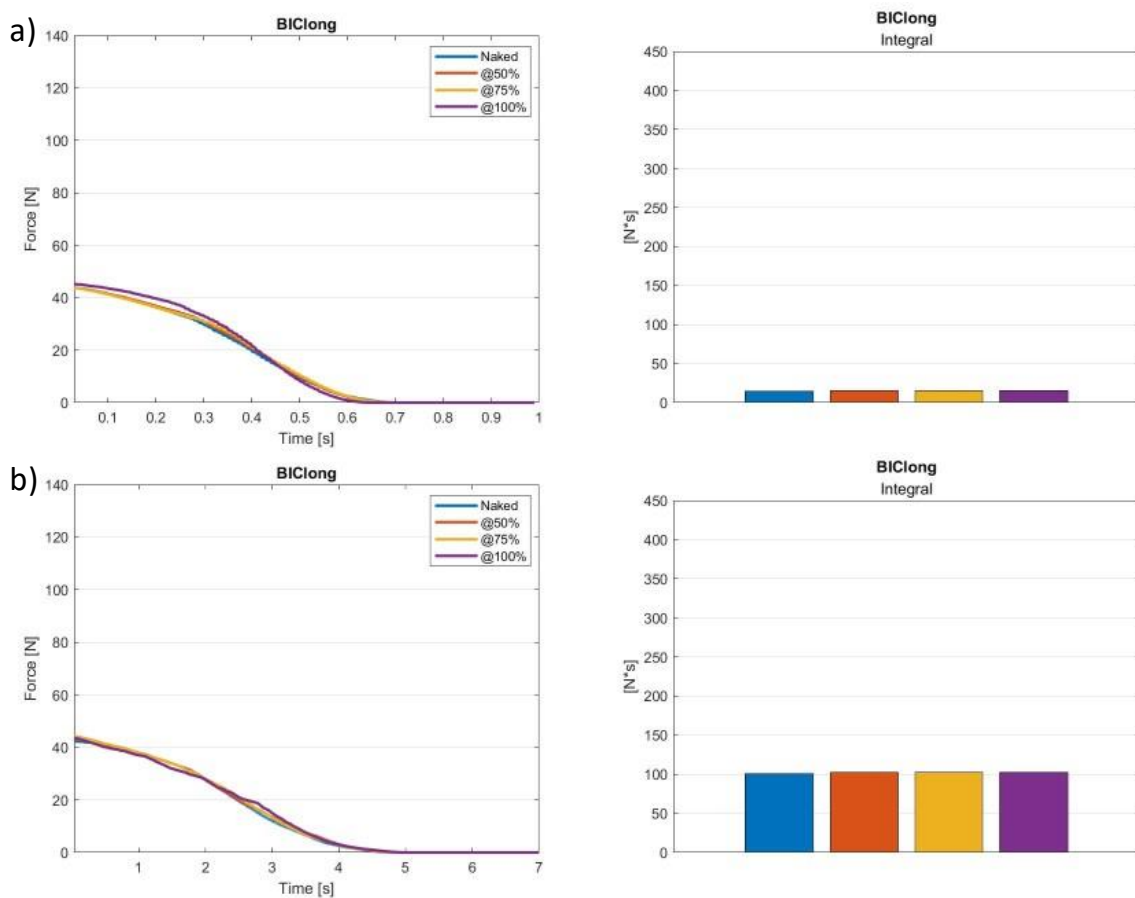
Figure 4.13: Left panels – Passive force of Biceps Long (BIClong) during elbow flexion extension movement lasting a) 1s and b) 7 s; right panels – Integral of each curve in the right panel, color labels are the same.
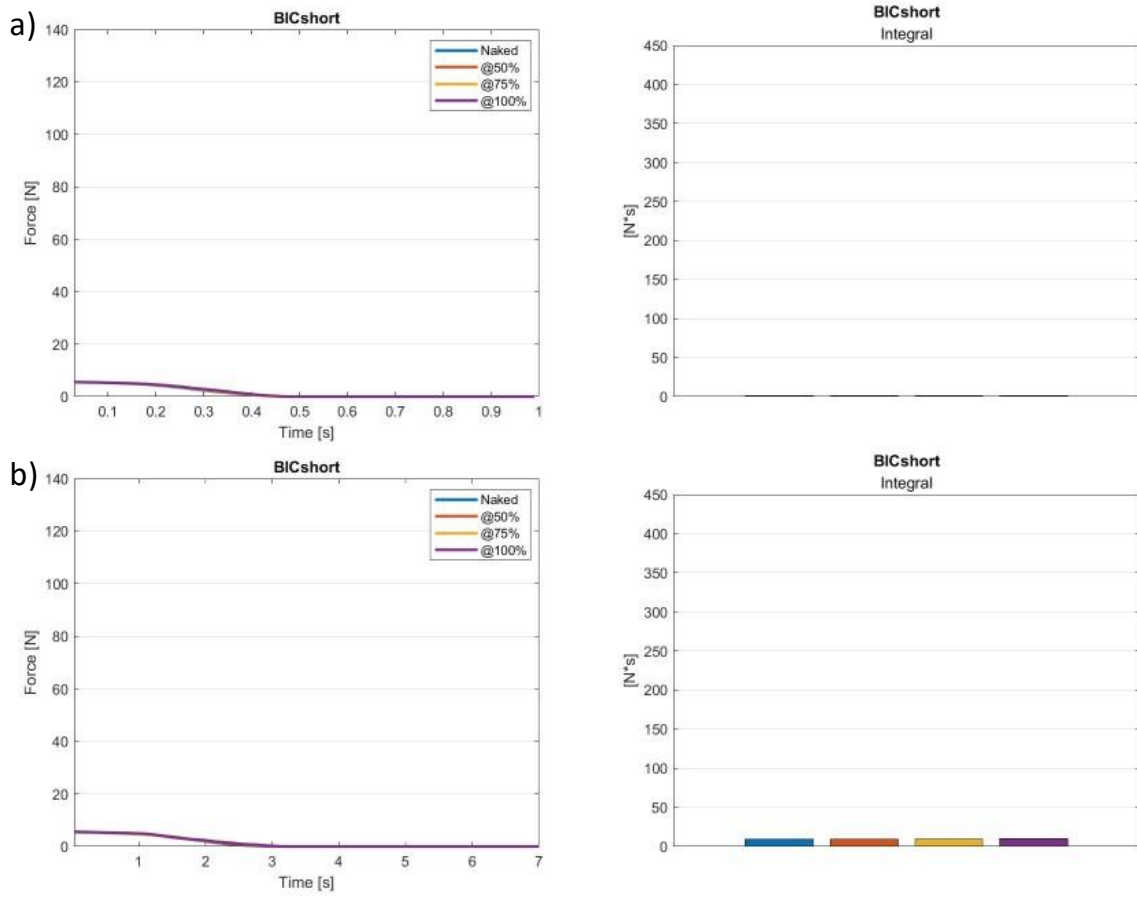
Figure 4.14: Left panels – Passive force of Biceps Short (BICshort) during elbow flexion extension movement lasting a) 1s and b) 7 s; right panels – Integral of each curve in the right panel, color labels are the same.
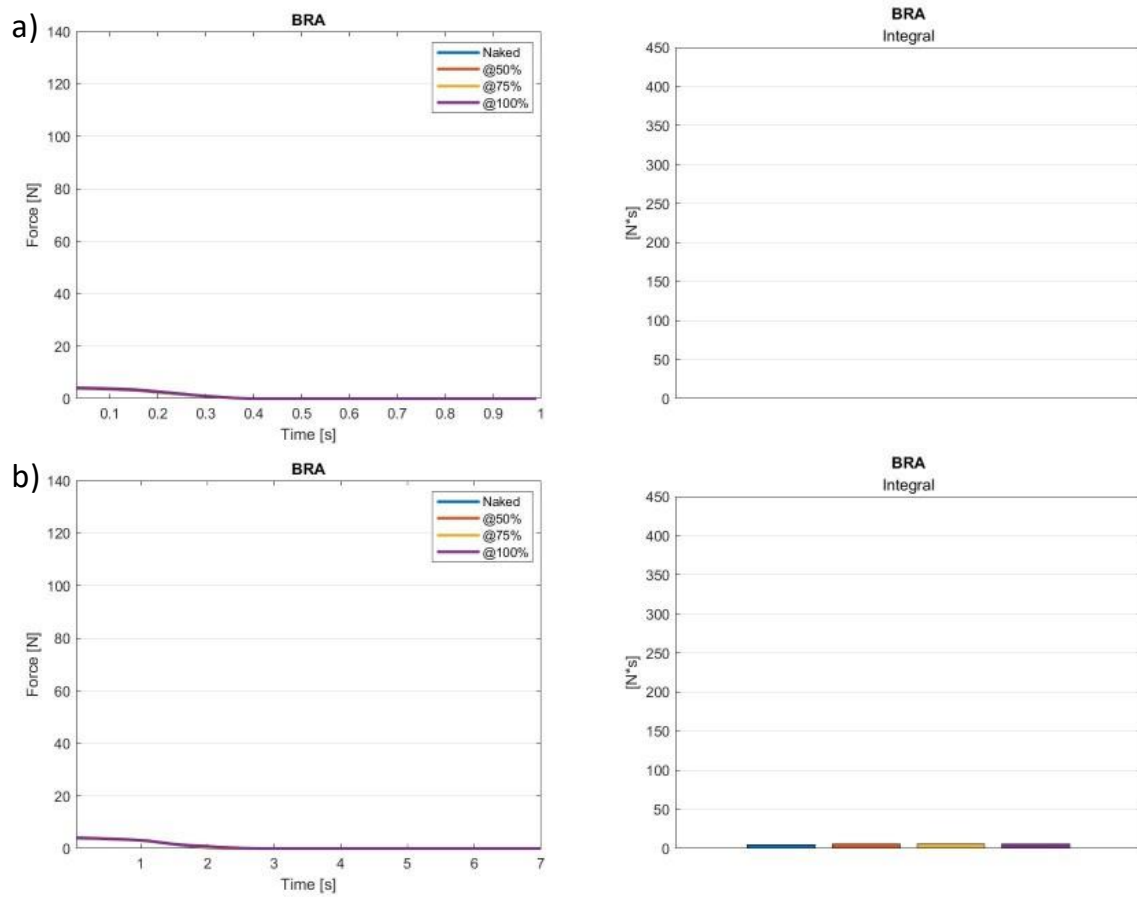
Figure 4.15: Left panel – Passive force of Brachialis (BRA) during elbow flexion extension movement lasting a) 1s and b) 7 s; right panels – Integral of each curve in the right panel, color labels are the same.
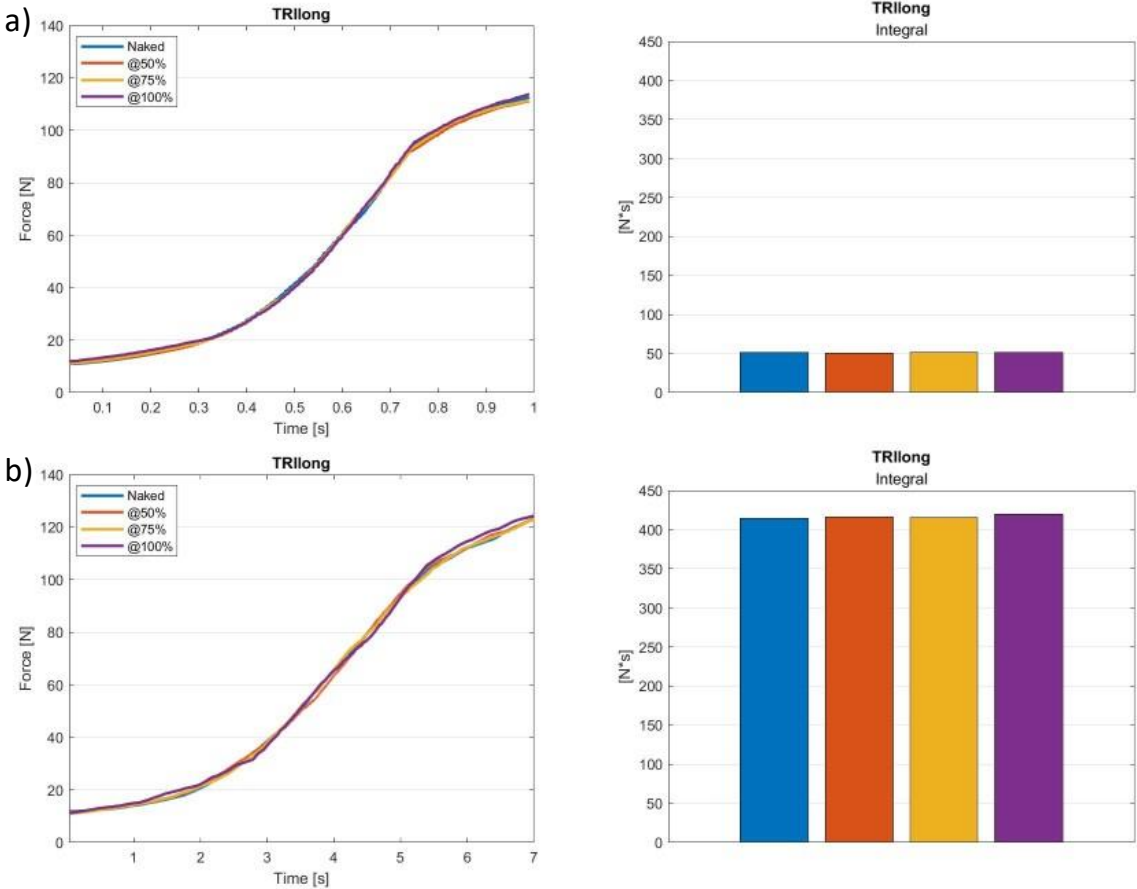
Figure 4.16: Left panels – Passive force of Triceps Long (TRIlong) during elbow flexion extension movement lasting a) 1s and b) 7 s; right panels – Integral of each curve in the right panel, color labels are the same.
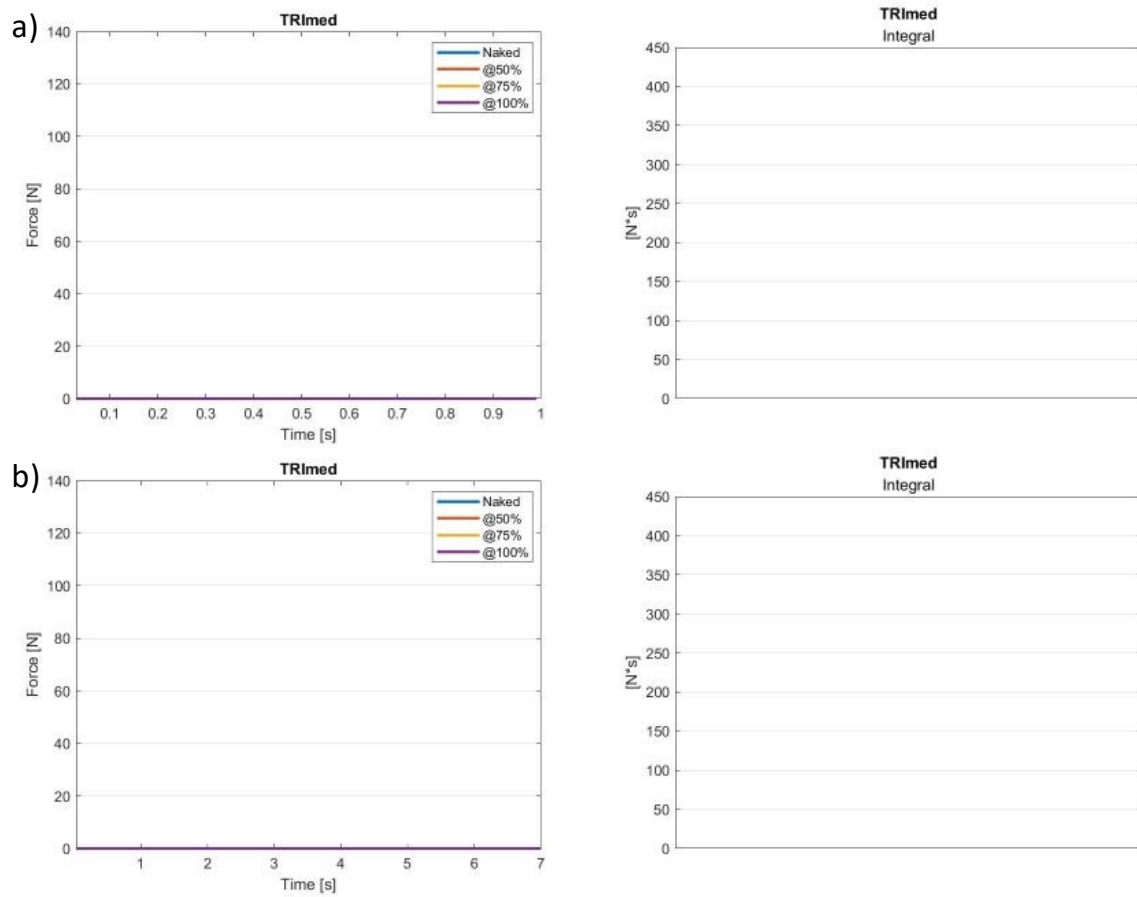
Figure 4.17: Left panels – Passive force of Triceps Medium (TRImed) during elbow flexion extension movement lasting a) 1s and b) 7 s; right panels – Integral of each curve in the right panel, color labels are the same.
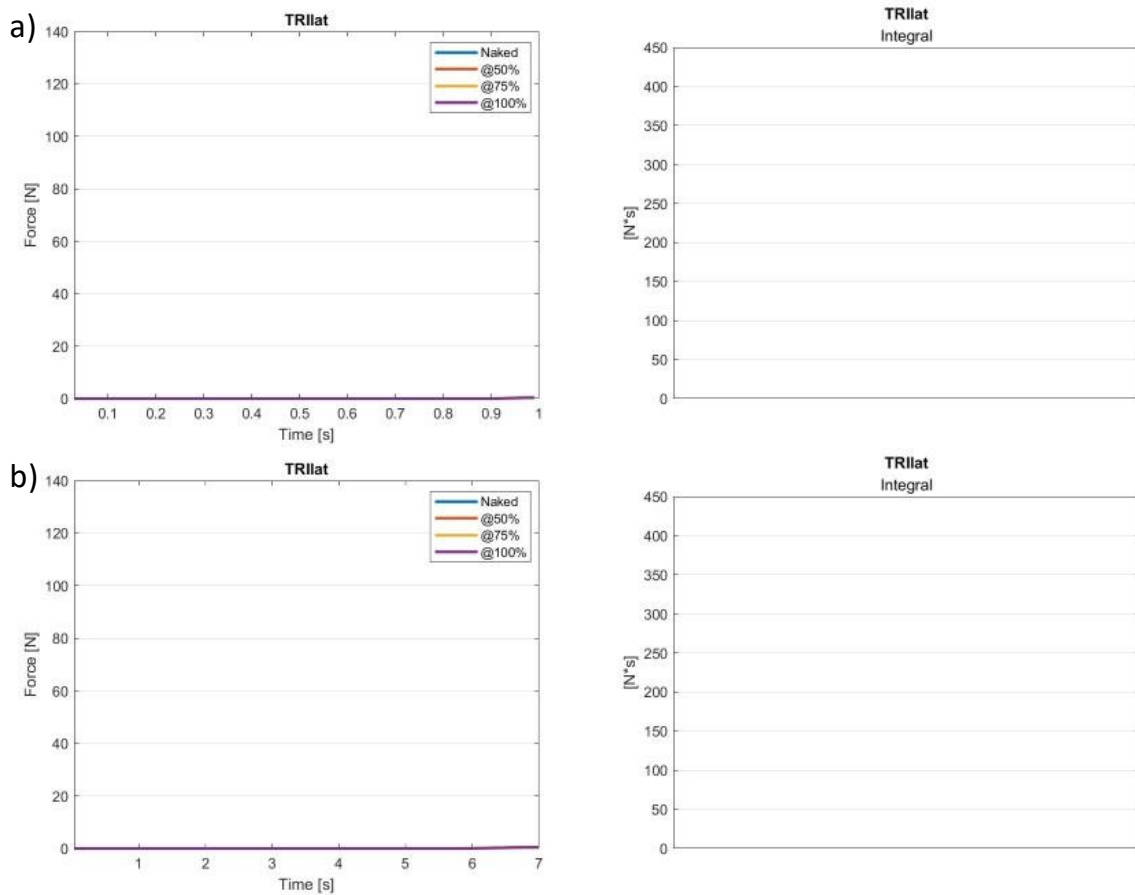
Figure 4.18: Left panels – Passive force of Triceps Lateral (TRIlat) during elbow flexion extension movement lasting a) 1s and b) 7 s; right panels – Integral of each curve in the right panel, color labels are the same.

Looking at these results (Figure 4.13-18), it is safe to say that providing assistance of any magnitude did not affect, with the only exception of TRIlat for which passive forces dropped of 23% for 100% of assistance, any of the muscles' passive behaviour, as no sensible changes were observed.

This also means that the device's action does not produce excessive muscles' strain, which could be a cause of concern since it could lead to muscles' reaping and tearing. As such, the device can be deemed safe to use under this point of view.

Changes from the *Naked* condition for each assistance percentage are shown in Table 4.2. Positive values represent an increase in the passive force generated by the muscle, while negative ones represent a decrease.

	@50%		@75%		@100%	
Muscle	1s	7s	1s	7s	1s	7s
BIClong	2%	2%	2%	2%	5%	1%
BICshort	2%	3%	4%	4%	7%	7%
BRA	2%	3%	7%	6%	8%	9%
TRIlong	-1%	0%	0%	0%	1%	1%
TRImed	0%	0%	0%	0%	0%	0%
TRIlat	-4%	-2%	1%	-2%	-23%	-22%

Table 4.2: Muscles' passive force reduction (in percentage) from the physiological case for each muscle in each condition tested. *@50%-@75%-@100%* represent the cables' assistance percentage provided, *1s-7s* stand for the different elbow flexion durations.

4.2.3 Metabolic costs

Metabolic cost is defined as the power consumed by a muscle over a period of time.

In the graphs shown (Figure 4.19-24), the progression of metabolic costs, expressed in Watts, over time while performing the elbow flexion movement are plotted.

Coupled with each graph, there is a bar plot representing the curves' integrals useful to better understand the quantity's changes for each different condition tested.

Values labeled as *@eq* represent the metabolic cost spent by the muscles to maintain the model in the equilibrium configuration (see 3.2.2). *Naked* values refer to results obtained by running simulations in which the model performed elbow flexion without the cables' assistance, while values labeled as *@50%-75%-@100%* represent results obtained providing the corresponding assistance percentage through the cables.

Figure 4.19: Left panels – Metabolic cost of Biceps Long (BIClong) during elbow flexion extension movement lasting a) 1s and b) 7 s; right panels – Integral of each curve in the right panel, color labels are the same.

Figure 4.20: Left panels – Metabolic cost of Biceps Short (BICshort) during elbow flexion extension movement lasting a) 1s and b) 7 s; right panels – Integral of each curve in the right panel, color labels are the same.
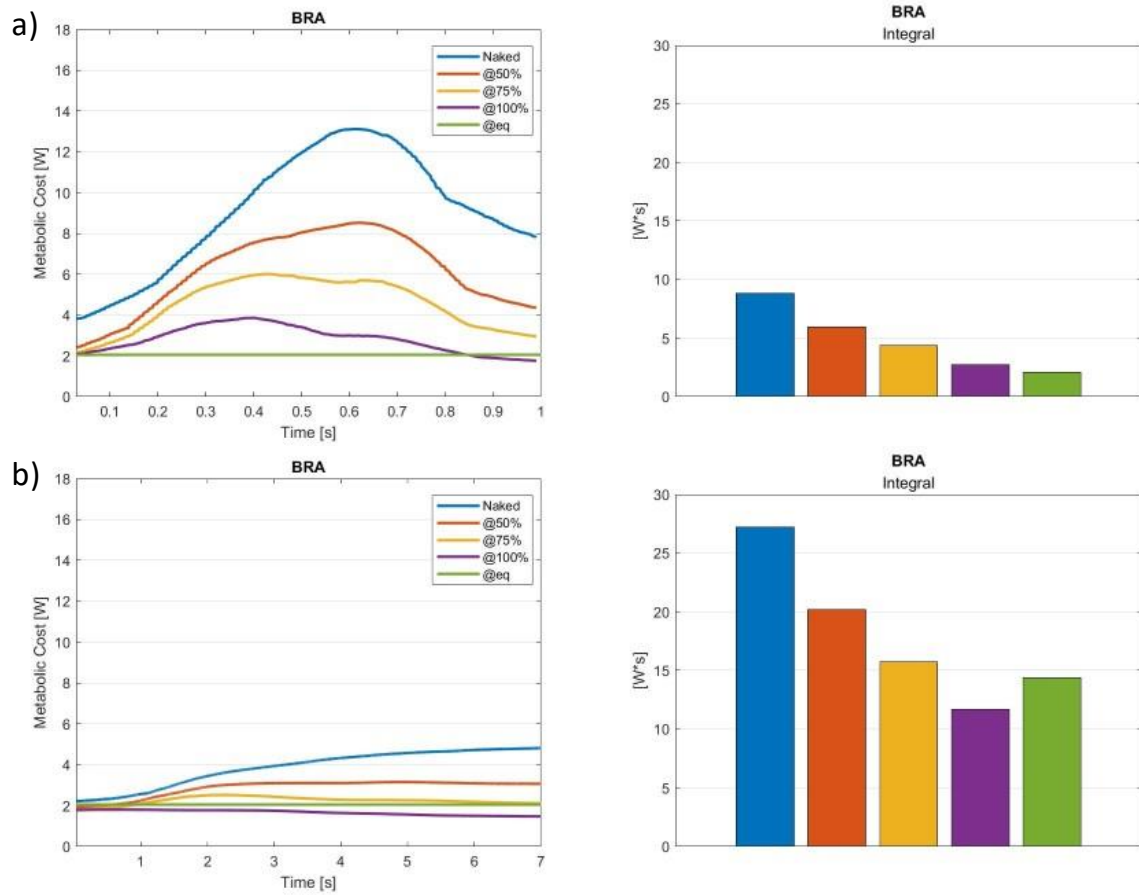
Figure 4.21: Left panels – Metabolic cost of Brachialis (BRA) during elbow flexion extension movement lasting a) 1s and b) 7 s; right panels – Integral of each curve in the right panel, color labels are the same.
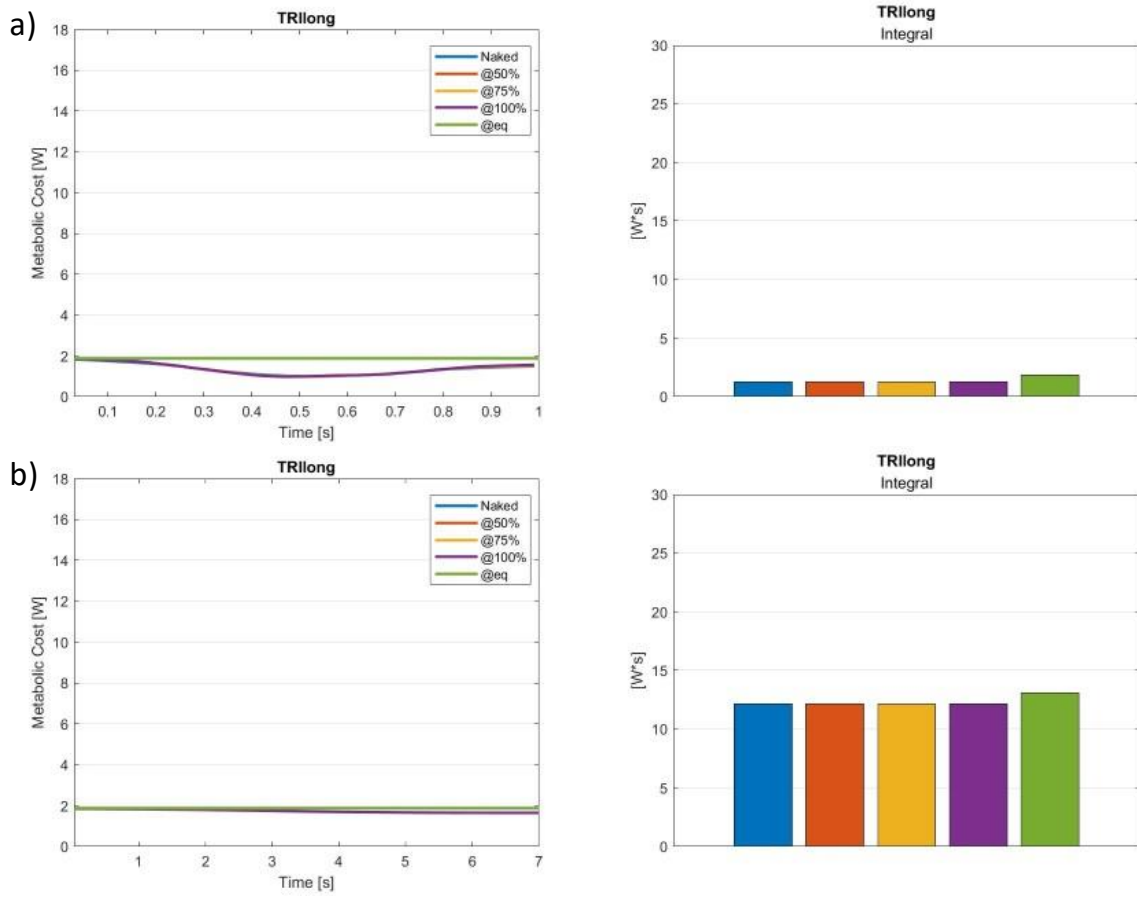
Figure 4.22: Left panels – Metabolic cost of Triceps Long (TRIlong) during elbow flexion extension movement lasting a) 1s and b) 7 s; right panels – Integral of each curve in the right panel, color labels are the same.
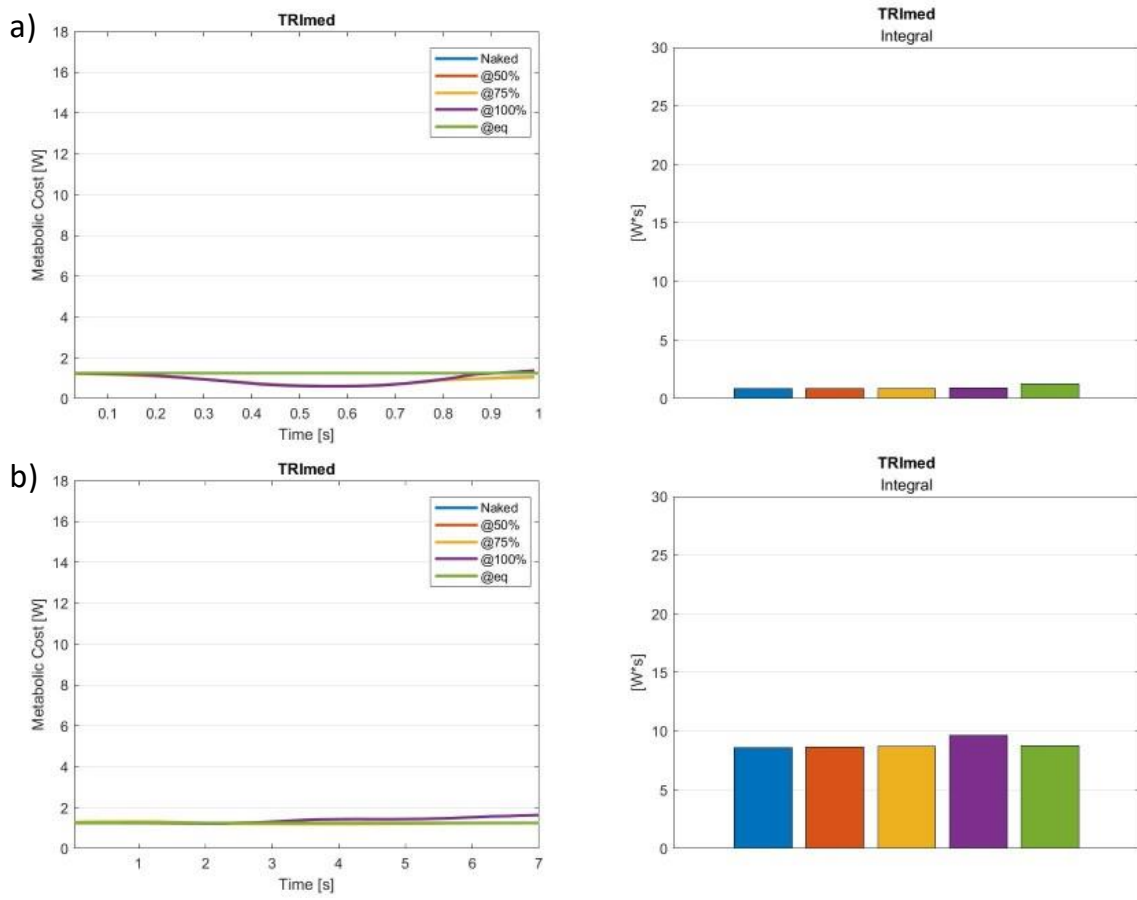
Figure 4.23: Left panels – Metabolic cost of Triceps Medium (TRImed) during elbow flexion extension movement lasting a) 1s and b) 7 s; right panels – Integral of each curve in the right panel, color labels are the same.
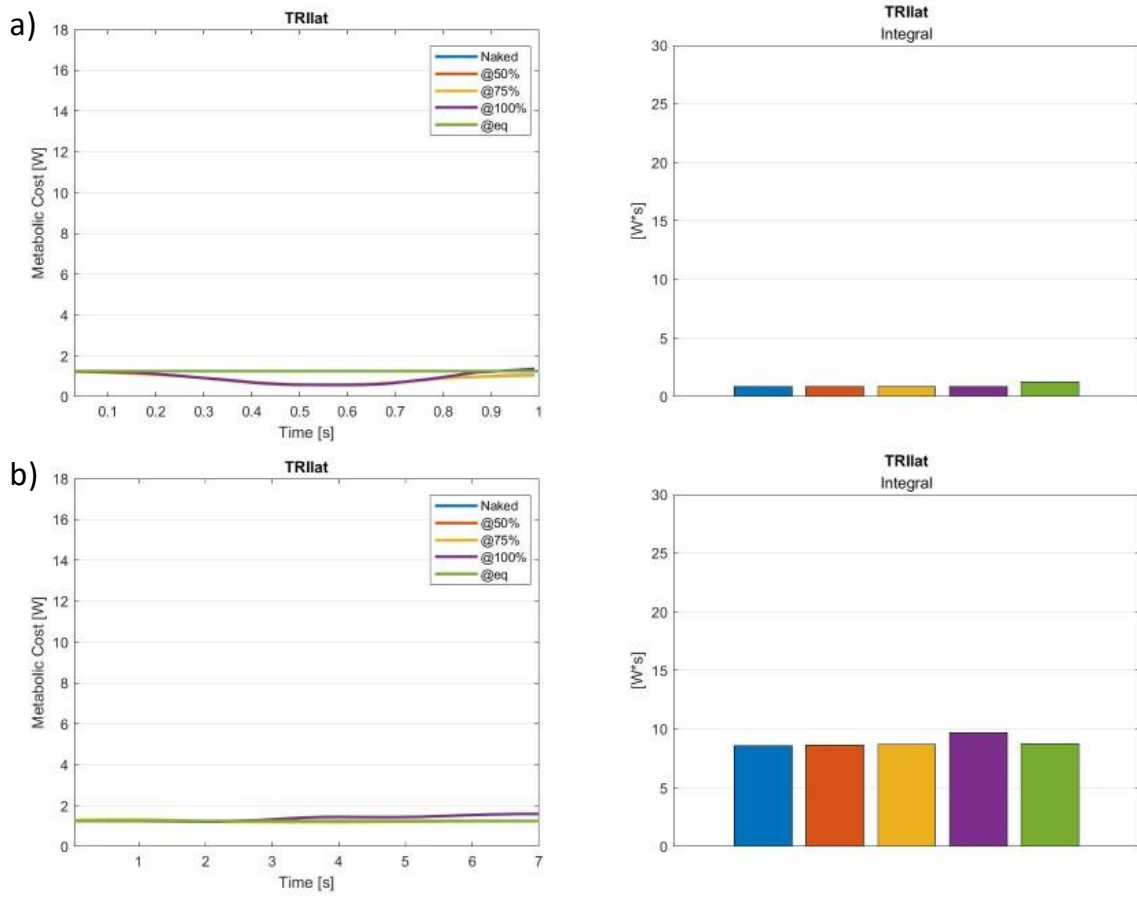
Figure 4.24: Left panels – Metablic cost of Triceps Laterla (TRIlat) during elbow flexion extension movement lasting a) 1s and b) 7 s; right panels – Integral of each curve in the right panel, color labels are the same.

Since metabolic cost is strictly related to muscle activation, it was expected to observe a reduction of the metabolic cost as the percentage of assistance increased, similarly to what is presented in section 4.2.1. This hypothesis proved to be correct, as for agonist muscles (BIClong, BICshort, BRA), metabolic costs do indeed get lower and closer to the *@eq* values. Basically this means that providing 100% of assistance, agonist muscles consume almost as much power as when they are in the elbow's resting condition. On the other hand, for antagonist muscles (TRIlong, TRImed, TRIlat), the values stay almost the same or slightly increase for higher degrees of assistance, in accordance with the results in muscles' activation.

In Table 4.3 the percentile changes in muscles' metabolic costs for each testing condition are shown, expressed as differences from the *Naked* values.

Muscle	@50%		@75%		@100%		@eq	
	1s	7s	1s	7s	1s	7s	1s	7s
BIClong	-41%	-36%	-61%	-52%	-79%	-68%	-88%	-73%
BICshort	-33%	-34%	-51%	-50%	-69%	-61%	-83%	-65%
BRA	-32%	-26%	-50%	-42%	-69%	-57%	-77%	-47%
TRIlong	0%	0%	1%	0%	1%	0%	47%	8%
TRImed	-1%	0%	-1%	1%	5%	12%	46%	2%
TRIlat	0%	1%	-1%	1%	5%	13%	50%	2%

Table 4.3: Muscles' metabolic cost reduction (in percentage) from the physiological case for each muscle in each condition tested. *@50%-@75%-@100%* represent the cables' assistance percentage provided, *1s-7s* stand for the different elbow flexion durations.

4.2.4 Joint reaction forces

In this section, results related to the joint reaction forces analysis are presented. To better understand the results displayed, a reference system centered on the ulna, since all forces and moments are expressed as applied on the ulna's head, is provided in Figure 4.25.
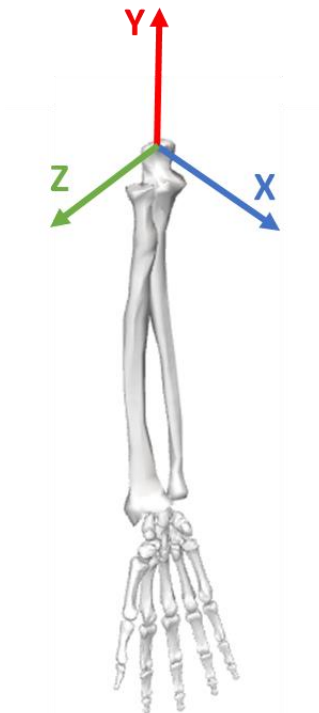
Figure 4.25: Reference system.

In the graphs shown (Figure 4.26-31), the progression of reaction forces and moments over time while performing the elbow flexion movement are plotted.

Coupled with each graph, there is a bar plot representing the curves' integral that are useful to better understand the quantity's changes for each different condition tested.

Values labeled as *Naked* refer to results obtained by running simulations in which the model performed elbow flexion without the cables' assistance, while values labeled as *@50%-75%-@100%* represent results obtained providing the corresponding assistance

percentage through the cables. Reaction forces are expressed in Newtons, while reaction moments are expressed in Newtons per meter.
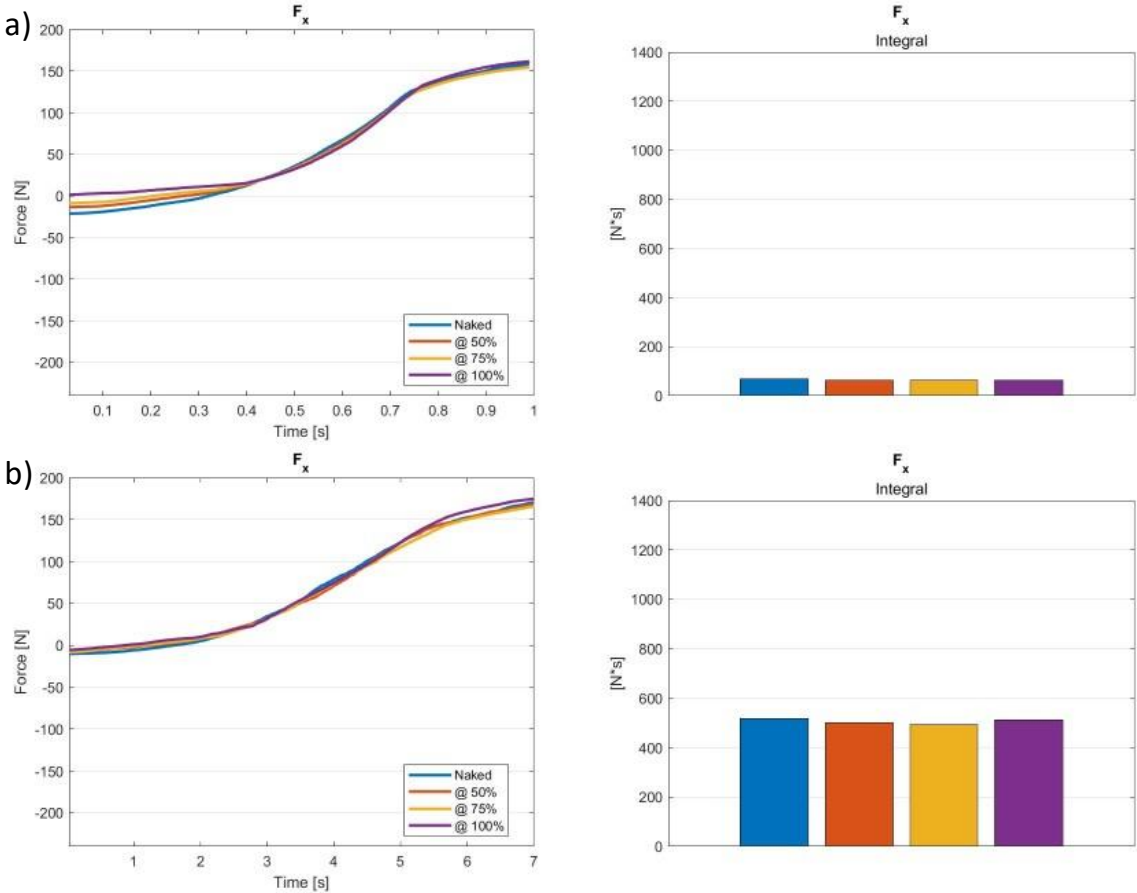
Figure 4.26: Left panels – Elbow reaction force along X axis (F_X) during elbow flexion extension movement lasting a) 1s and b) 7 s; right panels – Integral of each curve in the right panel, color labels are the same.
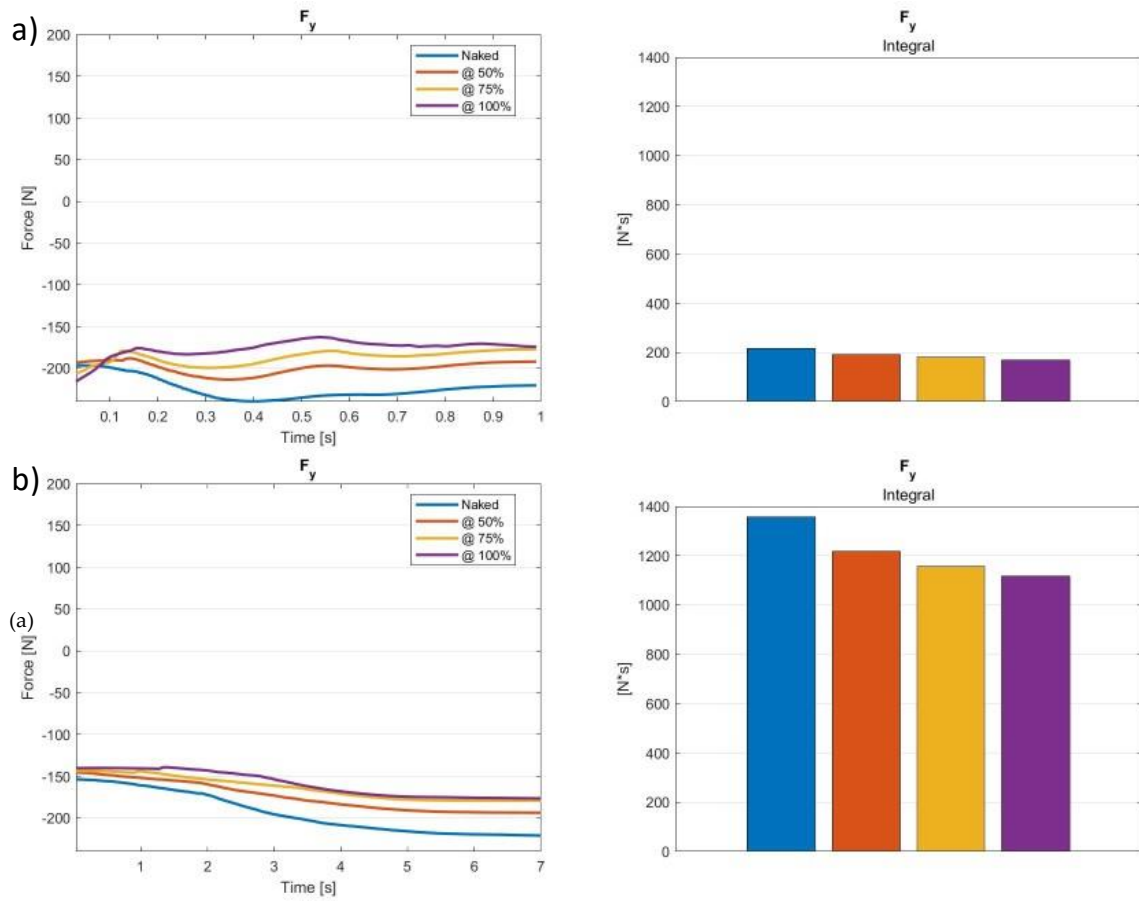
Figure 4.27: Left panels – Elbow reaction force along Y axis (F$_Y$) during elbow flexion extension movement lasting a) 1s and b) 7 s; right panels – Integral of each curve in the right panel, color labels are the same.
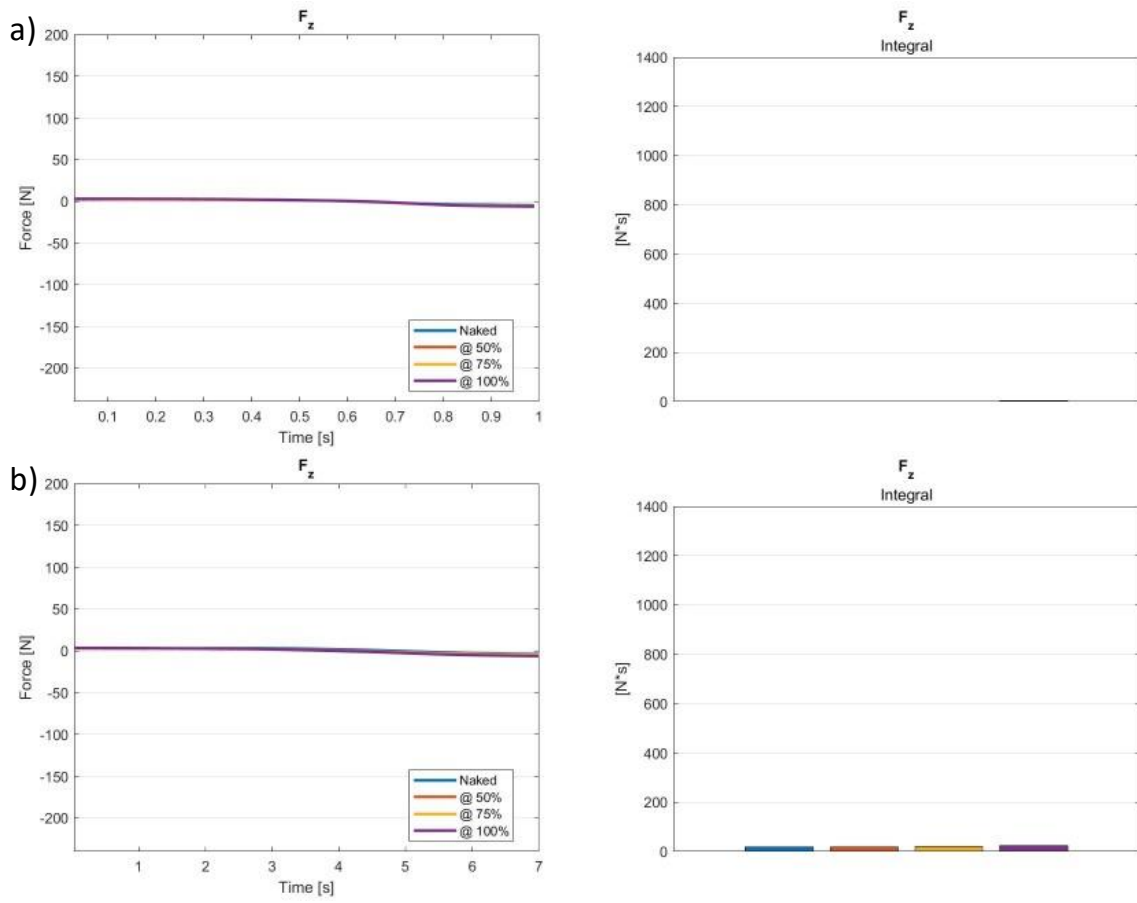
Figure 4.28: Left panels – Elbow reaction force along Z axis (Fz) during elbow flexion extension movement lasting a) 1s and b) 7 s; right panels – Integral of each curve in the right panel, color labels are the same.
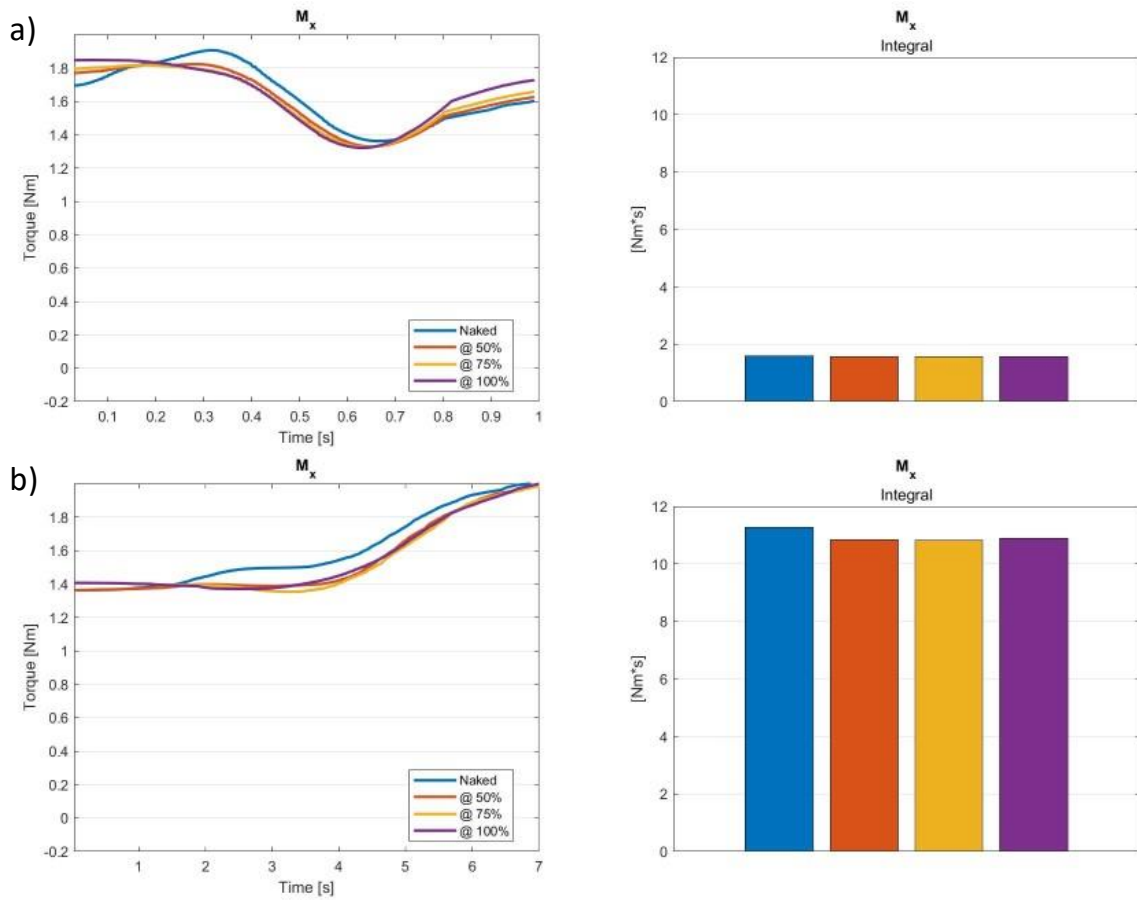
Figure 4.29: Left panels – Elbow reaction moment on X axis (Mx) during elbow flexion extension movement lasting a) 1s and b) 7 s; right panels – Integral of each curve in the right panel, color labels are the same.
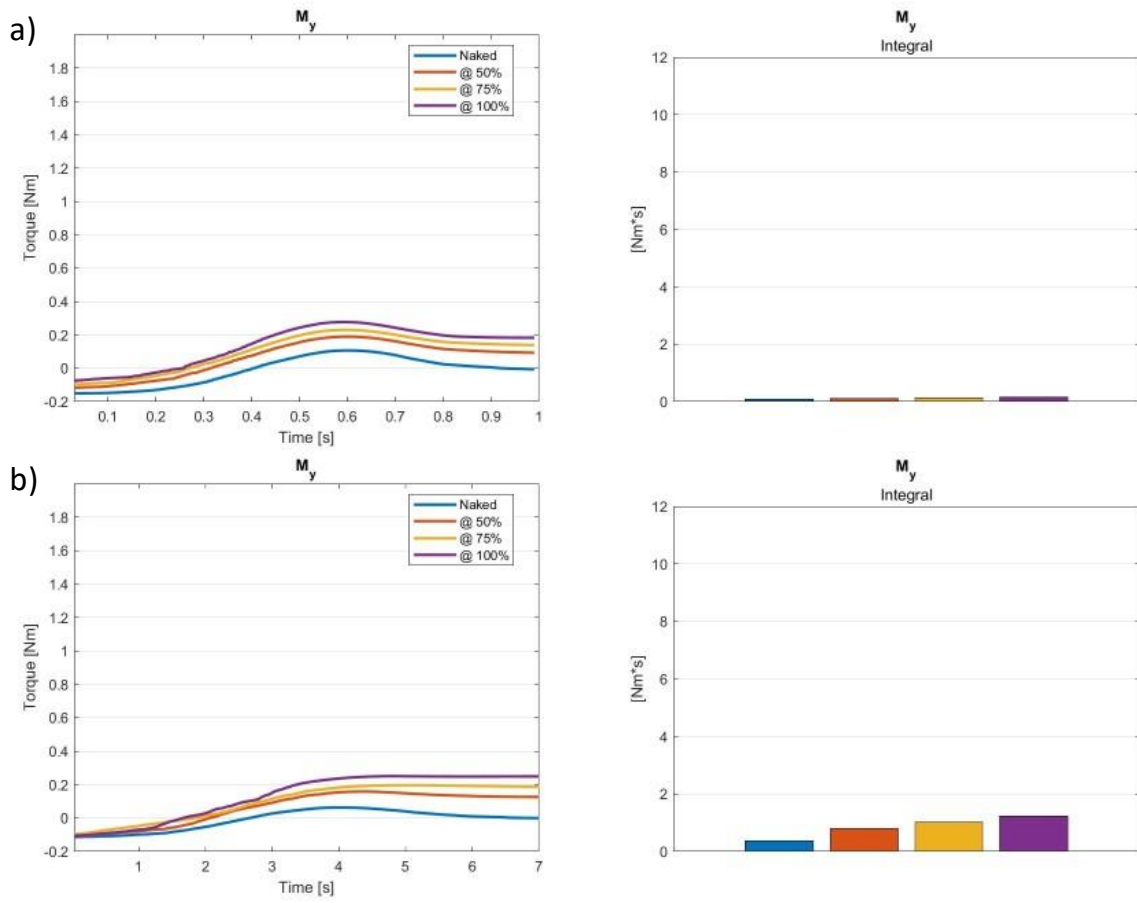
Figure 4.30: Left panels – Elbow reaction moment on Y axis (M$_Y$) during elbow flexion extension movement lasting a) 1s and b) 7 s; right panels – Integral of each curve in the right panel, color labels are the same.
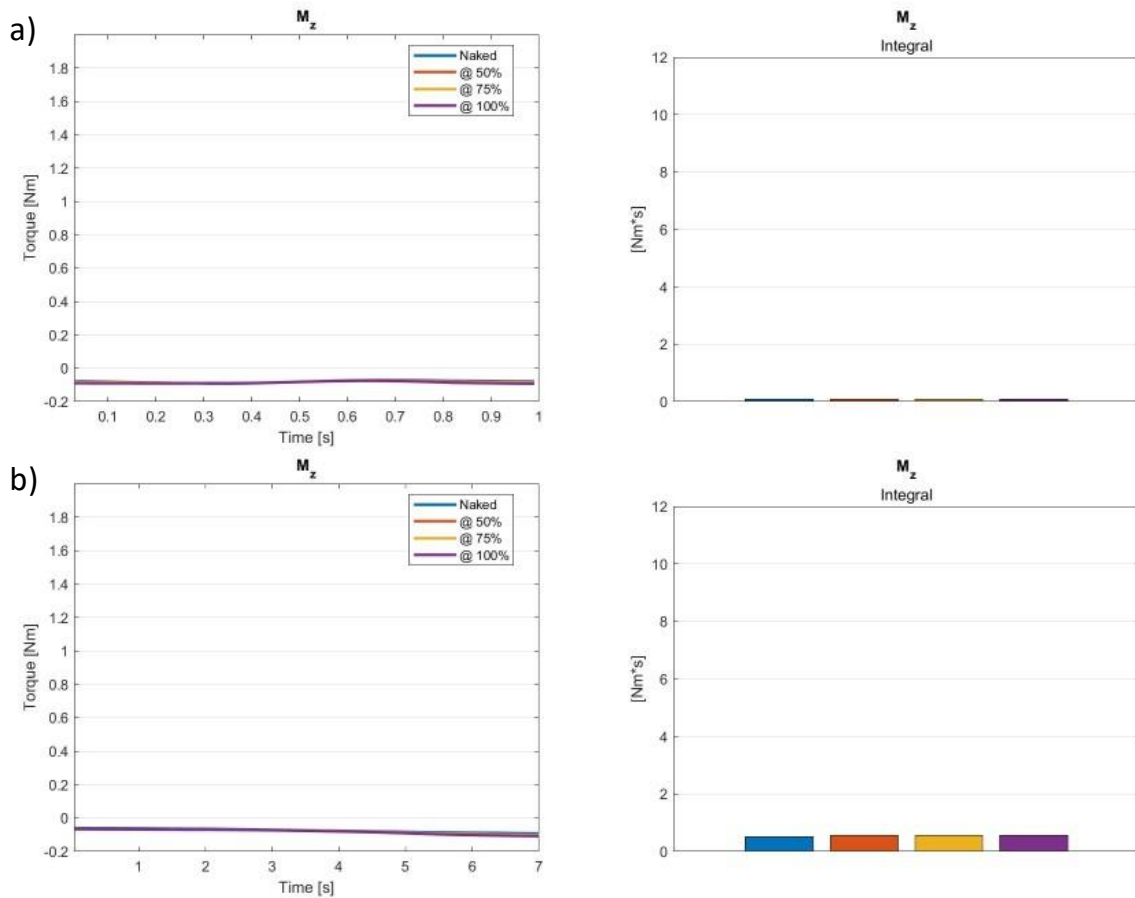
Figure 4.31: Left panels – Elbow reaction moment on Z axis (M$_z$) during elbow flexion extension movement lasting a) 1s and b) 7 s; right panels – Integral of each curve in the right panel, color labels are the same.

From the results, it can be stated that forces along X axis and moments on X and Z axis do not get affected in a relevant way by the cable's action.

The same cannot be said regarding forces along Z axis and the moment on Y axis, as they increase as the assistance degree raises, potentially affecting prono-supination of the forearm (but due to the model's limits it could not be verified). Anyways, this phenomenon could be explained by errors in the placement of the cables' anchor points, which may not be exactly symmetrical respect the limb's longitudinal axis. Also, the raise for higher degrees of assistance could be due to disparities in the cables' tension profiles. Anyway, assuming that the data obtained by the *Naked* case reliably

represents real life data, these results are not concerning since there are not excessive increases in forces and moments, and as such, it can be stated that the tensions applied by the cables on the limb of the user do not generate reaction forces at the elbow joint that could potentially harm the user themselves.

On the other hand, forces along Y axis decrease for higher degrees of assistance, thus the device's action reduces compressive stress on the elbow joint.

In Table 4.4 the percentile changes in joint reaction forces and moments for each testing condition are shown, expressed as differences from the *Naked* values.

Force/Moment	@50%		@75%		@100%	
	1s	7s	1s	7s	1s	7s
F_x	-5%	-4%	-7%	-5%	-6%	-1%
F_y	-11%	-10%	-17%	-15%	-22%	-18%
F_z	-1%	4%	0%	9%	12%	25%
M_x	-1%	-4%	-1%	-4%	0%	-3%
M_y	46%	111%	76%	170%	108%	229%
M_z	2%	5%	4%	7%	6%	9%

Table 4.4: Joint reactions' reduction (in percentage) from the physiological case for each rection force/moment at the elbow in each condition tested. *@50%-@75%-@100%* represent the cables' assistance percentage provided, *1s-7s* stand for the different elbow flexion durations.

4.3   Device prototype

In this chapter's final paragraph, results regarding the sizing of the device and a first schematic of the actuation unit will be presented.

4.3.1 Actuation unit

The results of the analyses regarding the cables' lengthening and lengthening velocity during the elbow flexion movement performed in 1s are shown (Figure 4.32).
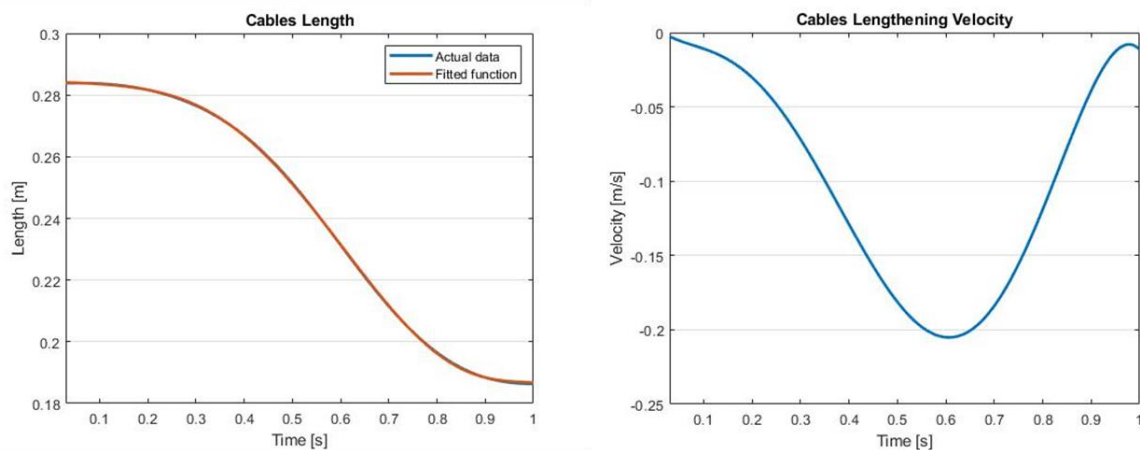
Figure 4.32: Cables average length while performing elbow flexion in 1s (left) and computed cables' lengthening velocity.

Once the lengthening speed progression was obtained, the maximum lengthening speed has been found with an absolute value of 21 m/s.

The maximum force required, considering the peak of both cables, was about 70 N, but to account for possible lack of power due to friction, possible higher weight of the arm and to potentially allow faster movements, 80 N were used in the computations.

At this point, together with the information provided by the components' datasheets, all the data required to size the actuation system's spool was available (Table 4.5).

Quantity	Value
Max cable speed	-0.21m/s
Max tension	80N
Reductor's max angular speed	31.15rpm
Reductor's max torque	15N

Table 4.5: Data used to size the spool. *Max cable speed* is negative because the cables shorten over time.

Using (3.10) and the data in Table 4.5, the minimum and maximum length of the spool was computed.

The minimum value is bound both to the maximum lengthening velocity required and the maximum output angular speed provided by the reductor (computed as the maximum output angular speed provided by the motor divided by the reductor's reduction factor). On the other hand, the maximum spool's radius value depends on the maximum output torque provided by the reductor and the maximum tension required to pull both cables.

Quantity	Value
Min radius	0.062m
Max radius	0.18m

Table 4.6: Spool's minimum and maximum radius' length.

In Figure 4.33, the actuation system's maximum output angular velocity (calculated from the maxium lengthening velocity required) and maximum output torque (calculated from the maximum cables' tension set) are displayed as functions of the spool's radius, computed using (3.10).
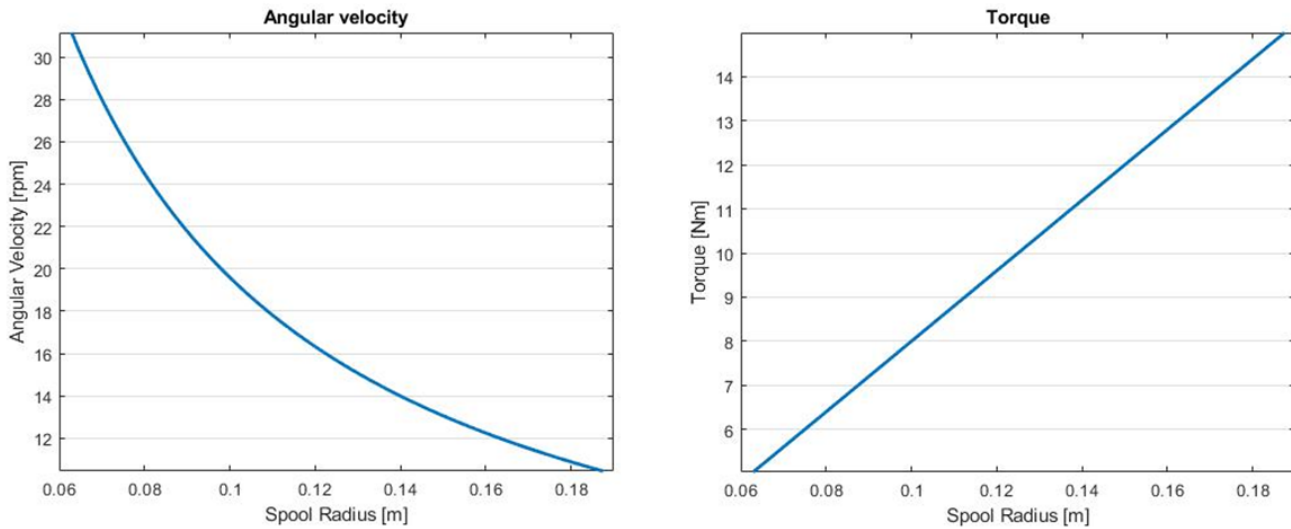
Figure 4.33: Maximum output angular velocity (left) and torque (right) expressed as functions of the spool's radius.

Angular velocity and torque values are bound to the current available components' specifics (see 3.2.6), while the radius length covers an interval defined between its minimum and maximum values.

Angular velocity is expressed in rotations per minute, torque in Newtons per meter, and the spool's radius in meters.

Finally, the schematic in Figure 4.34 has been developed using the data acquired.

To keep the device to a reasonable size and potentially allow to perform movements at higher speeds, the spool's radius has been set to 0.07 meters. This radius also allows to use the motor under the maximum of its operational range.

In addition, in the attempt to limit the encumbrance, the spool has been placed on the side with its axis parallel to the main axis of the motor-reductor system, and a pair of straight bevel gears have been used to set the spool in motion.

In the schematic are show only the motor, the reductor, the spool and a couple of cables wrapped around it.
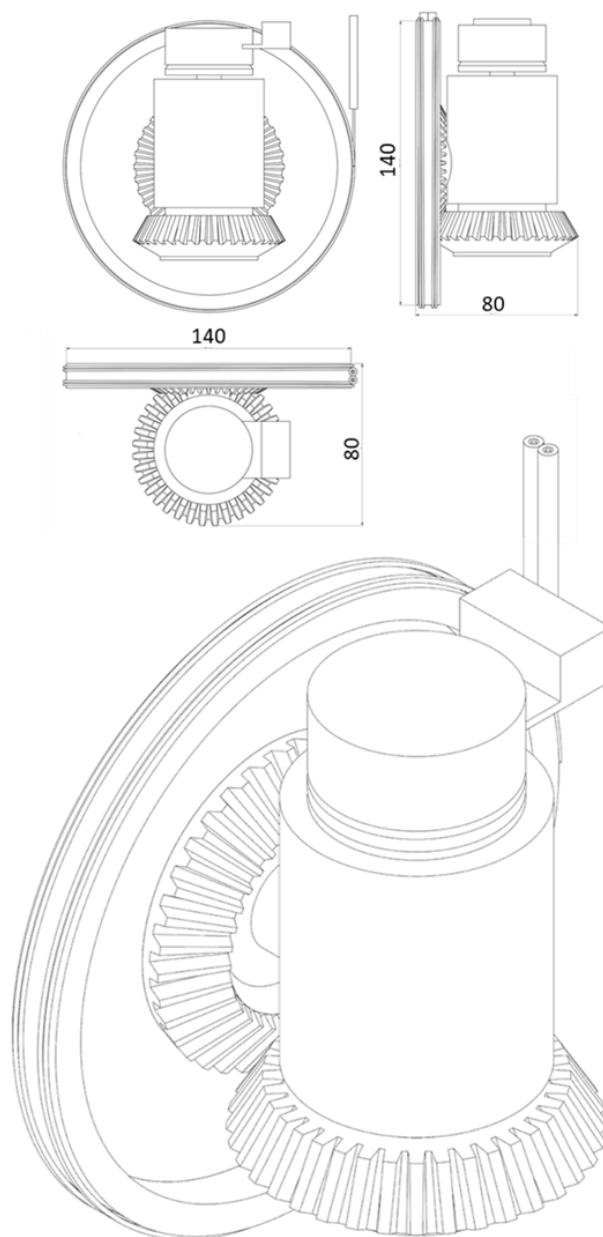
Figure 4.34: First prototype's schematic. All measures are in millimeters

5. Chapter five: Conclusion & future developments

This thesis' work had as main objective that of developing a simulation-based optimization process for the cable routing of a cable-driven exosuit.

First, a musculoskeletal model of the upper human body has been found. Given the model's characteristics, the optimization process has been designed with elbow flexion as the target movement of the exosuit.

This model has then been customized, adding tensile cables (implemented as linear actuators) in different configurations.

Each configuration has been then evaluated, with the aim to identify the one that would lead to minimal mechanical requirements to be implemented in real life. Specifically, the best configuration would require the least maximum and average tension to pull the cables, also accounting for tension equality between the cables. These specific quantities were considered as they are directly linked to motor's performance minimal requirements (the lower the tension required, the lower the maximum output torque needed and the smaller the motor can be) and to the possibility to restrict the actuation system encumbrance using a single spool to actuate all cables.

Once the best configuration had been identified, further simulations have been run to assess its efficacy by evaluating its effects on the biomechanics of the model. Quantities such as muscular activation, passive forces, metabolic costs and joint reaction forces have been studied.

In this final chapter, conclusions drawn from the results obtained and suggestions for future developments of the project are presented.

5.1   Conclusions

5.1.1 Cables arrangement

The analysis regarding the best cables' configuration (4.1) led to an important conclusion: in order to optimize the tension profile during elbow flexion, double cable systems are better than those relying on a single cable.

Indeed, as explained and shown in 4.1, using a single cable requires the highest amount of tension among all the other configurations.

5.1.2 Device evaluation

Looking at the results from 4.2.1, it is safe to say that the employment of the device (approximated as the cables only in the simulations) succeeded in reducing the recruitment of the model's agonists muscles (BIClong, BICshort, BRA) needed to perform the desired elbow flexion movement, which lowers as the assistance provided by the cables raises. The same cannot be said about the antagonist muscles (TRIlong, TRImed, TRIlat). In fact, it was initially expected to record no sensible change in these muscles' activation, as the cables action was thought not to affect their behaviour.

However, their slight rise in activation that was found for higher percentages of assistance may be functional in correcting the movements trajectory.

The same conclusions may be drawn from the results shown in 4.2.3, as muscle's activation and muscle's metabolic consumption are related to one another.

Regarding the remaining results, presented in sections 4.2.2 and 4.2.4, the aim was to make sure that cables' action wouldn't result in possible harmful situations, such as excessive strain on muscle, leading to high passive forces, or high reaction forces at the elbow joint.

As the data computed by simulations suggests, since there are no sensible increases on any of those values, using the exosuit with the proposed cables configuration should not result in said harmful situations. However, the raise of M_y as a result of the cables's action may affect forearm prono-supination.

5.2   Limitations

The main limits to further developments in this project were determined by the musculoskeletal model used.

The Arm_26 is characterized by its extreme simplicity. It features a very limited number of muscles and degrees of freedom, implementing only 6 muscles and 2 degrees of freedom.

Also, this model did not behave realistically when elbow extension was studied. Infact, when in forward dynamics simulations the model was set in a configuration having the arm fully raised and the elbow completely flexed, passive forces generated by the muscles caused the arm to extend on its own, acting against gravity, even without any active intervention of the muscles.

For these reasons, the project development was limited in studying the design of the device only regarding elbow flexion, while other arm movements (such as elbow extension, forearm pronation and supination) could not be addressed.

Regarding the prototype of the actuation system, limits were imposed by the current components available. The results presented in 4.3.1 about the dimensioning of the spool according to force and velocity requirements are underwhelming. Indeed, given the current motor and reductor, the actuation system (alone) would be way too cumbersome, with dimensions of about 14x14x8 centimeters.

5.3   Future developments

5.3.1 Simulation environment

As stated in 3.2.1, the ideal model to perform the kind of studies done in this thesis would have to be as realistic as possible to a real human arm, implementing all of its degrees of freedom and at least most of its muscles. Moreover, the muscles behaviour in forward dynamics simulations should be realistic as well, unlike what was found out by using both the MoBL_ARM and the DAS3 models.

For these reasons, in order to further develop the project, to design and study cables' routing to assist other arm movements such as elbow extension, forearm pronation and supination and shoulder elevation, it is fundamental to find or develop and validate a more appropriate and realistic musculoskeletal model.

5.3.2 Device prototype

The final goal of the project in which this thesis took place, is to fully develop a portable exosuit to assist the upper limb. In particular, the device should assist elbow flexion-

extension. Being portability one of the main requirements of the device, the exosuit's components, such as the motor and gear, the spool and the batteries should be as small as possible.

A possible solution to reduce the actuation system's size is to use a different motor and reductor, allowing the possibility to reach the appropriate maximum angular speed needed to perform physiological movements. With respect to the torque requirements, it is possible to reduce the gear ratio, since the present gear ratio is highly conservative. By reducing the gear ratio, not only the gear weight and dimensions could be reduced, but also the spool's radius length range would be shifted towards lower values and, therefore, the whole system's dimension would be reduced, lowering its weight, volume and thus increasing its portability.

Bibliography

[1]   M. Xiloyannis *et al.*, "Soft Robotic Suits: State of the Art, Core Technologies, and Open Challenges," *IEEE Trans. Robot.*, pp. 1–20, Jun. 2021, doi: 10.1109/TRO.2021.3084466.

[2]   Y. Shen, P. W. Ferguson, and J. Rosen, "Upper Limb Exoskeleton Systems— Overview," *Wearable Robot. Syst. Appl.*, pp. 1–22, Jan. 2020, doi: 10.1016/B978-0-12-814659-0.00001-1.

[3]   "Media information: Paexo exoskeleton | Ottobock SE & Co. KGaA." https://www.ottobock.com/en/company/newsroom/media/media-information-exoskelett-paexo/ (accessed Nov. 23, 2021).

[4]   J. L. Pons, "Witnessing a wearables transition," *Science (80-.).*, vol. 365, no. 6454, pp. 636–637, Aug. 2019, doi: 10.1126/SCIENCE.AAW9407.

[5]   N. Li *et al.*, "Bio-inspired upper limb soft exoskeleton to reduce stroke-induced complications," *Bioinspiration and Biomimetics*, vol. 13, no. 6, Aug. 2018, doi: 10.1088/1748-3190/aad8d4.

[6]   J. L. Samper-Escudero, A. Gimenez-Fernandez, M. A. Sanchez-Uran, and M. Ferre, "A Cable-Driven Exosuit for Upper Limb Flexion Based on Fibres Compliance," *IEEE Access*, vol. 8, pp. 153297–153310, 2020, doi: 10.1109/ACCESS.2020.3018418.

[7]   D. C. Scuola *et al.*, "Design and Embedded Control of a Soft Elbow Exosuit HUMAN-MACHINE INTERFACES BASED ON ELECTRO-BIOLOGICAL SIGNALS FOR ROBOTIC APPLICATIONS AND NEUROREHABILITATION View project CENTAURO-Robust Mobility and Dexterous Manipulation in Disaster Response by Full," doi: 10.1109/ROBOSOFT.2018.8405386.

[8]   S. Lessard, P. Pansodtee, A. Robbins, J. M. Trombadore, S. Kurniawan, and M. Teodorescu, "A Soft Exosuit for Flexible Upper-Extremity Rehabilitation," *IEEE Trans. Neural Syst. Rehabil. Eng.*, vol. 26, no. 8, pp. 1604–1617, Aug. 2018, doi: 10.1109/TNSRE.2018.2854219.

[9]   C. S. Simpson, A. M. Okamura, and E. W. Hawkes, "Exomuscle: An inflatable device for shoulder abduction support," *Proc. - IEEE Int. Conf. Robot. Autom.*, pp. 6651–6657, 2017, doi: 10.1109/ICRA.2017.7989785.

[10]   T. H. Koh, N. Cheng, H. K. Yap, and C. H. Yeow, "Design of a soft robotic elbow sleeve with passive and intent-controlled actuation," *Front. Neurosci.*, vol. 11, no. OCT, Oct. 2017, doi: 10.3389/FNINS.2017.00597.

[11]   H. Kobayashi and K. Hiramatsu, "Development of muscle suit for upper limb," *Proc. - IEEE Int. Conf. Robot. Autom.*, vol. 2004, no. 3, pp. 2480–2485, 2004, doi: 10.1109/ROBOT.2004.1307433.

[12]   M. Ding, J. Ueda, and T. Ogasawara, "Pinpointed muscle force control using a power-assisting device: System configuration and experiment," *Proc. 2nd Bienn. IEEE/RAS-EMBS Int. Conf. Biomed. Robot. Biomechatronics, BioRob 2008*, pp. 181–186, 2008, doi: 10.1109/BIOROB.2008.4762829.

[13]   S. Sridar *et al.*, "Soft Robotic Shoulder Assist Device: Towards Prevention of Shoulder Overuse Syndrome in Wheelchair Users," *Front. Biomed. Devices,*

BIOMED - 2018 Des. Med. Devices Conf. DMD 2018, Jun. 2018, doi: 10.1115/DMD2018-6808.

[14] T. Abe *et al.*, "Fabrication of '18 weave' muscles and their application to soft power support suit for upper limbs using Thin McKibben Muscle," *IEEE Robot. Autom. Lett.*, vol. 4, no. 3, pp. 2532–2538, Jul. 2019, doi: 10.1109/LRA.2019.2907433.

[15] D. Park and K.-J. Cho, "Development and evaluation of a soft wearable weight support device for reducing muscle fatigue on shoulder," *PLoS One*, vol. 12, no. 3, p. e0173730, Mar. 2017, doi: 10.1371/JOURNAL.PONE.0173730.

[16] A. Seth *et al.*, "OpenSim: Simulating musculoskeletal dynamics and neuromuscular control to study human and animal movement," *PLOS Comput. Biol.*, vol. 14, no. 7, p. e1006223, Jul. 2018, doi: 10.1371/JOURNAL.PCBI.1006223.

[17] C. L. Dembia, N. A. Bianco, A. Falisse, J. L. Hicks, and S. L. Delp, "OpenSim Moco: Musculoskeletal optimal control," *PLOS Comput. Biol.*, vol. 16, no. 12, p. e1008493, Dec. 2020, doi: 10.1371/JOURNAL.PCBI.1008493.

[18] S. L. Delp *et al.*, "OpenSim: Open-source software to create and analyze dynamic simulations of movement," *IEEE Trans. Biomed. Eng.*, vol. 54, no. 11, pp. 1940–1950, 2007, doi: 10.1109/TBME.2007.901024.

[19] "How CMC Works - OpenSim Documentation - Global Site." https://simtk-confluence.stanford.edu:8443/display/OpenSim/How+CMC+Works (accessed Oct. 29, 2021).

[20] B. ND *et al.*, "Tensile properties of the superior glenohumeral and coracohumeral ligaments," *J. shoulder Elb. Surg.*, vol. 5, no. 4, pp. 249–254, 1996, doi: 10.1016/S1058-2746(96)80050-4.

[21] B. LU, P. RG, S. LJ, F. EL, P. RJ, and M. VC, "Tensile properties of the inferior glenohumeral ligament," *J. Orthop. Res.*, vol. 10, no. 2, pp. 187–197, 1992, doi: 10.1002/JOR.1100100205.

[22] Y. C, G. A, S. W, Y. H, and S. K, "In vivo three-dimensional evaluation of the functional length of glenohumeral ligaments," *Clin. Biomech. (Bristol, Avon)*, vol. 25, no. 2, pp. 137–141, Feb. 2010, doi: 10.1016/J.CLINBIOMECH.2009.10.009.

[23] M. DC, M. EM, P. MN, and S. K, "Spatial Dependency of Glenohumeral Joint Stability during Dynamic Unimanual and Bimanual Pushing and Pulling," *J. Biomech. Eng.*, vol. 141, no. 5, May 2019, doi: 10.1115/1.4043035.

[24] M. E. Vidt *et al.*, "Modeling a rotator cuff tear: Individualized shoulder muscle forces influence glenohumeral joint contact force predictions," *Clin. Biomech. (Bristol, Avon)*, vol. 60, p. 20, Dec. 2018, doi: 10.1016/J.CLINBIOMECH.2018.10.004.

[25] B. I. Binder-Markey and W. M. Murray, "Incorporating the length-dependent passive-force generating muscle properties of the extrinsic finger muscles into a wrist and finger biomechanical musculoskeletal model," *J. Biomech.*, vol. 61, pp. 250–257, Aug. 2017, doi: 10.1016/J.JBIOMECH.2017.06.026.

[26] M. M, U. T, S. A, and D. SL, "Flexing computational muscle: modeling and simulation of musculotendon dynamics," *J. Biomech. Eng.*, vol. 135, no. 2, 2013, doi: 10.1115/1.4023390.

[27] L. M. Schutte, M. M. Rodgers, F. E. Zajac, and R. M. Glaser, "Improving the Efficacy of Electrical Stimulation-Induced Leg Cycle Ergometry: An Analysis Based on a Dynamic Musculoskeletal Model," *IEEE Trans. Rehabil. Eng.*, vol. 1, no. 2, pp. 109–125, 1993, doi: 10.1109/86.242425.

[28] M. A. Sherman, A. Seth, and S. L. Delp, "WHAT IS A MOMENT ARM? CALCULATING MUSCLE EFFECTIVENESS IN BIOMECHANICAL MODELS USING GENERALIZED COORDINATES," *Proc. ASME Des. Eng. Tech. Conf.*, vol. 2013, 2013, doi: 10.1115/DETC2013-13633.

[29] S. KR *et al.*, "Benchmarking of dynamic simulation predictions in two software platforms using an upper limb musculoskeletal model," *Comput. Methods Biomech. Biomed. Engin.*, vol. 18, no. 13, pp. 1445–1458, Oct. 2015, doi: 10.1080/10255842.2014.916698.

[30] E. K. Chadwick, D. Blana, R. F. Kirsch, and A. J. Van Den Bogert, "Real-time simulation of three-dimensional shoulder girdle and arm dynamics," *IEEE Trans. Biomed. Eng.*, vol. 61, no. 7, pp. 1947–1956, 2014, doi: 10.1109/TBME.2014.2309727.

[31] B. Brahmi, M. Saad, C. Ochoa-Luna, M. H. Rahman, and A. Brahmi, "Adaptive Tracking Control of an Exoskeleton Robot with Uncertain Dynamics Based on Estimated Time-Delay Control," *IEEE/ASME Trans. Mechatronics*, vol. 23, no. 2, pp. 575–585, Apr. 2018, doi: 10.1109/TMECH.2018.2808235.

List of Figures

List of Tables

6. Acknowledgements